Hydrates in sediments and strategies for hydrate reservoir exploitation

CCOP Workshop Da Nang, Vietnam
December 9, 2009

Professor Bjørn Kvamme
Department of Physics and Technology,
University of Bergen, Bergen, Norway
Bjorn.kvamme@ift.uib.no

Gas Hydrates: A Major Energy Resource:

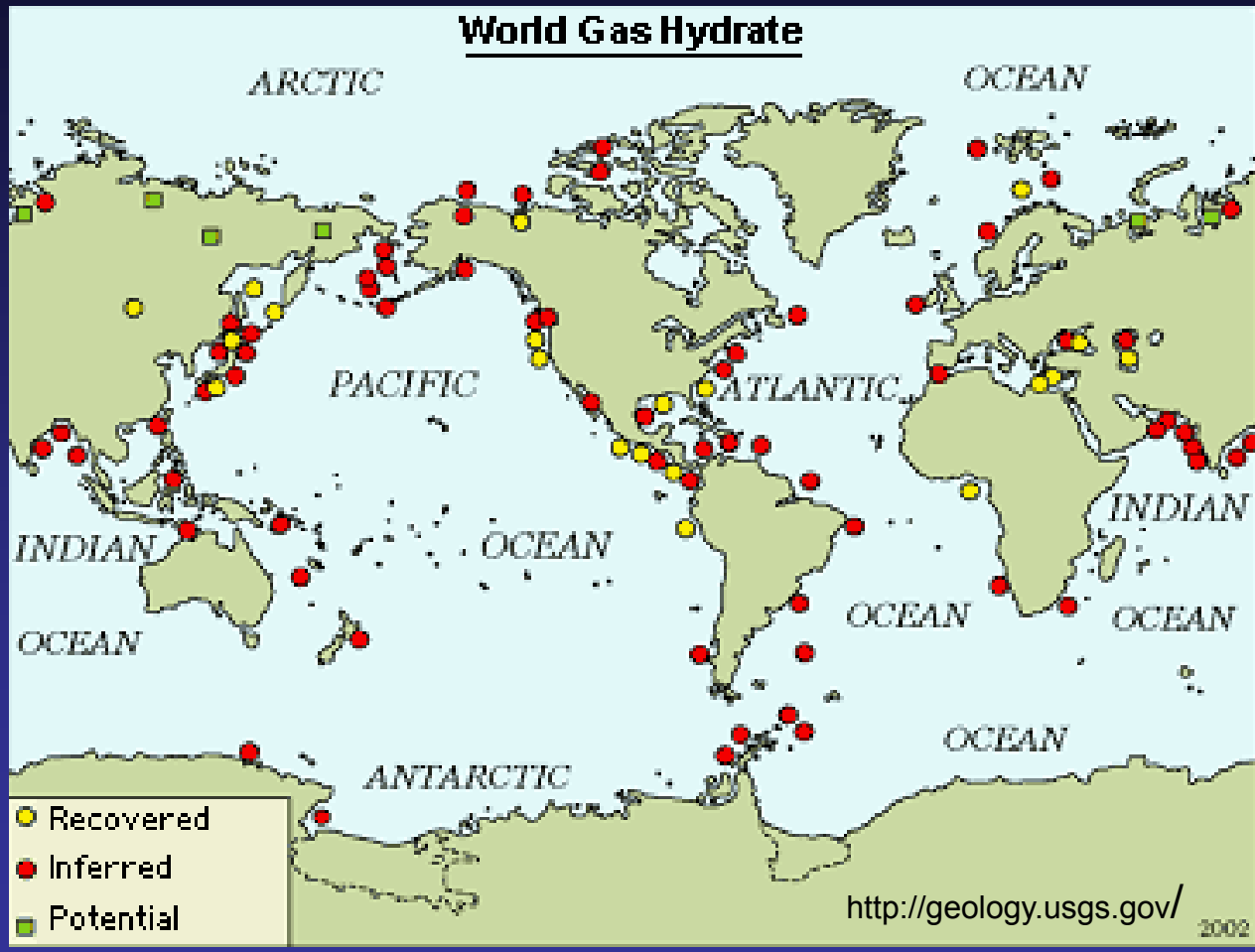

Hydrate Structures:

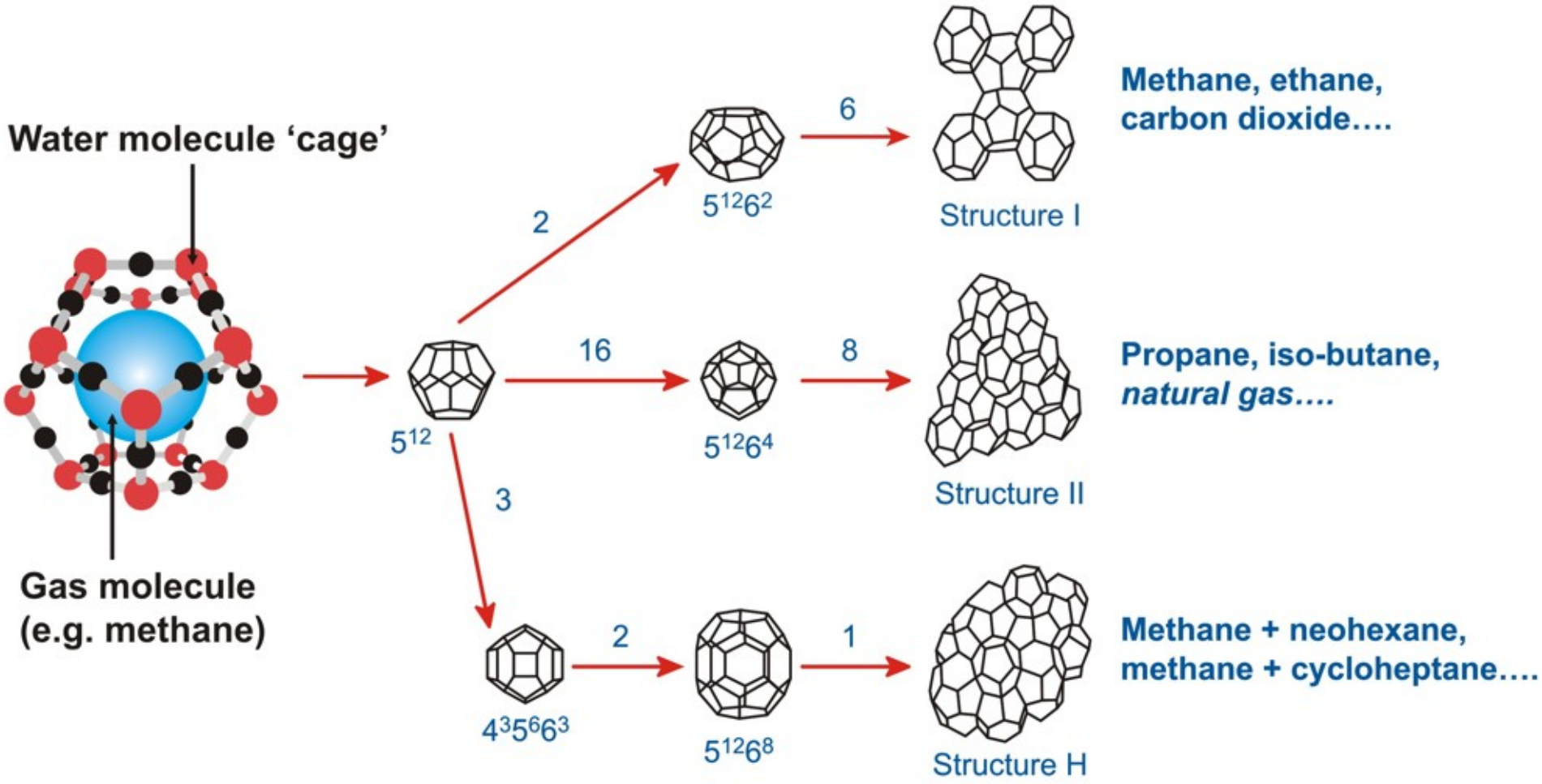

www.pet.hw.ac.uk/

Regions of pressure and temperature for stability of some hydrates

Solid line is liquid/ice coexistence curve

Dashed line is for methane hydrate

Dash-dot is for 2 per cent ethane in methane

+ are hydrate formed from water and an ethane-rich mixture with methane (3 per cent)

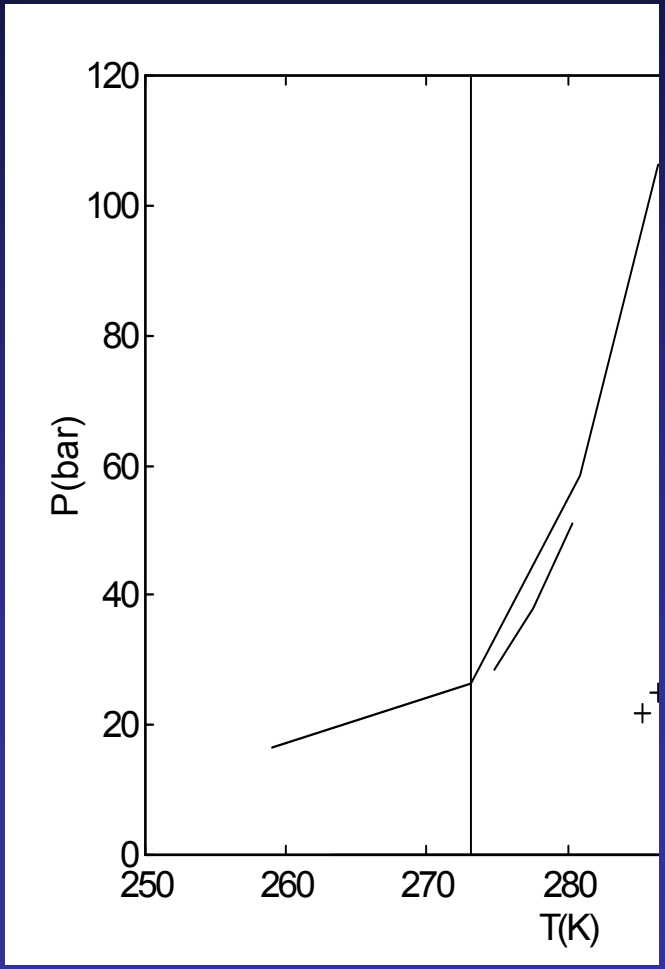

Where do the hydrate formers come from

- ***Biogenic sources***
- **Microbial activity in the upper several hundred meters of deep-sea sediment (about 99%)**

- ***Thermogenic sources***
- **Thermal breakdown of organic material at greater depths**

Seismic detection of hydrates

- Seismic methods: contrasts in density and elastic moduli associated with the presence of gas hydrate within sediment pore spaces versus saline pore fluid or free methane gas

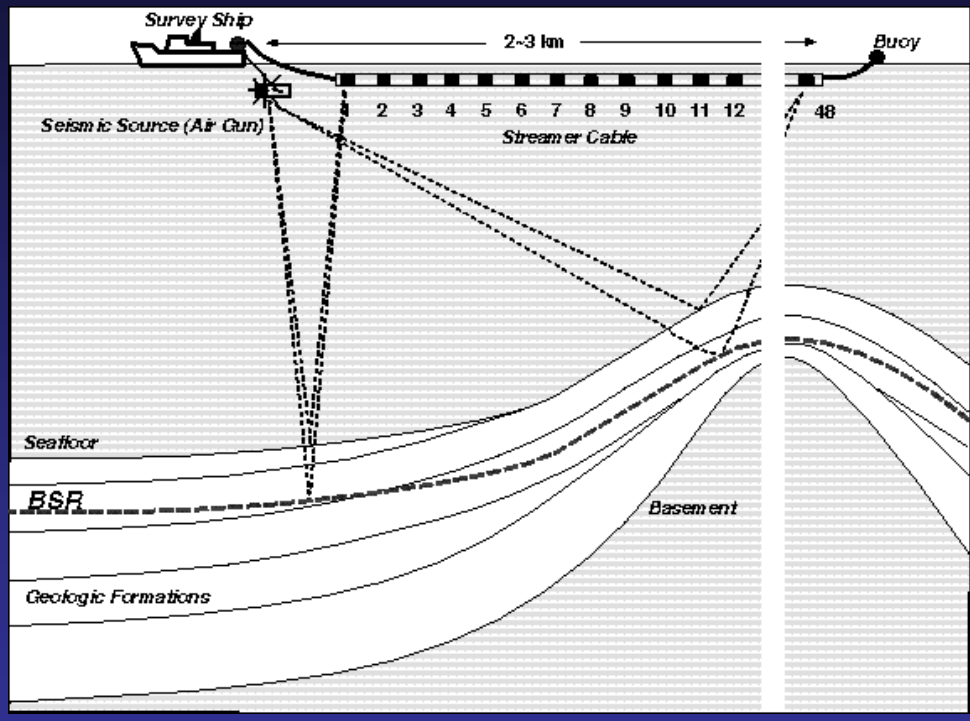

Sampling of acustic reflection from seismic shots (from towed devices on ocean, close to bottom or bottom mounted acoustic signal generators)

Geophysical characterization and quantification of gas hydrates

P-cable: High resolution 3D seismic concept

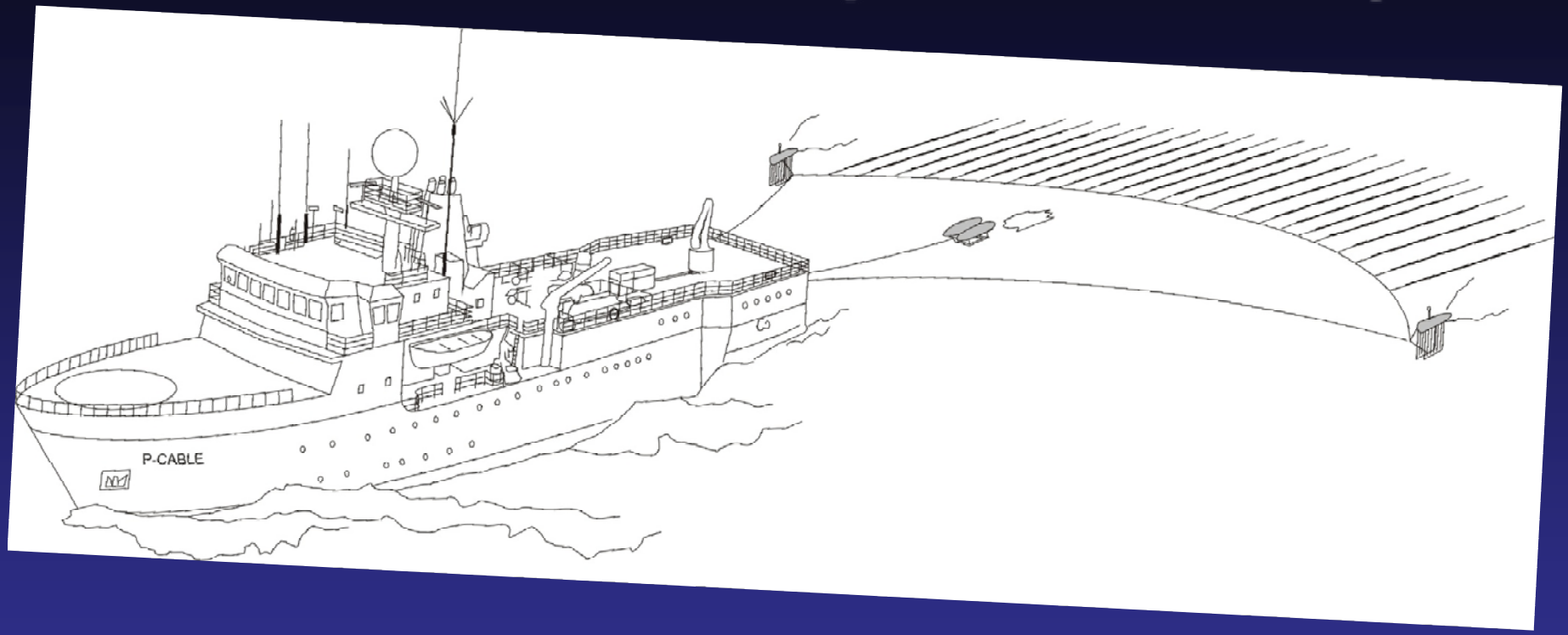

- "Shallow" 3-D reflection seismic with high frequencies (50-250 Hz)
- A seismic cable towed perpendicular to the vessel's steaming direction
- Many seismic streamers attached to a wire (cross cable) held in place by two doors
- Used configuration with 12 (8) streamers towed parallel (streamer offset of ~10 m).

Geophysical evidence for gas hydrates

Seismic example from west Svalbard margin

Bottom-simulating reflector (BSR):

- Mimics seafloor
- Phased-reversed compared to seafloor reflection
- Reflection enhancement underneath

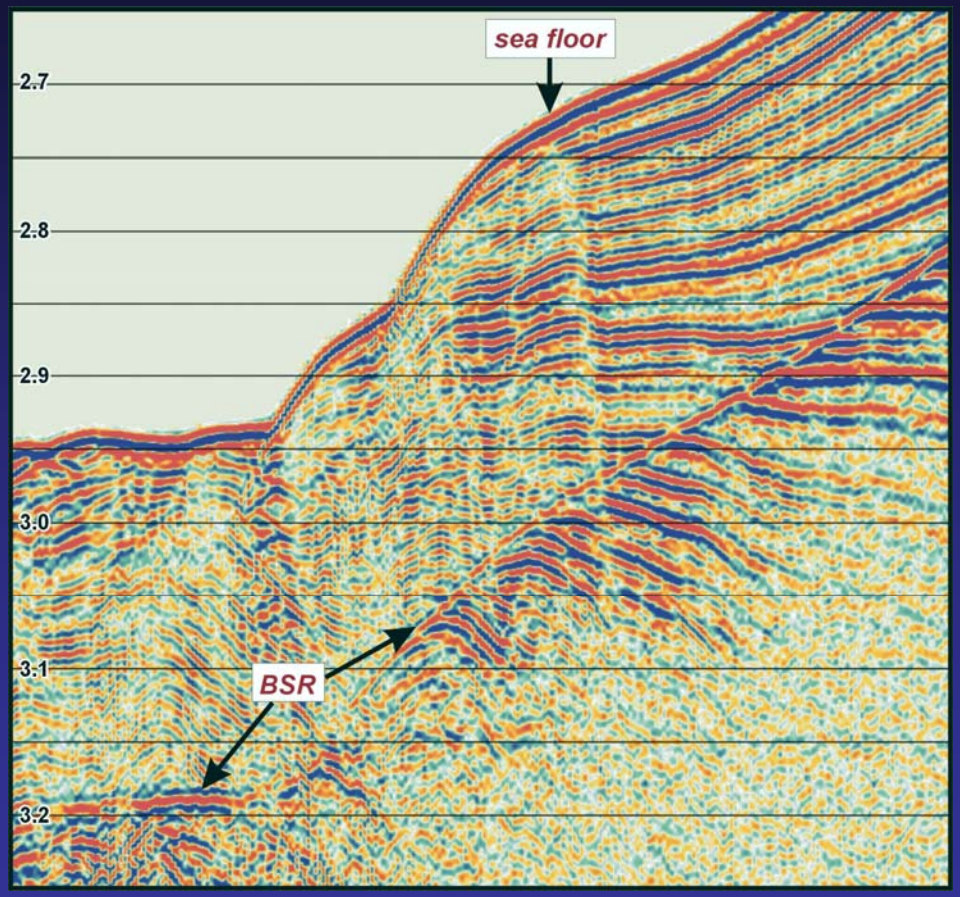

Geophysical evidence for gas hydrates

Seismic example from south Vøring Plateau

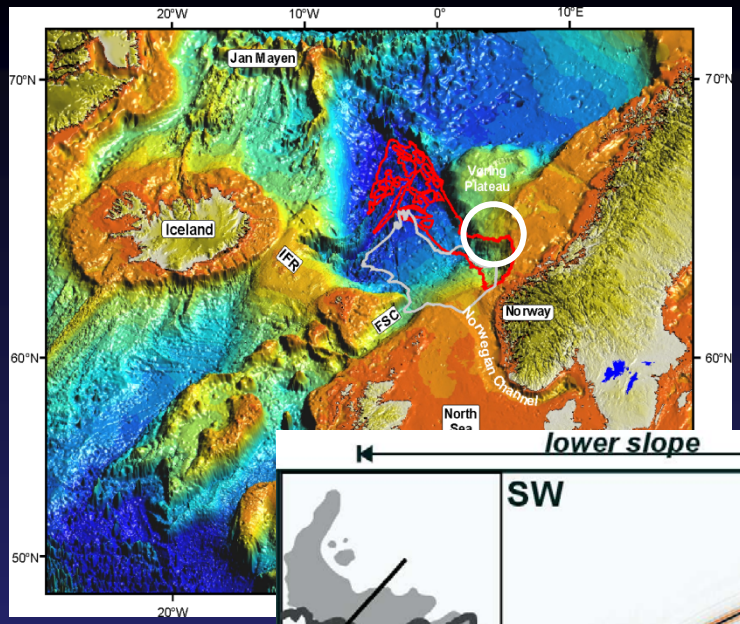

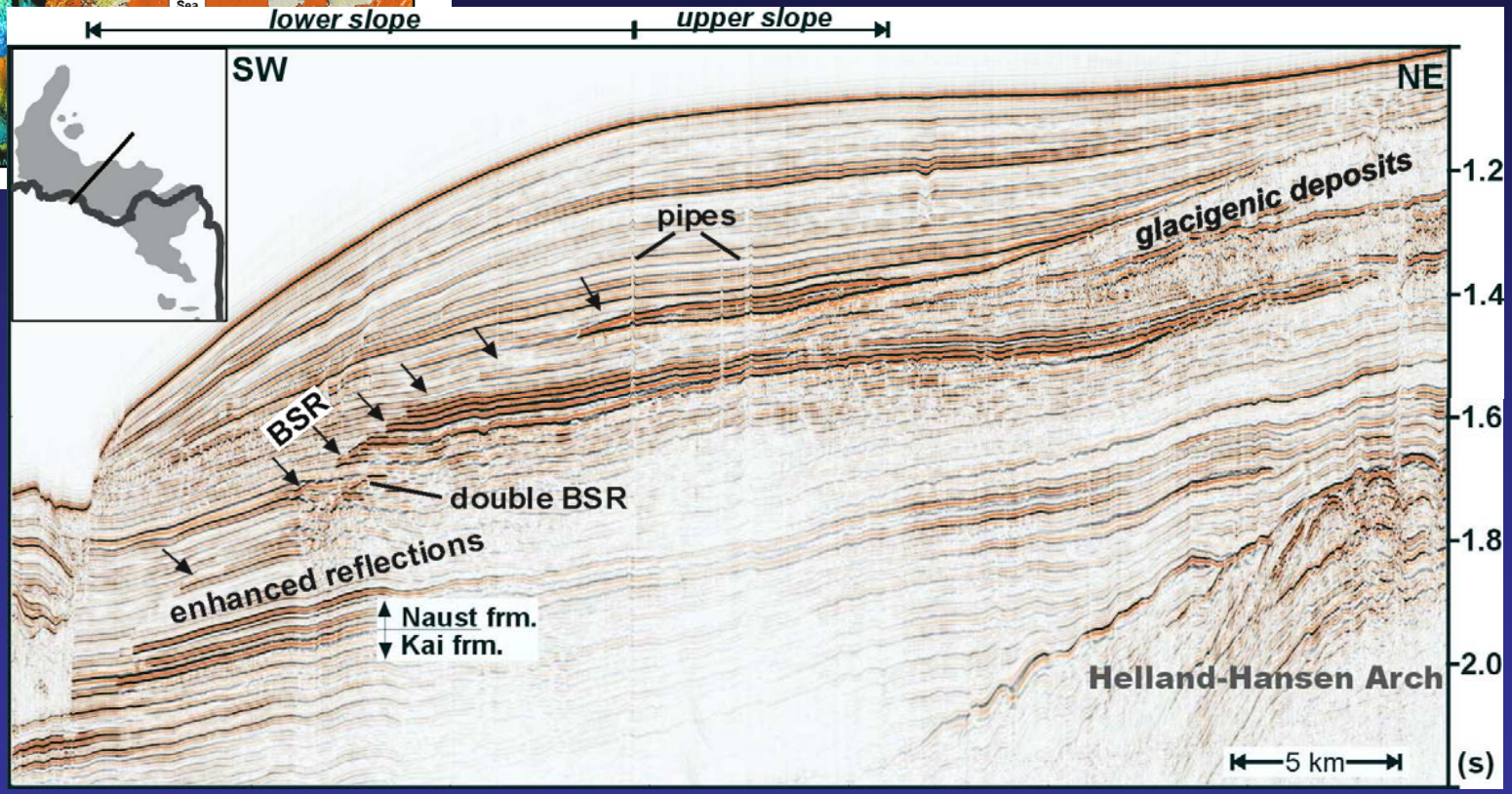

Buenz et al. (2003)

3D seismic system cube; from Vestnesa Ridge, W-Spitsbergen

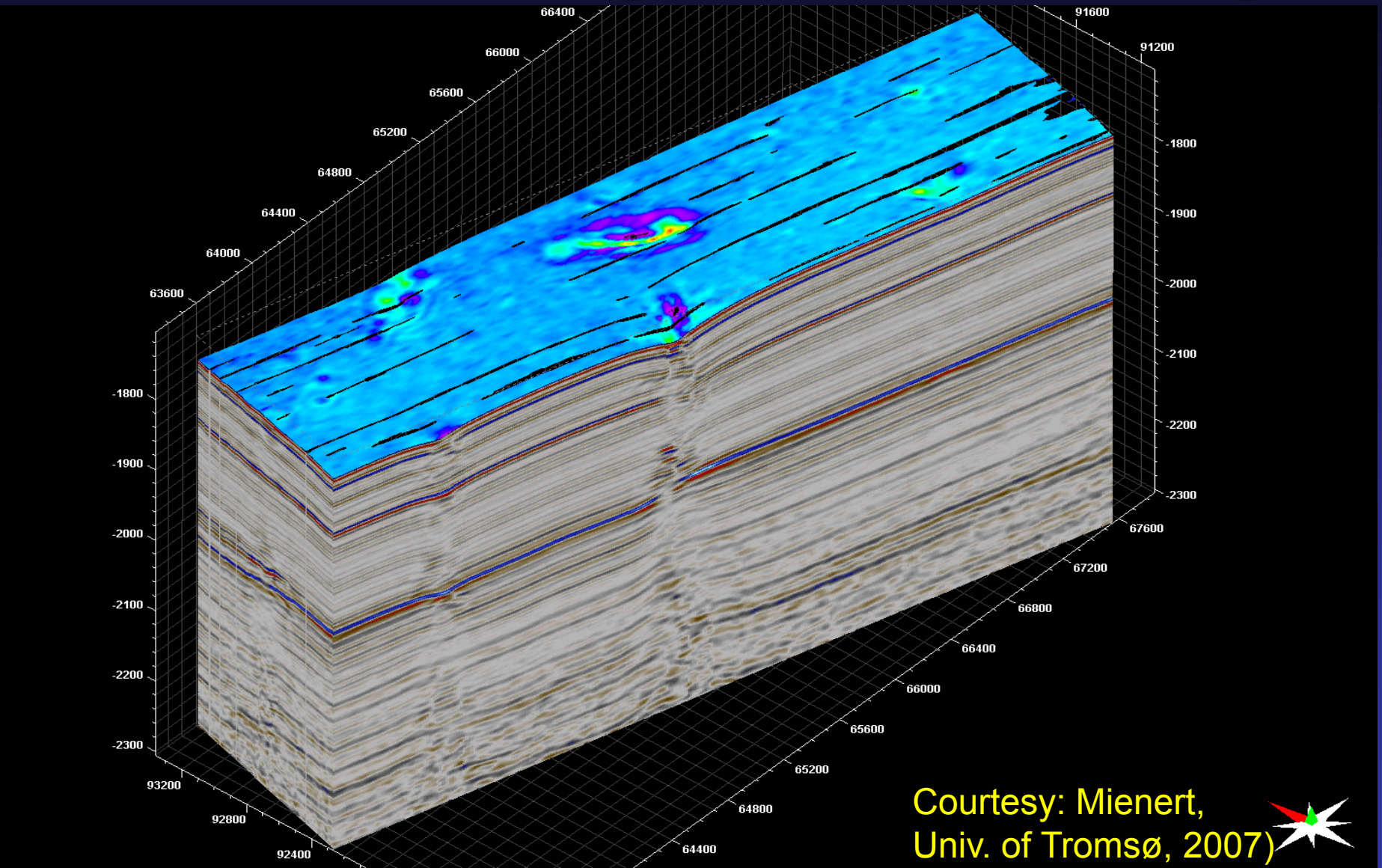

Courtesy: Mienert, Univ. of Tromsø, 2007)

Detection of hydrates through resistivity measurements

- Electrical methods are based on contrasts in electrical conductivity, or its inverse, resistivity.
- Gas hydrate is essentially an insulator, in contrast to saline pore fluids with resistivities on the order of 1 ohm-m or less

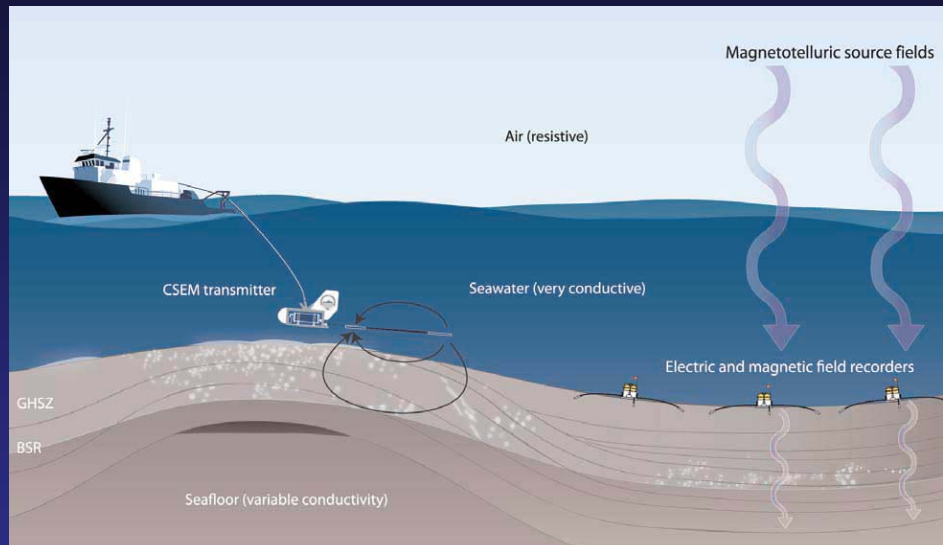

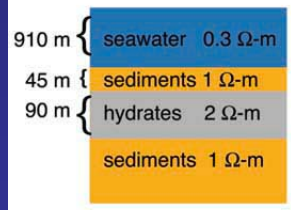

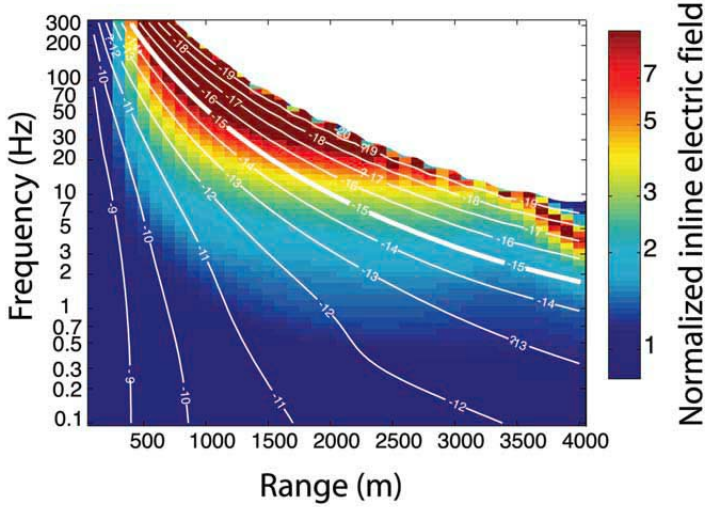

Source:http://marineemlab.ucsd.edu/~kkey/Pubs/Weitemeyer2006a.pdf

Example (Moridis & Collett, 2008)

DOE Merit Review, August 26-27, 2008Pittsburgh, PENNSYLVANIA

- Resistivity typically estimates higher hydrate saturation than analysis from P-Wave velocity (seismic)
- *(Even though these data appear to be open on the net the best is to request DOE for details on these data if interested in detailed location)*

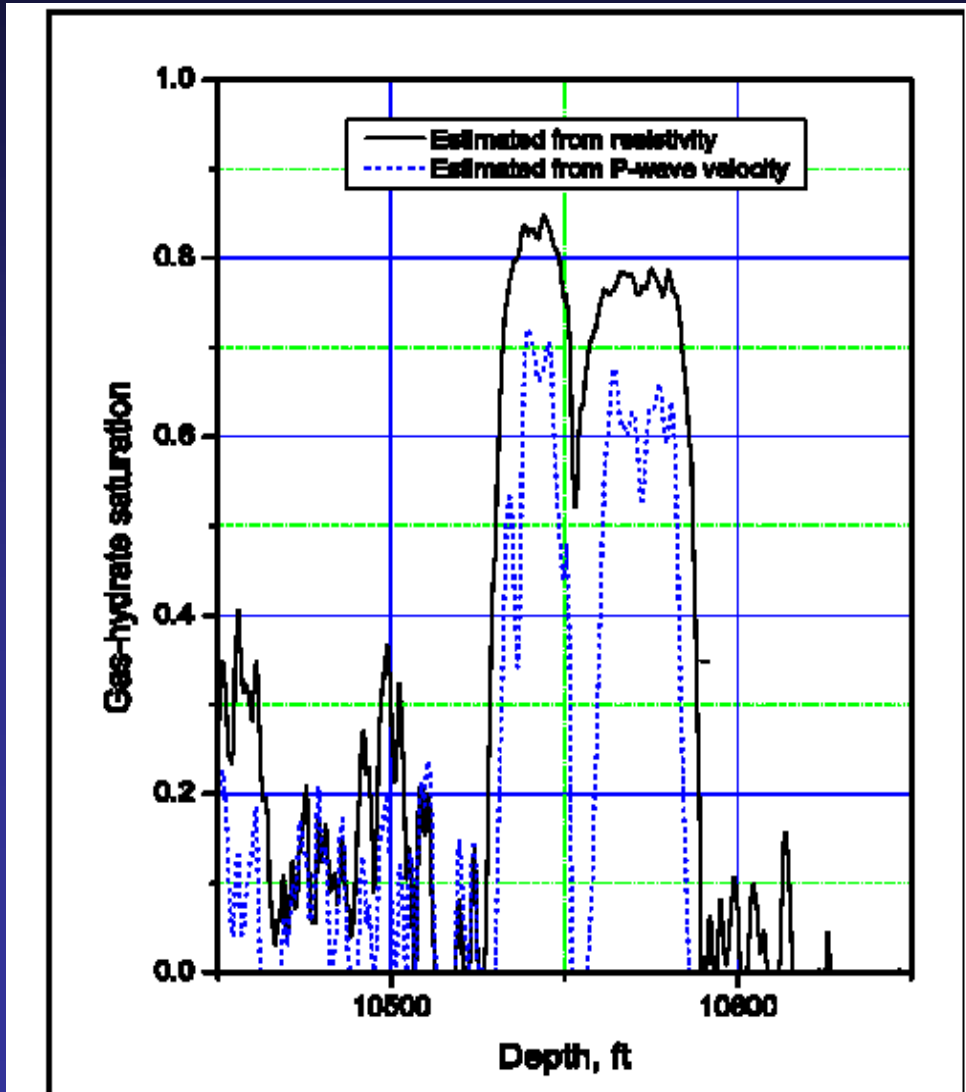

OUTLINE

- Before discussing exploration – a few words about hydrates in sediments
- A few words about classical approaches for exploitation of hydrate reservoirs
- Simultaneous safe storage of CO2 and exploitation of hydrate reservoirs
- Theoretical modelling
- Conclusions

What is the present status of hydrate as a source of energy?

- The main worldwide motivations are essentially combinations of the following:
- 1) Desire for higher degree of energy supply independence (USA)
- 2) Limited own traditional oil and gas resources (Japan) or declining resources of conventional sources (India, South-East Asia)
- 3) Increased value of excisiting processing and transport infrastructure by connecting hydrate production to excisiting infrastructure.

So what is special about hydrates in sediments?

- Each different mineral has a specific structure and ***surface structure of atoms***
- Interactions between these atoms and surrounding molecules does ***not facilitate stability of regular hydrate lattice in contact with the solid surfaces***
- Exceptions are hydrates in contact with clay minerals, in which the ionic content of the clay liquids assist in ”bridging” the hydrate to clay

Calcite cleaved along the dominant plane in contact with aqueous CO_2:

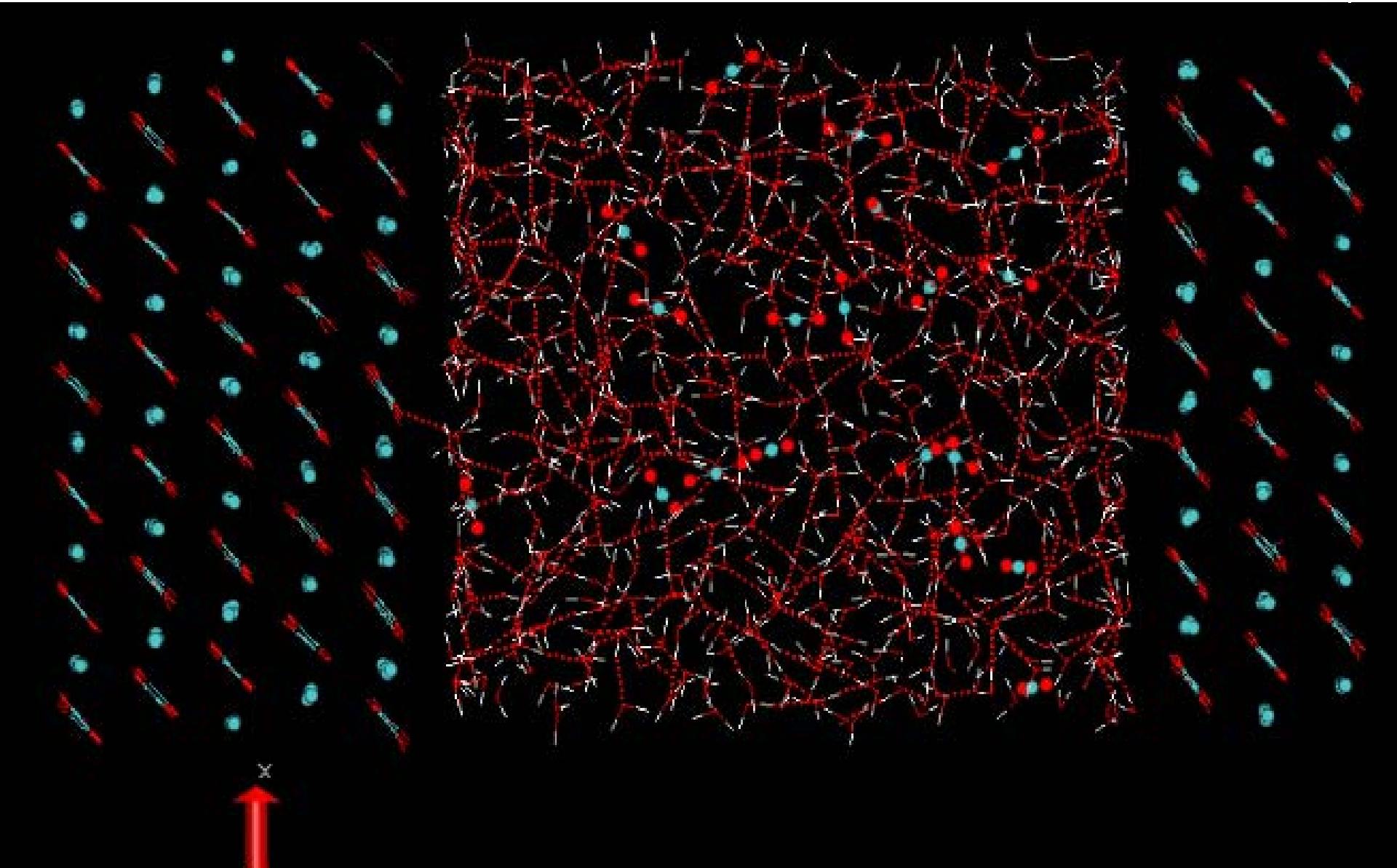

Calcite cleaved along the second most stable $\{10\bar{1}0\}$ plane in contact with aqueous CO_2: VMD-generated snapshot

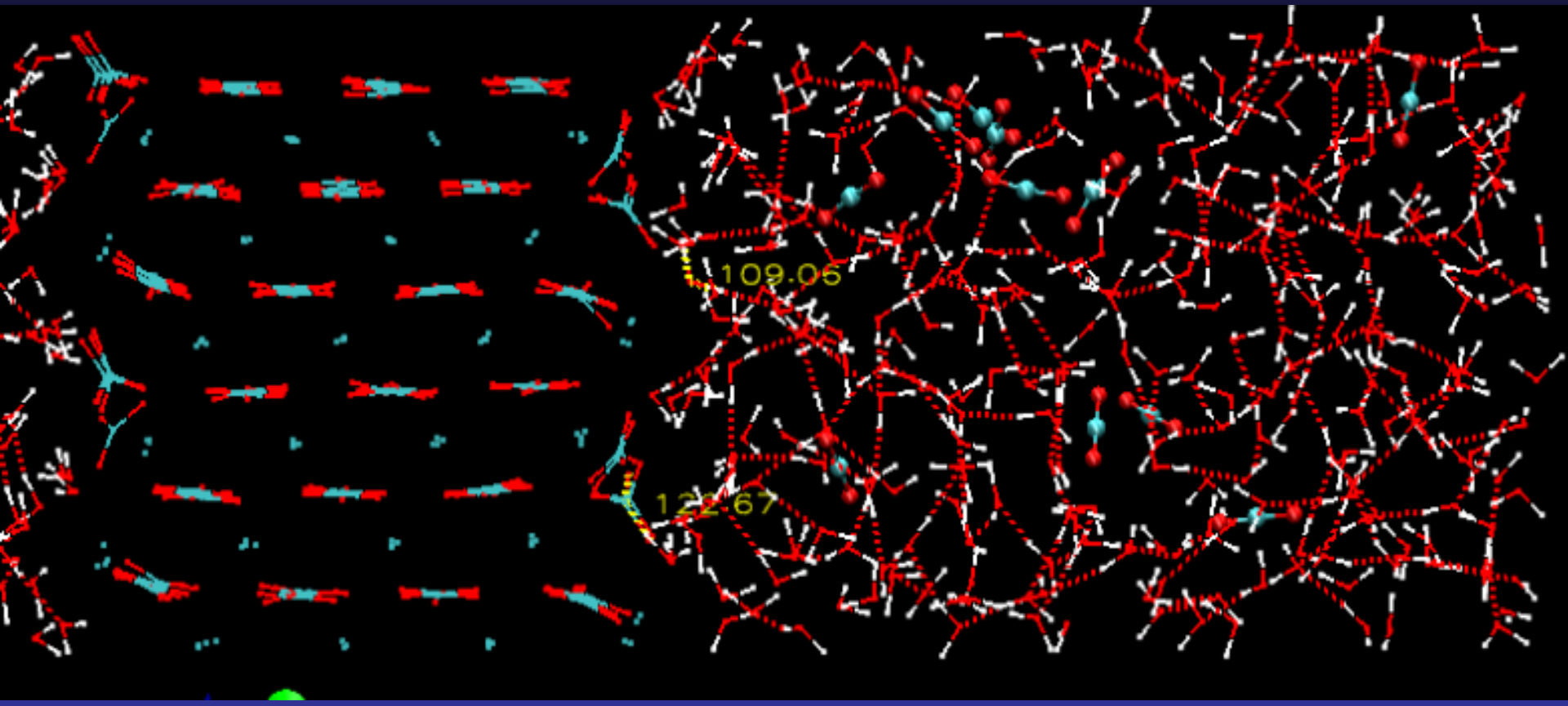

Calcite cleaved along the second most st$\{10\bar{1}0\}$ plane in contact with aqueous CO_2: density profiles

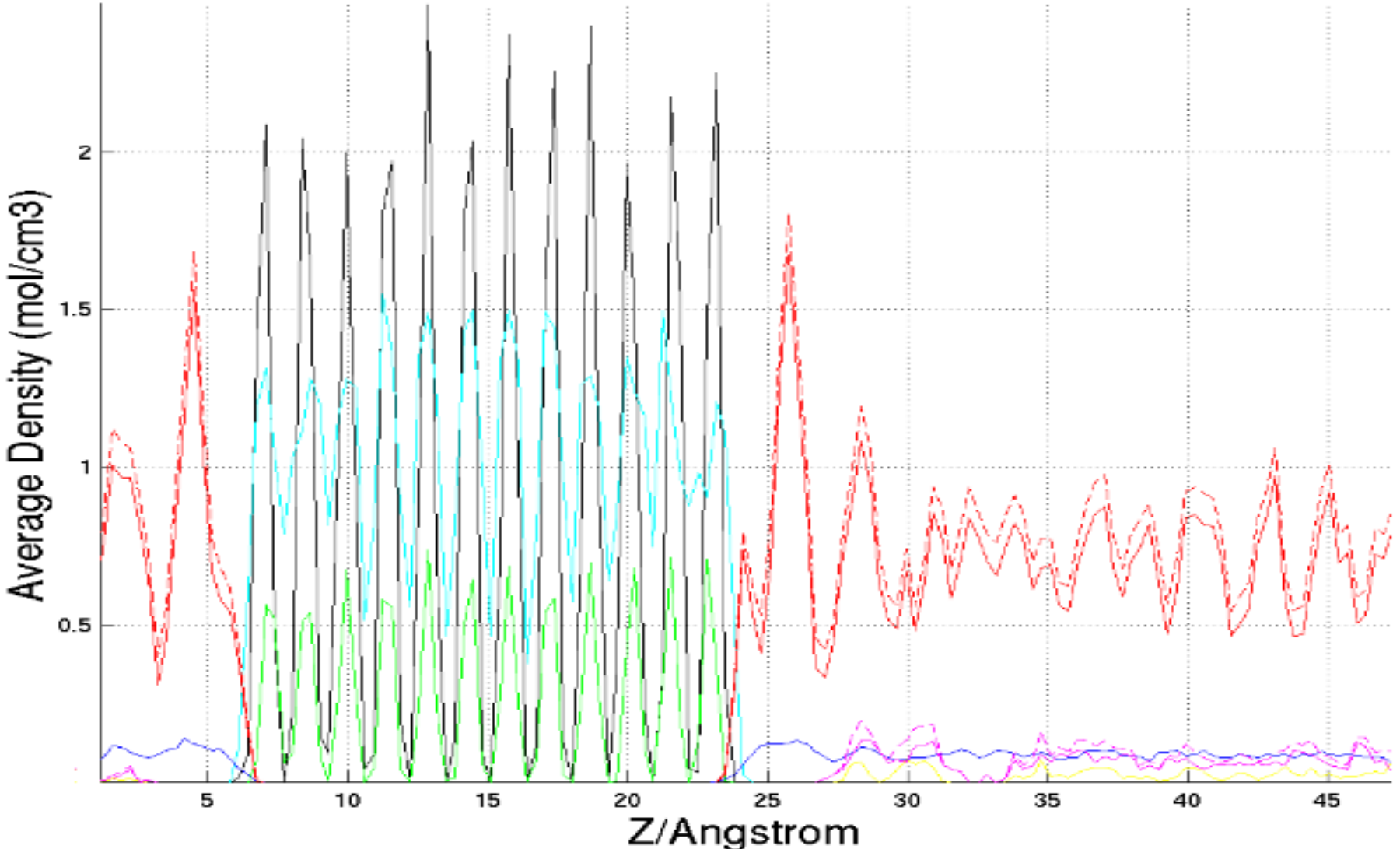

Example with a spherical hydrate particle growing from dissolved CO2 in saturated aqueous solutions at 1 C and 150 bar (x=0.033) x in minimum free energy for solution coexisting with the hydrate is x=0.016 System size is 40 nm x 40 nm and simulation time is 0.5 microseconds

- **The chemical potential of the water molecules are approximated to vary linearly from the interface and assumed to be of bulk liquid properties 8 molecular diameters from the interface (based on structure sampling)**
- **Note that growth rate is highly sensitive to shape and a spherical particle has been chosen as a simple example**
- **A growing hydrate film shows similar behavior of ”avoiding” the solid surface but the growth rate is slower**

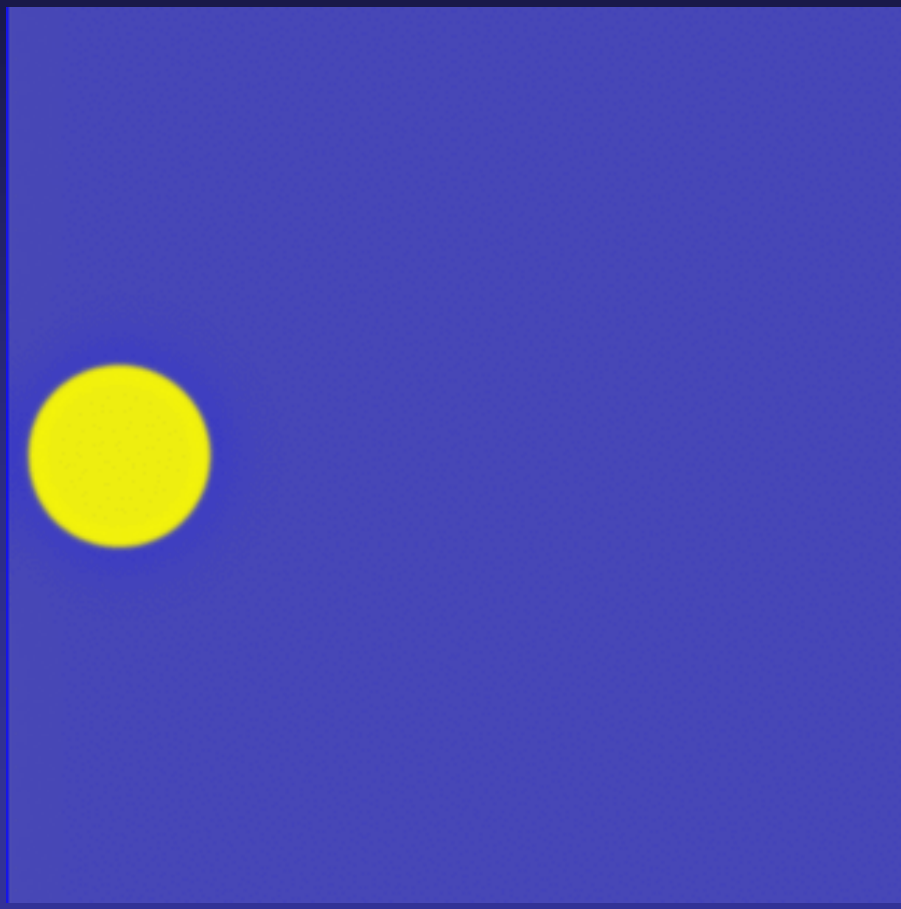

So what is the impact of this?

- Hydrate dissociation occurs wherever hydrate is exposed to ***fluid channels undersaturated with respect to "guest "*** types in the hydrate ***and hydrate exposed towards undersaturated gas***

- I.e.: Hydrate phase transitions in porous media can occur on ***very large surfaces and channels between hydrate and minerals assists in mass transport***

- ***For the opposite process it is enough to compare hydrate formation kinetics towards a liquid water surface as a reference (See later overheads for more detailed exp. setup)***

Experiments with methane and water at 83 bar and 3 C
Similar experiment with CO2 did not show any penetration of the hydrate film after 500 hour (resolution ~ 100 micrometer)

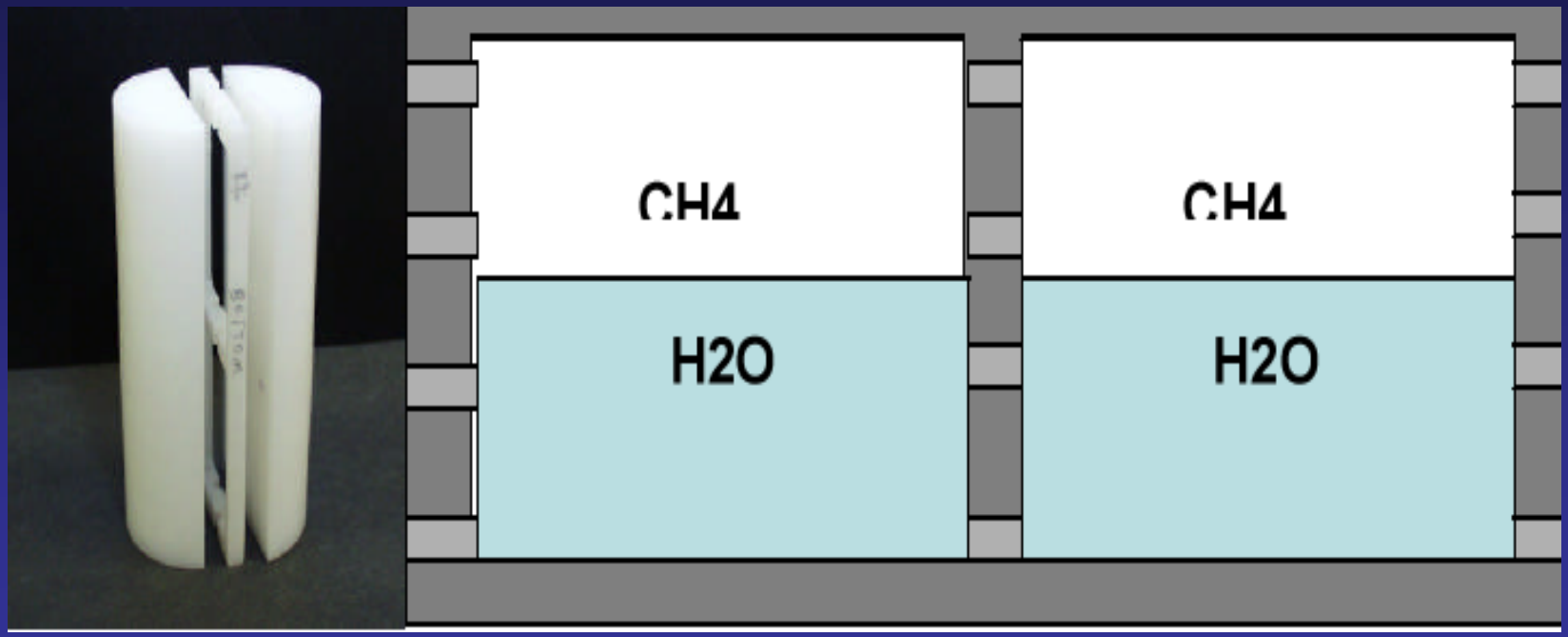

Note that methane is the wetting component on the polypropylene

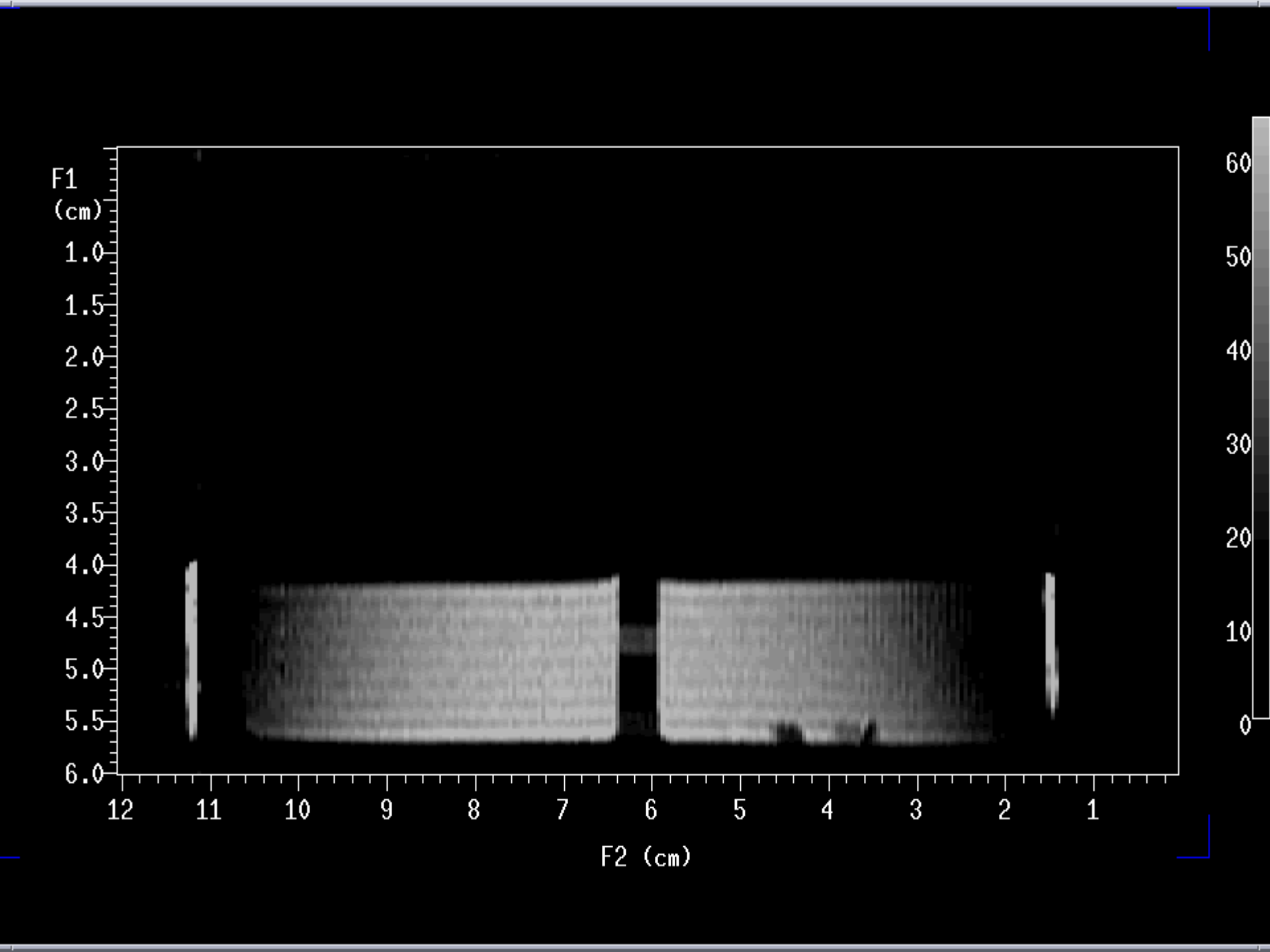
F1
(cm)
1.0
1.5
2.0
2.5
3.0
3.5
4.0
4.5
5.0
5.5
6.0
12
11
10
9
8
7
6
5
4
3
2
1
F2 (cm)
60
50
40
30
20
10
0

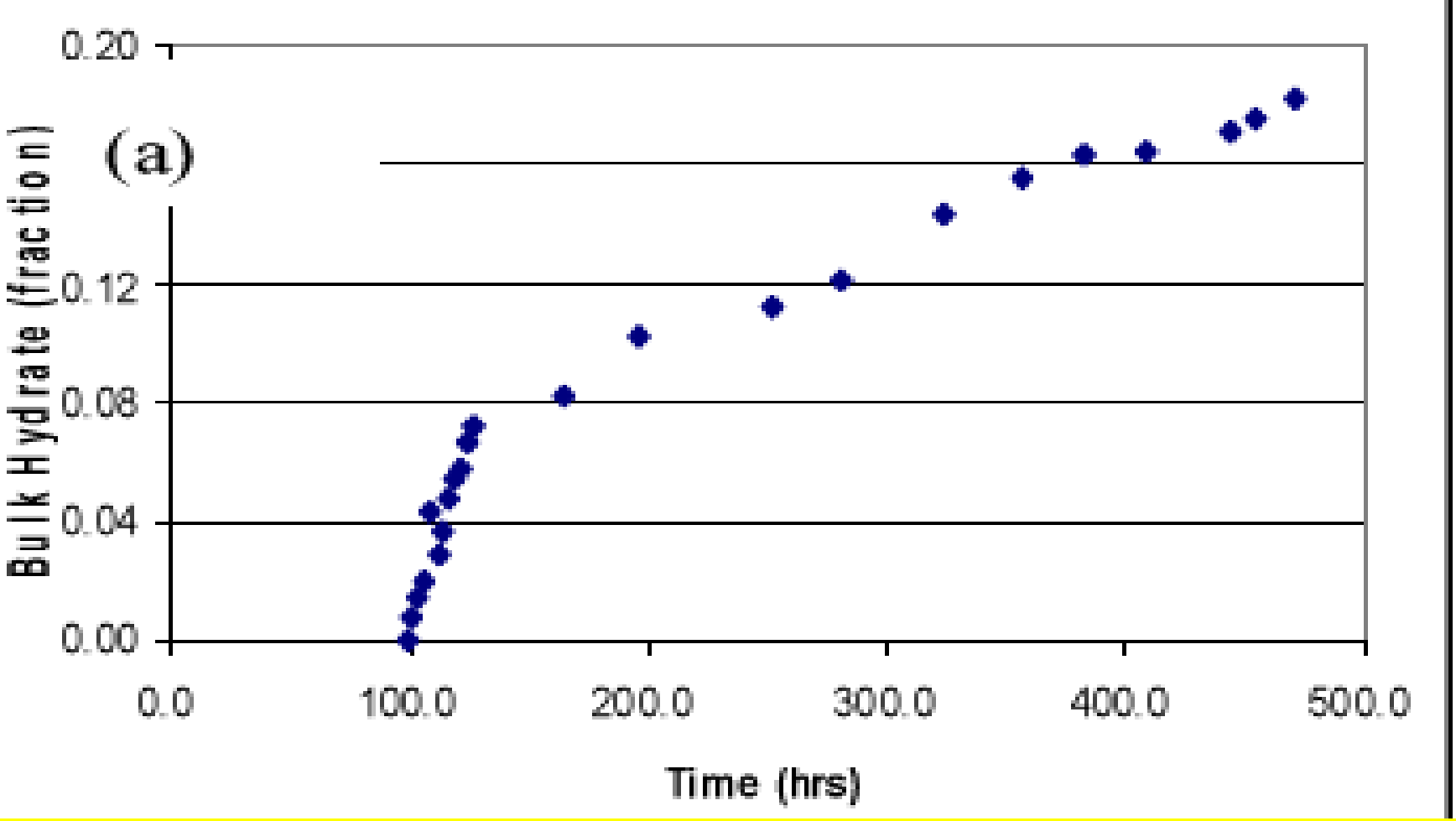

Why? Two primary factors:

1) A methane hydrate film will rapidly form on the water/methane interface and reduce efficiently further growth untill film penetratesdue to local competition based on first and second laws of thermodynamics
2) Methane is the wetting component of the silicone rubber and some methane will migrate along the walls downwards in the chamber due

Heterogeneous hydrate formation (yellow) on the interface between CO2 (inner red) and liquid water initially saturated with CO2 (outer red)

T = 274 K p = 150 bar
500 × 200 grid n = 100
Δx = 0.4 nm t = 0.27 μs

Thermodynamics:

Fugacity coefficients for CO2 from SRK equation of state

Aquous description and hydrate description as in the homogeneous case

Simulations started with an extremely thin film of hydrate.

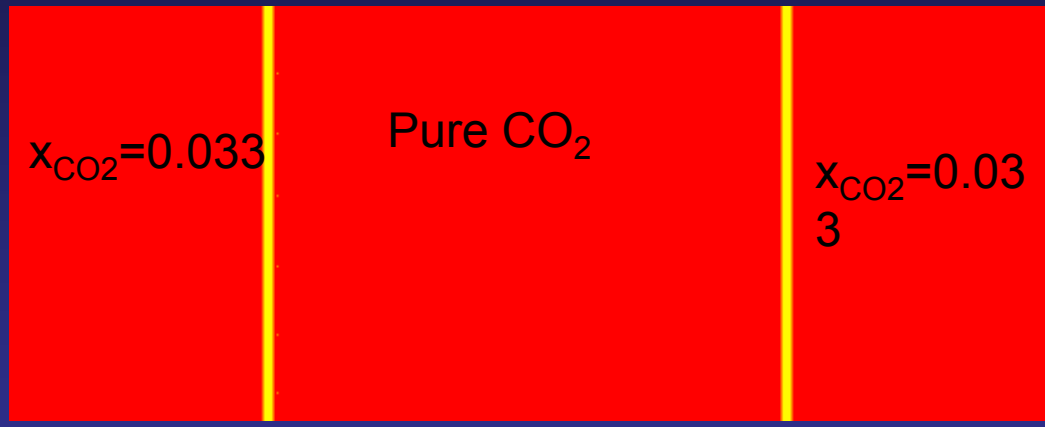

Note that simulation times are very short for this simulation and the average growth rate at later stages are expected to be significantly smaller (as experienced for the homogeneous case)

Heterogeneous hydrate formation (red front) on the interface between CO2 (yellow) and liquid water (blue)

This simulation is veryy short and rates should be considered as initial rates and compared to thelnitial rates from the homogeneous simulation the rate Is 7.5 times higher

DCO2=1.0•10-9 (liquid like) gives steady growth rate of 0.3 m/s

Experiment at T=277.4 K and 39 bar (lower thermodynamic driving force) Reported by Uchida et.al. (2003) indicates growth rate from 0.0001 m/s to 0.01 m/s

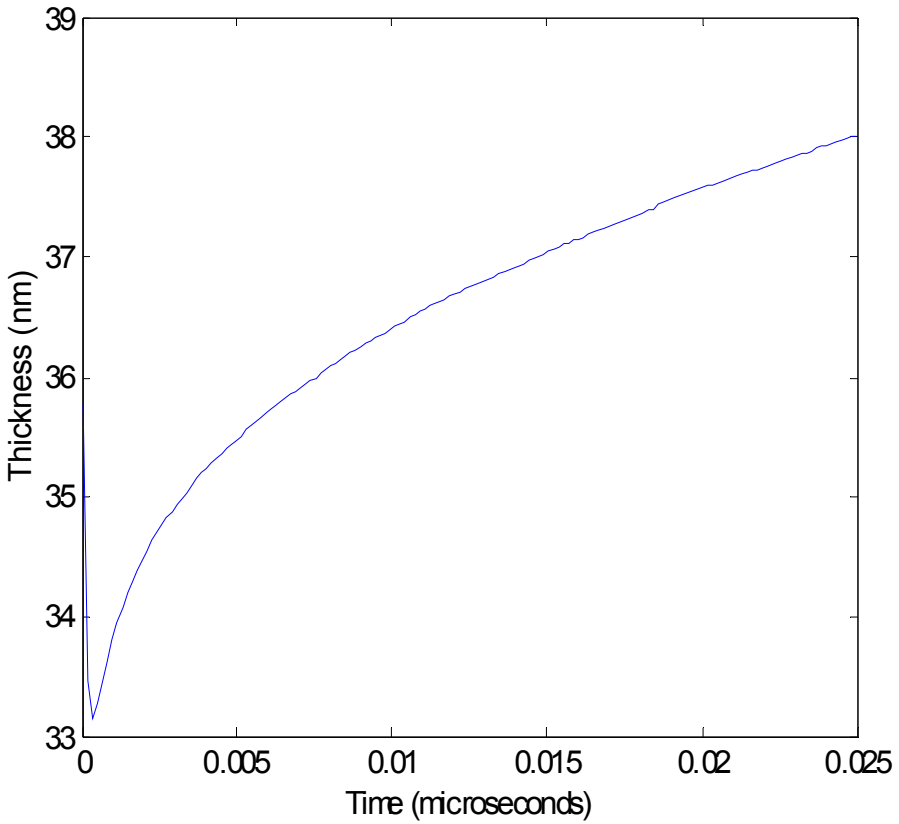

Similar simulation starting with a small hydrate nucleus

Average growth rate in this case is 0.24 m/s and diffusion-controlled. Note the short simulation time and recall that average rates for later growth are expected to be significantly lower

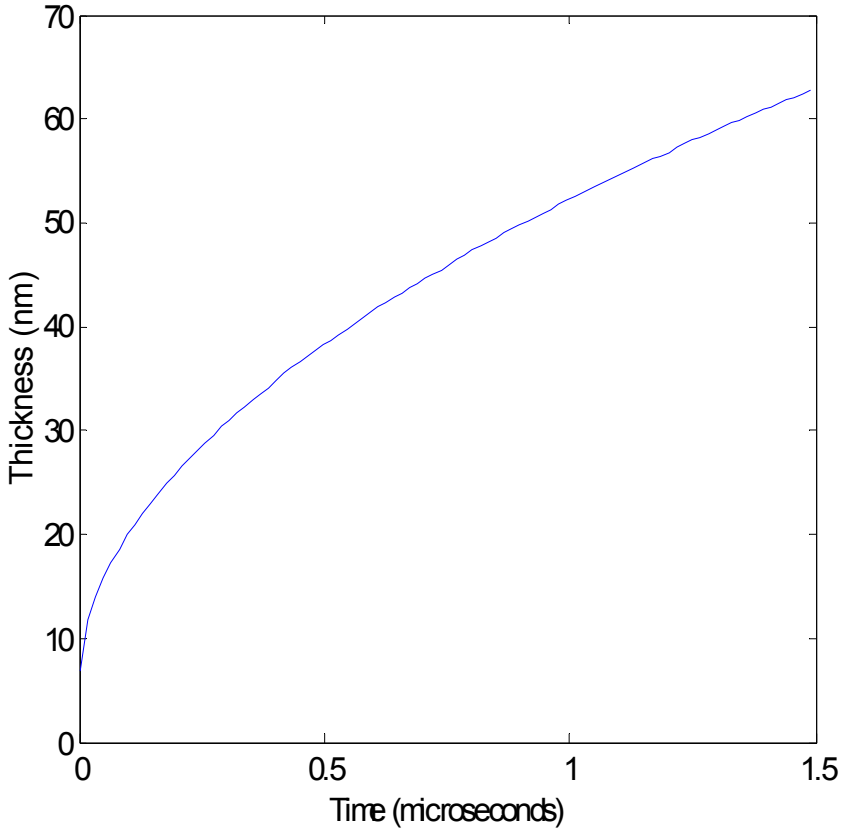

Now starting with several small hydrate nuclei on the interface between CO2 and water

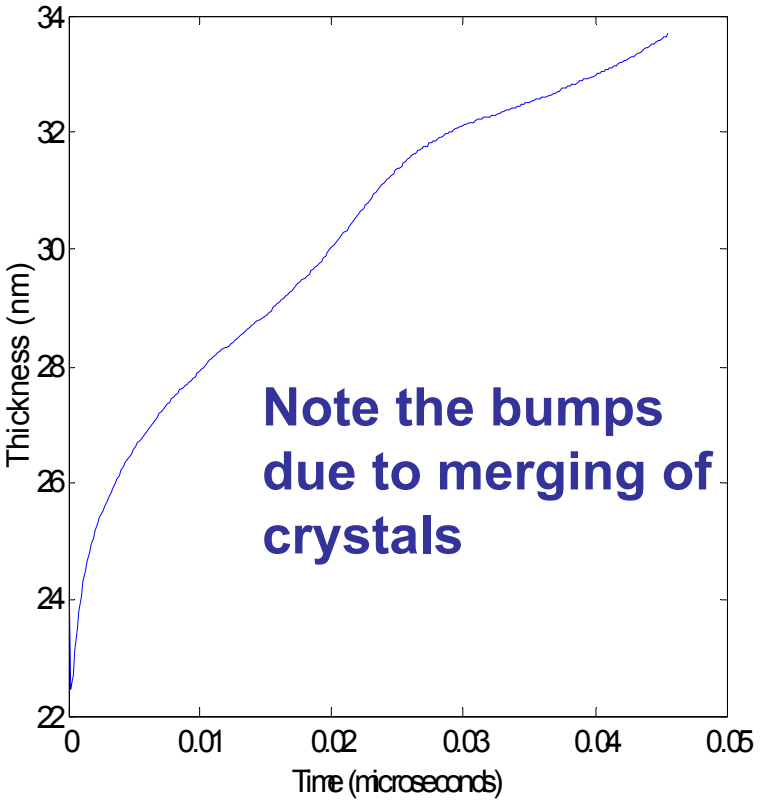

Asymptotically the system behaves proportional to t in the exponent of 0.3 in contrast to 0.5 for total mass transport control

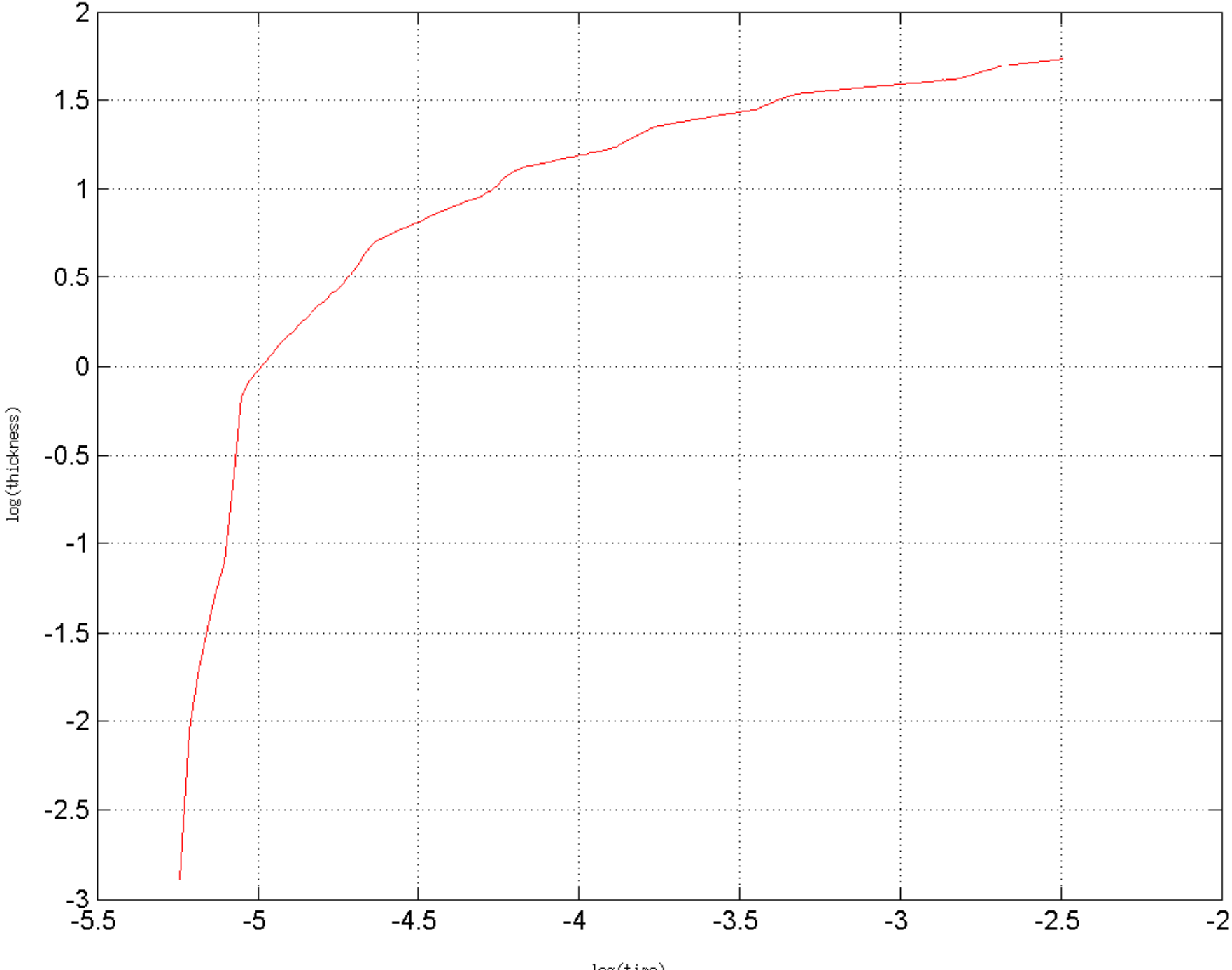
2
1.5
1
0.5
0
-0.5
-1
-1.5
-2
-2.5
-3
log(thickness)
-5.5
-5
-4.5
-4
-3.5
-3
-2.5
-2

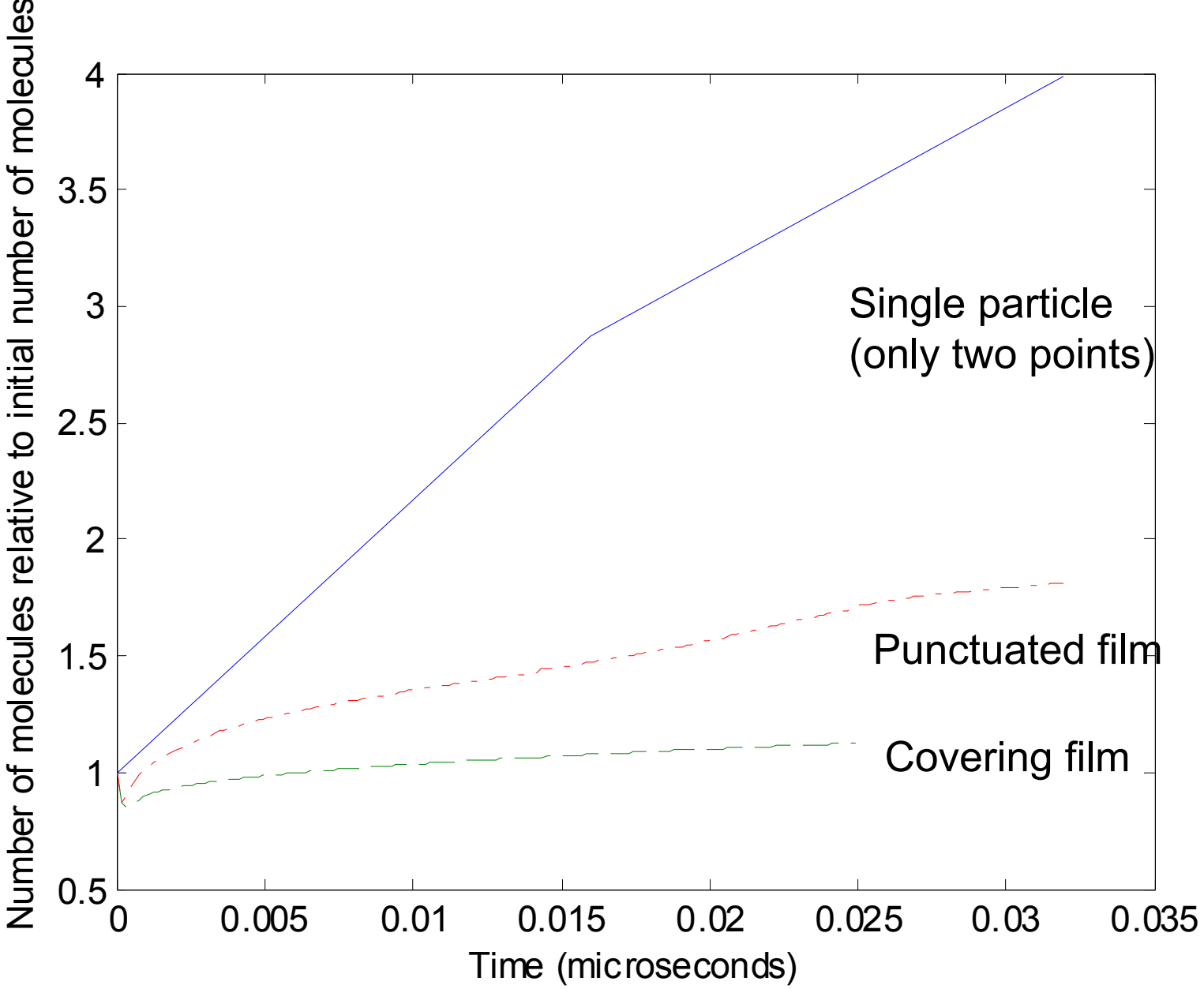

Growth rates from dissolved CO_2 much slower than heterogenous growth on exposed interfaces

So what is the consequence of this?

- Reservoir hydrate will never attach to the surface of the minerals
- The film of structured water, and possibly gas, will have a minimum thickness in the order of three water molecules but will normally be significantly thicker in a reservoir with significant fluid flow due to fractures and corresponding leakages

Consequence of mineral surfaces cont.?

- In practical terms this implies that real hydrate sections will have permeabillity, and a fluid filled porosity.
- But the magnitude of permeability may vary from very low to significant depending on the fluid flow dynamics of the reservoir (fractures, faults, feeding of fresh hydrocarbons from below etc)

Remarks

- Hydrate reservoirs which are tightly sealed (clay and shale layers) may enter a situation of extremely slow dynamics and local quasi equilibrium which will preserve the hydrate as ”rich” in hydrocarbons. Example is Nankai Through

- Reservoirs which have symptoms of extensive ”poc marks” of exposed hydrate may need more detailed examination since all leakage channels will have dissociated hydrate and the extent of rich and poor areas is uncertain

Hydrate Experiments Setup

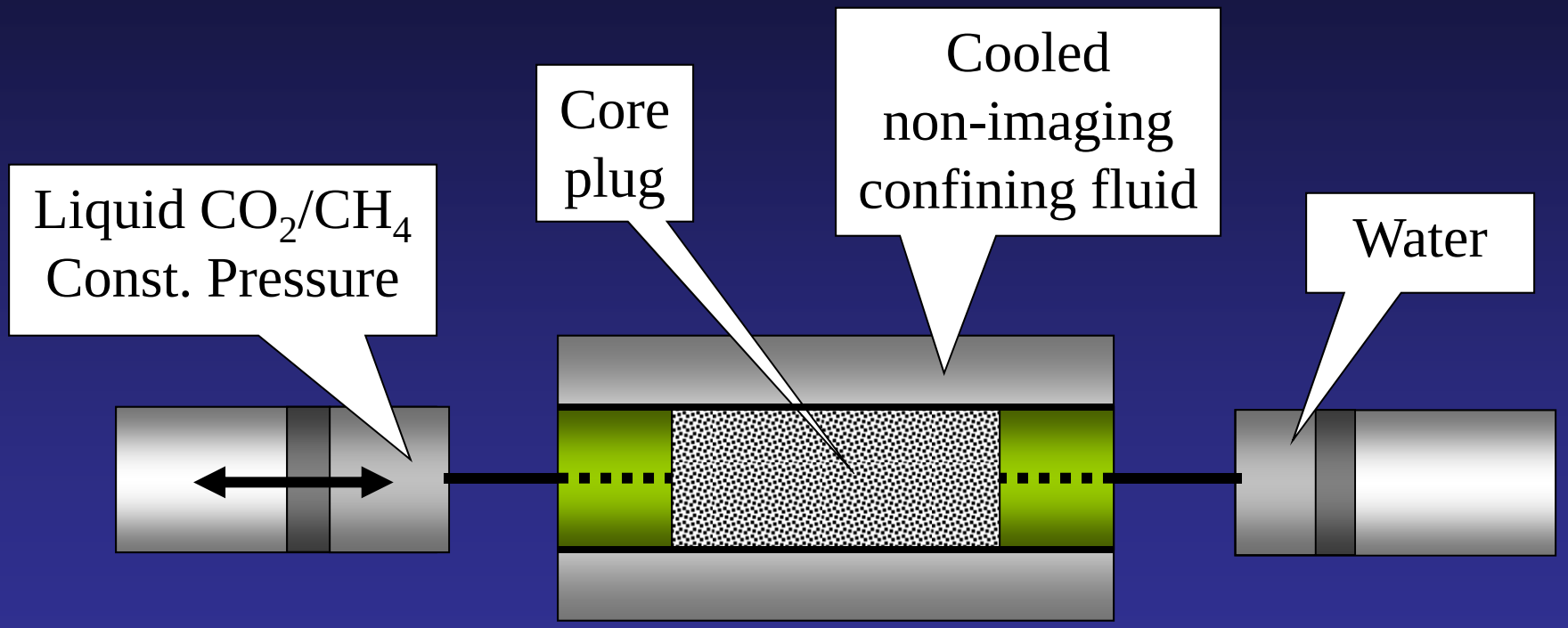

A Bentheimer sandstone core, 4 cm diameter, 10 cm long is embedded into a heat controlled core holder

The hydrogen spin in liquid water and hydrate water is different. Exposing the system to magnetic field and sampling responses gives accurate (relative) feedback on amount of hydrate (invisible water hydrogen)

Permeability System

Additional measurements of pressure drop during hydrate formation gives possibility for recalculation of permeability

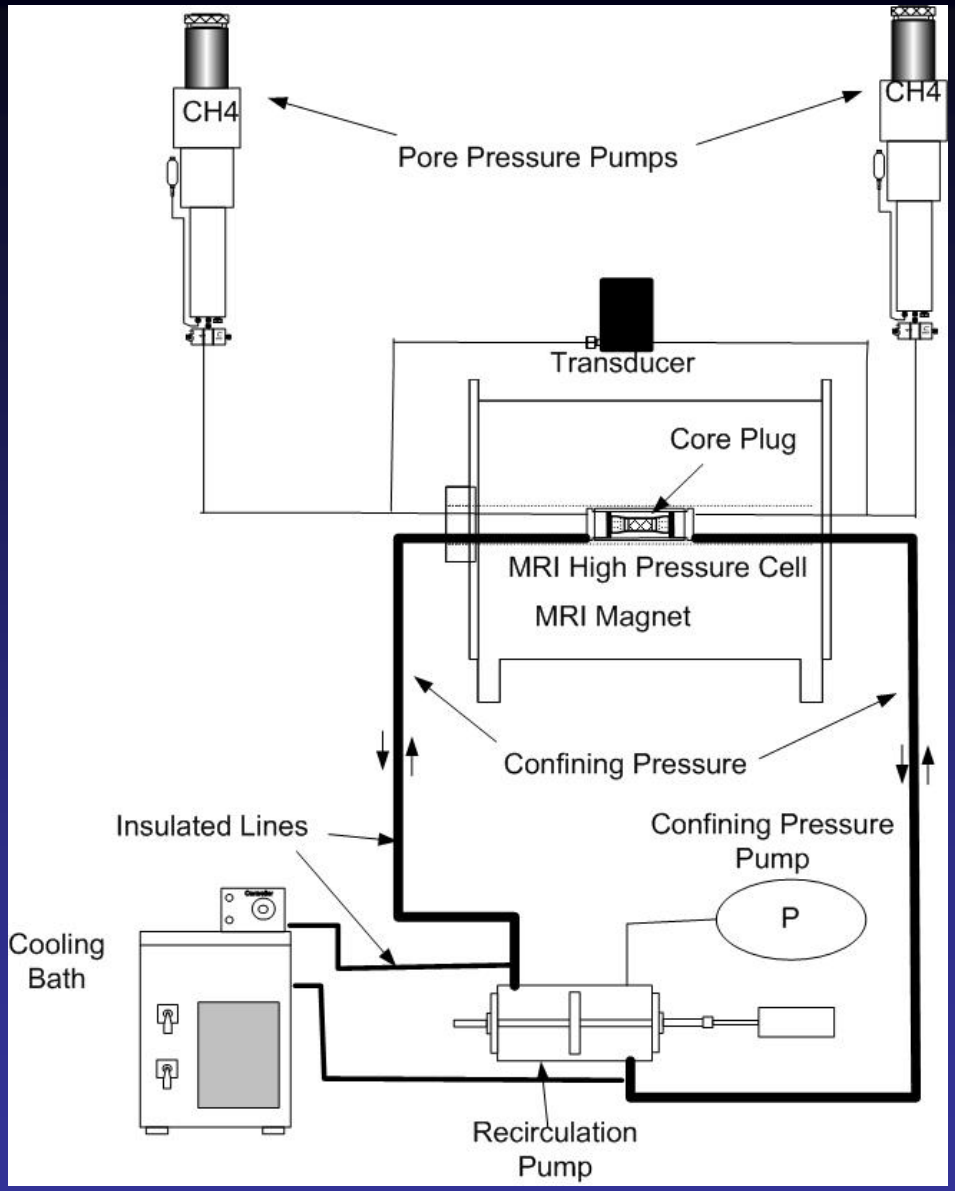

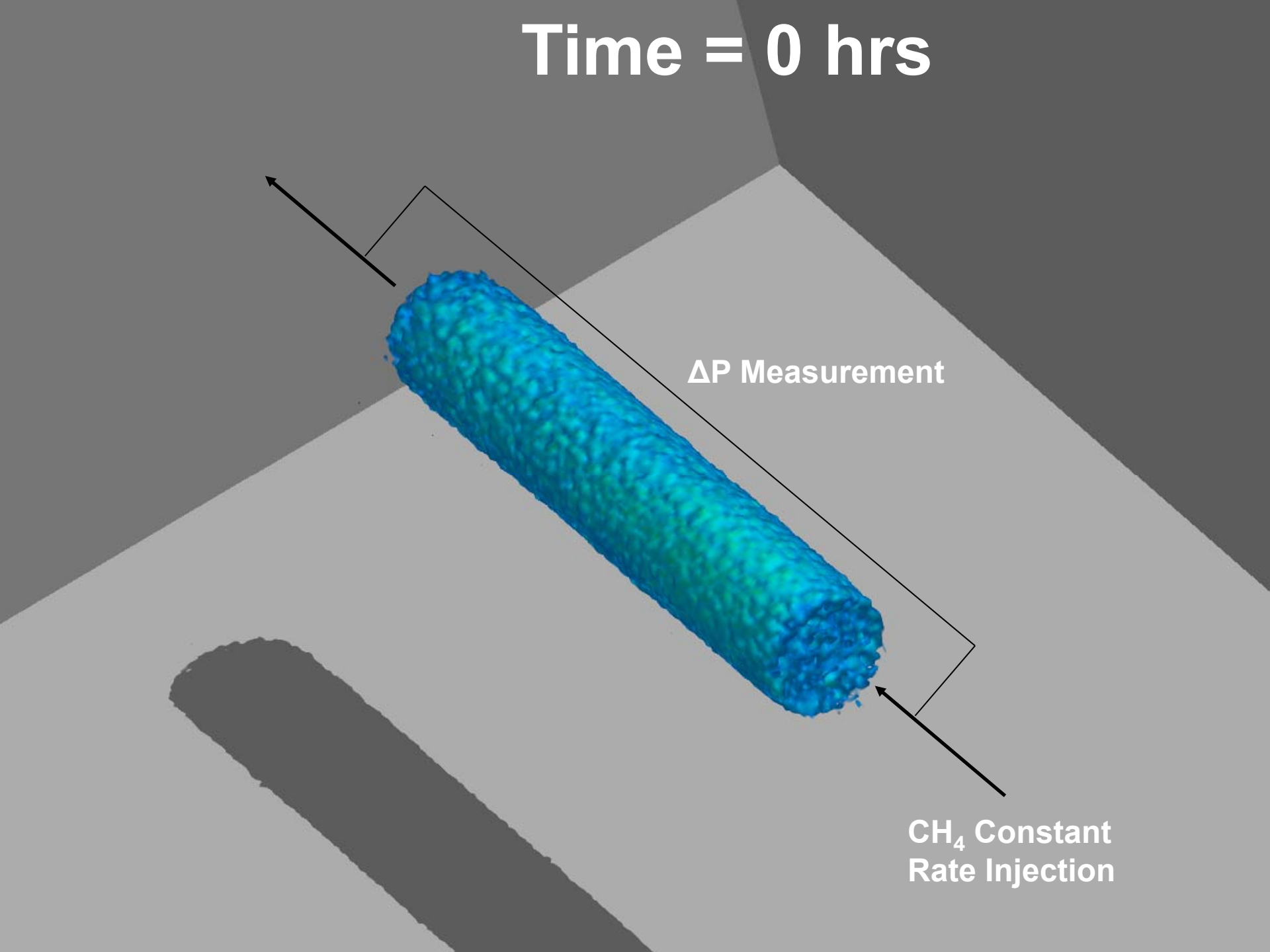
Time = 0 hrs
ΔP Measurement
CH_4 Constant
Rate Injection

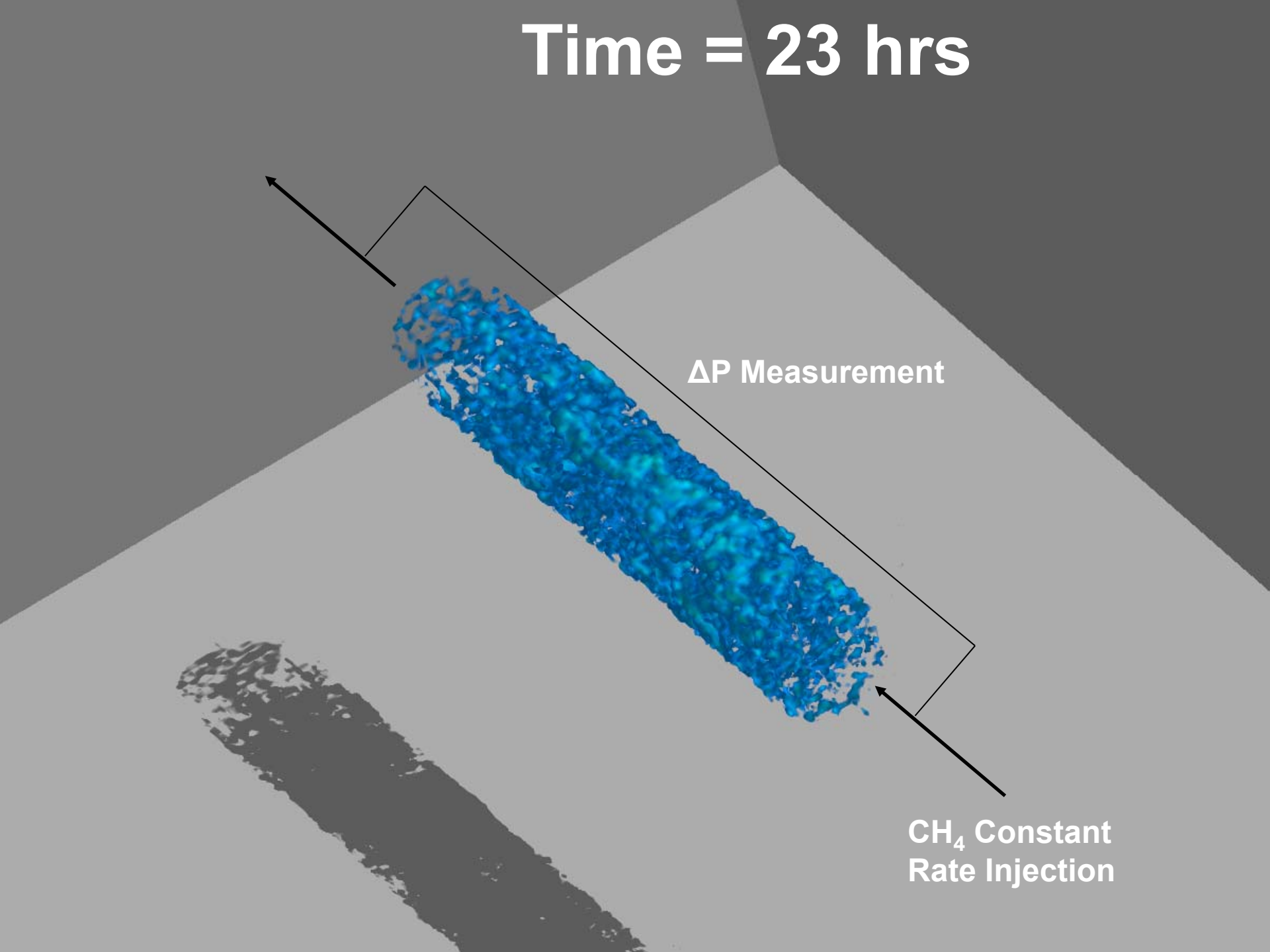
Time = 23 hrs
ΔP Measurement
CH_4 Constant
Rate Injection

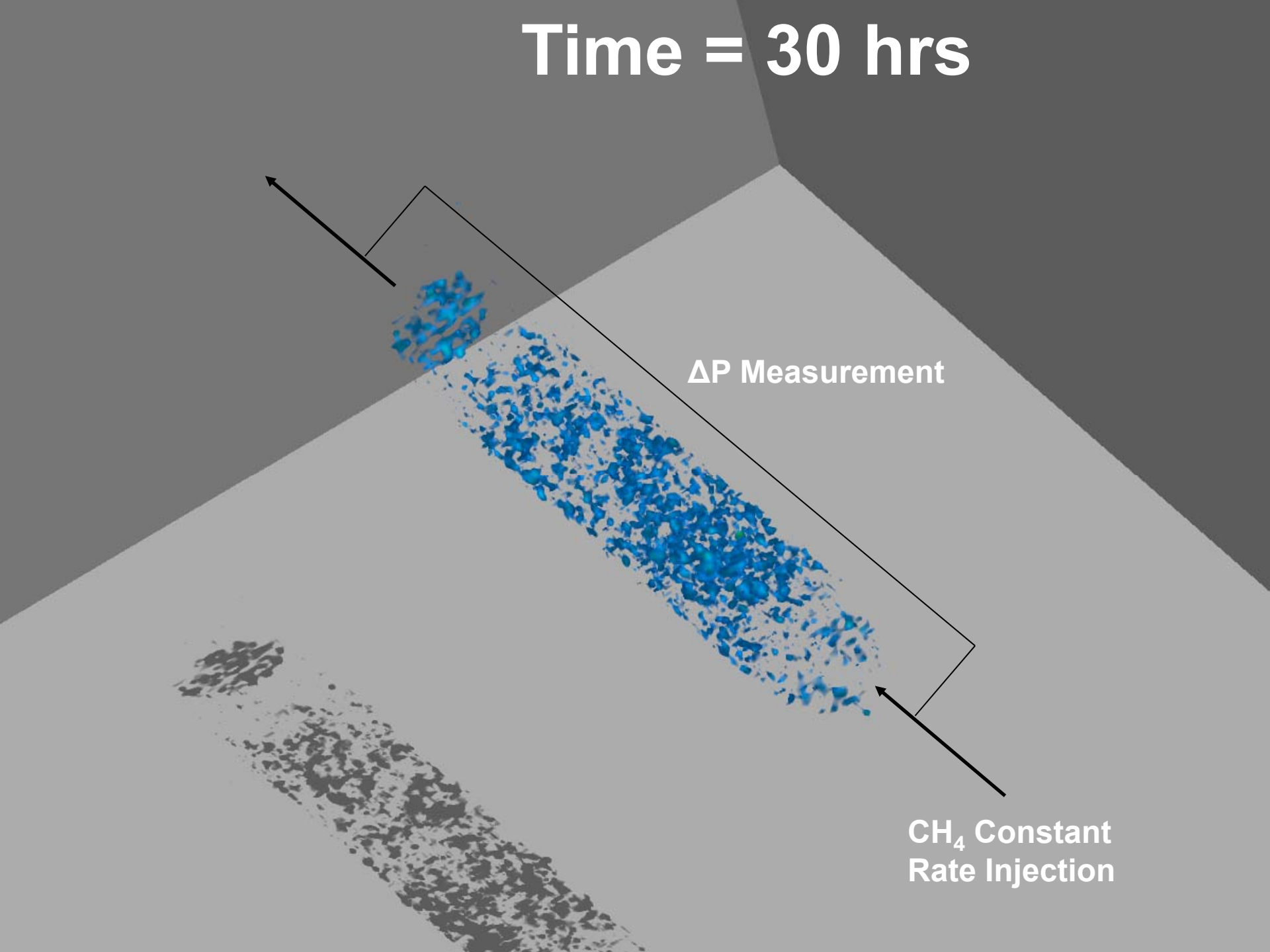
Time = 30 hrs
ΔP Measurement
CH_4 Constant
Rate Injection

Time = 36 hrs

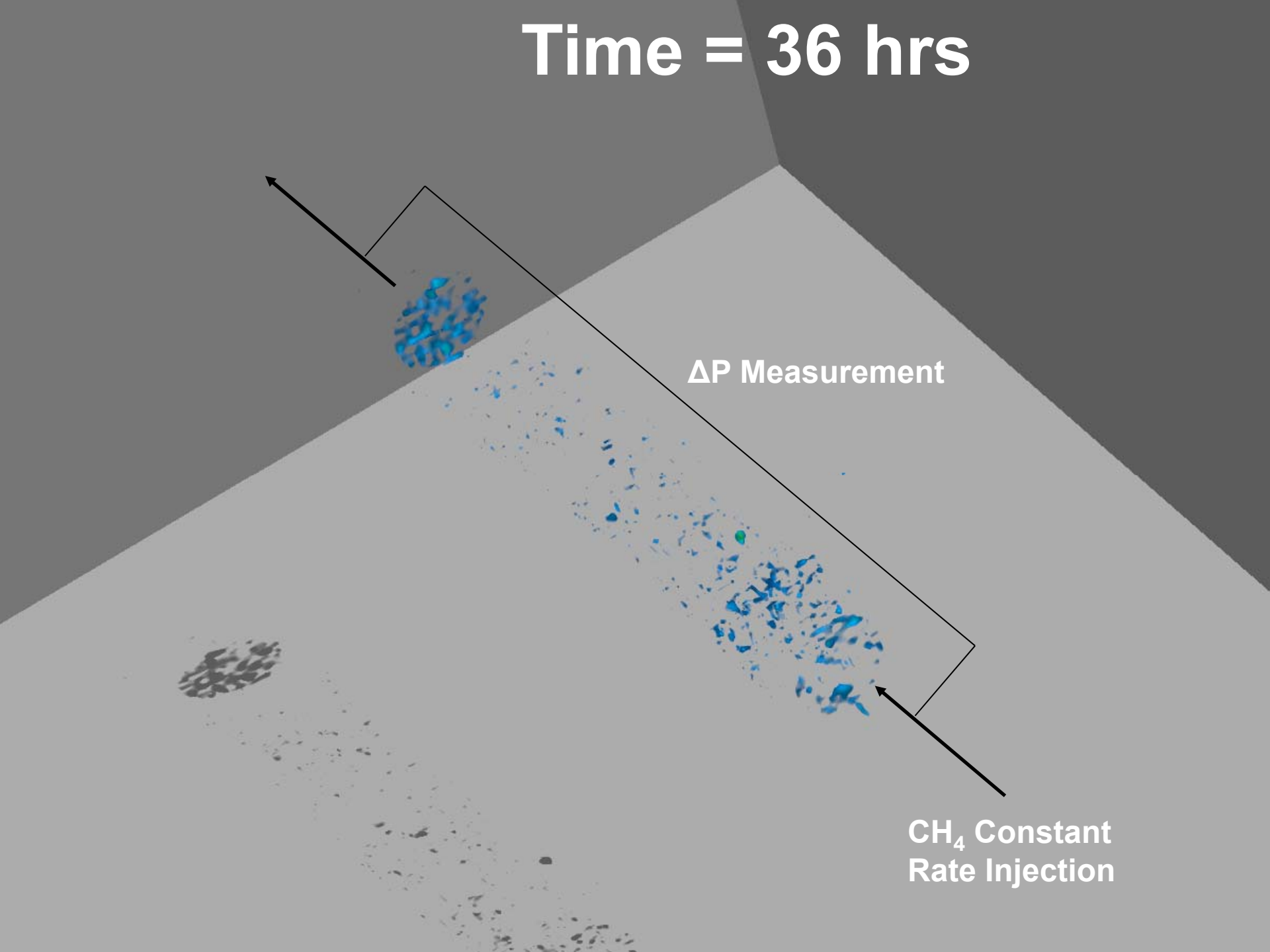

Permeability in Hydrates

- MRI Intensity Loss Indicates Hydrate Formation. Correlates with Permeability Decrease.

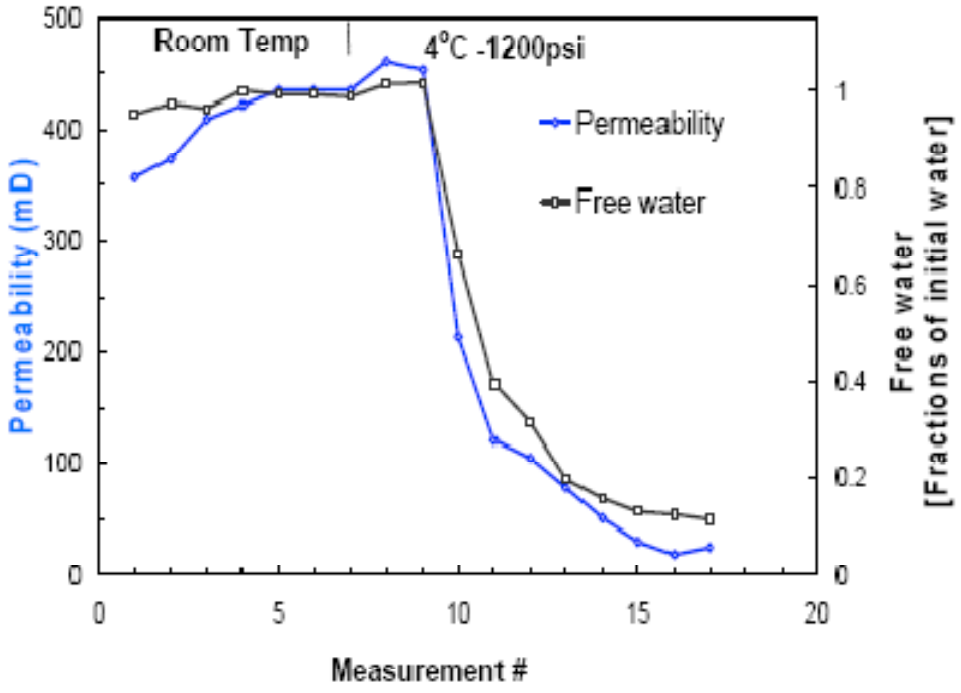

Exp #	$S_w/S_g/S_h$	k_{app}(mD)
1	33/67/0	670
	2/57/41	143
2	34/66/0	410
	11/60/29	217
3	47/53/0	356
	11/44/45	25
4	48/52/0	157
	3/41/56	13
5	51/49/0	115
	4/36/60	4
6	36/64/0	248
	2/40/58	7

”Classical” approaches to hydrate production

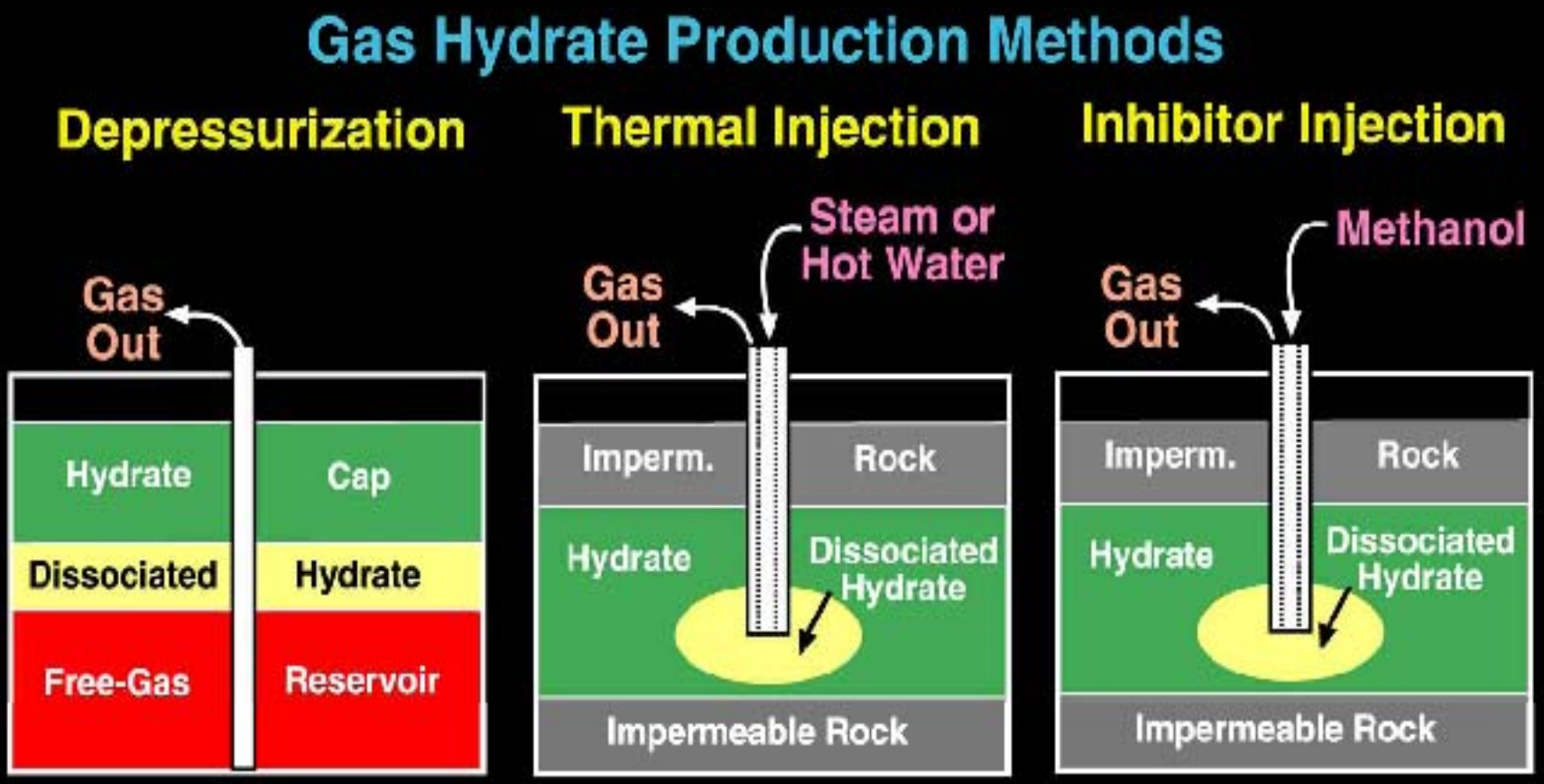

Brings the system out of P,T stability zone but dissociation heat must be supplied from surroundings or added

Dissociation alone costs roughly 5% of produced HC

Costly and require extra processing. Dilution from dissociated water Limits efficiency

Pressure and temperature are only two thermodynamic variable

Pressure reduction

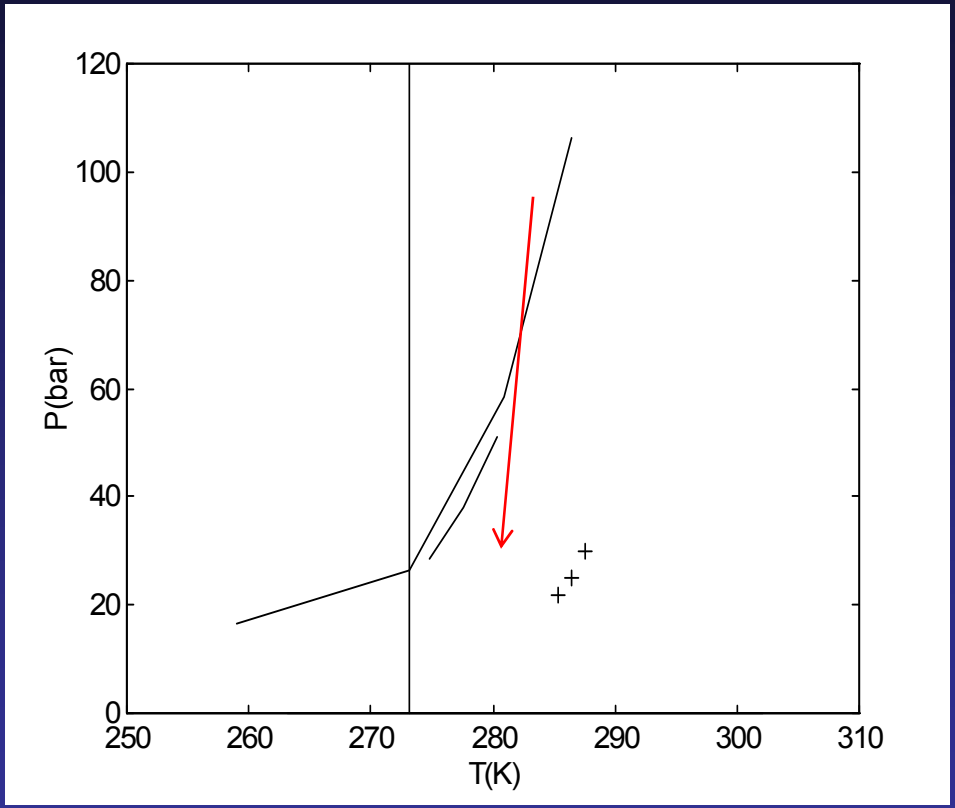

Addition of heat

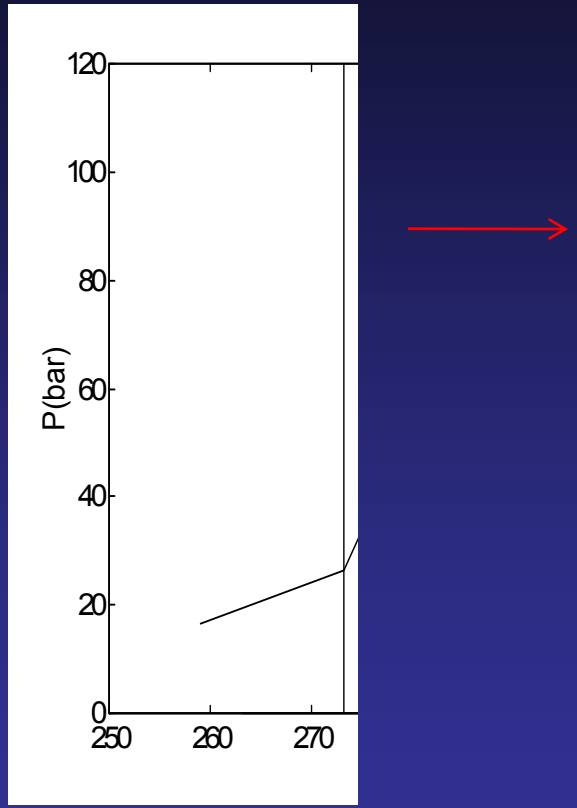

Inside or outside PT curve is just a minimum critera. Surrounding fluid concentrations and properties as well as mineral surfaces (adsorbed phase thermodynamics) are governing factors for hydrate phase transition dynamics

The phase transition dynamics related to different exploitation schemes is a function of mass transport, heat transport and phase transition kinetics

$$\Delta G$$

- *The free energy difference is the driving force for the phase transitions kinetics (see next overheads)*

- *And the corresponding dissociation enthalpy must be transported from the surrounding at kinetic rates determined by the composite (mineral, hydrate, fluid) heat transport properties*

$$\Delta H = -RT^2 \left(\frac{\partial \left[\frac{\Delta G}{RT} \right]}{\partial T} \right)_{P,\bar{N}}$$

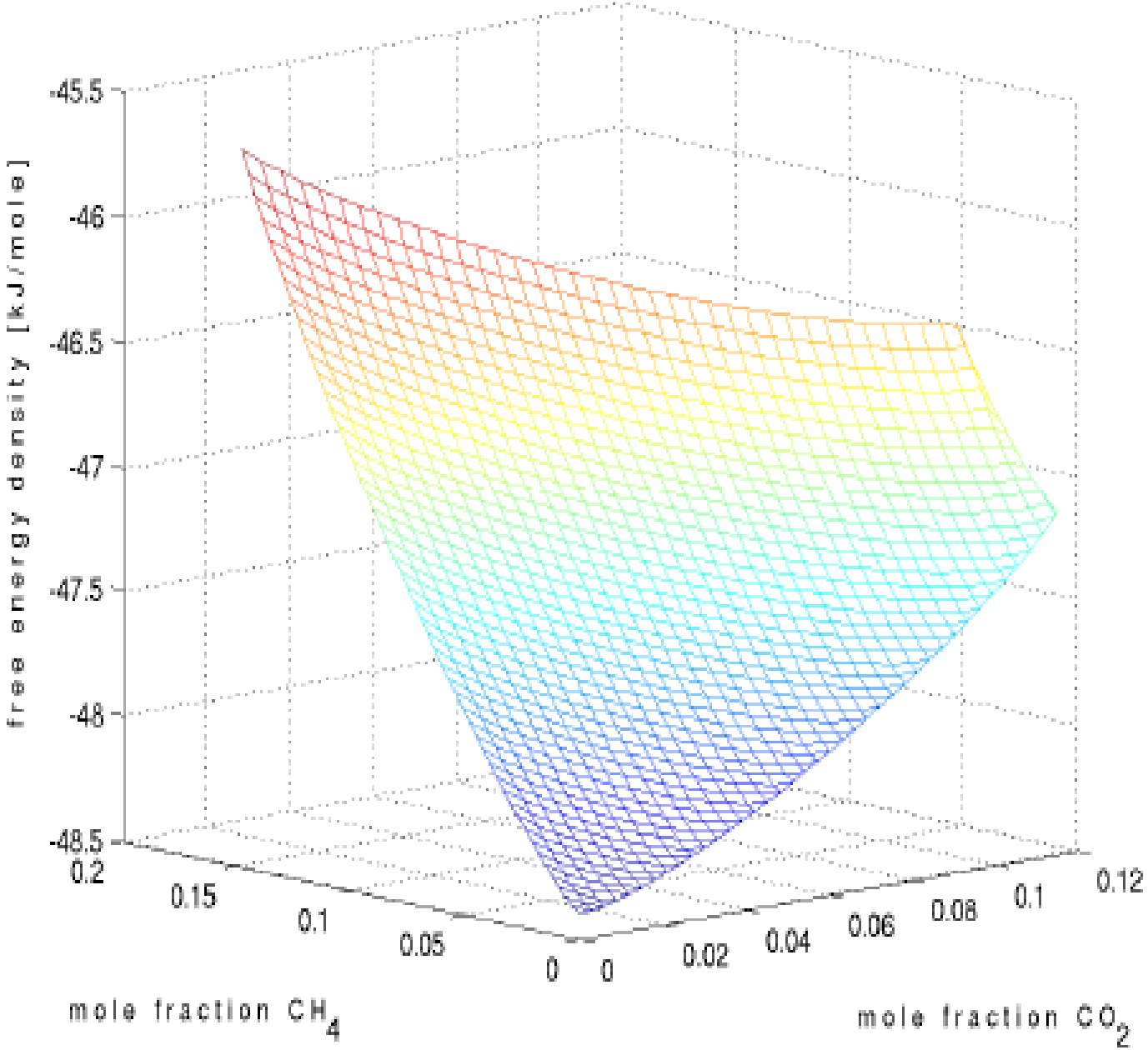

Fig. 1 Free energy density of the hydrate as a function of the mole fractions of CH_4 and CO_2 at 1°C and 40 bars.

CO_2 hydrate is more stable than methane hydrate

The free energy profile is constructed from MD simulations (Kvamme & Tanaka,1995) and verified to reproduce experimental stability regions (Svandal et.al., 2006)

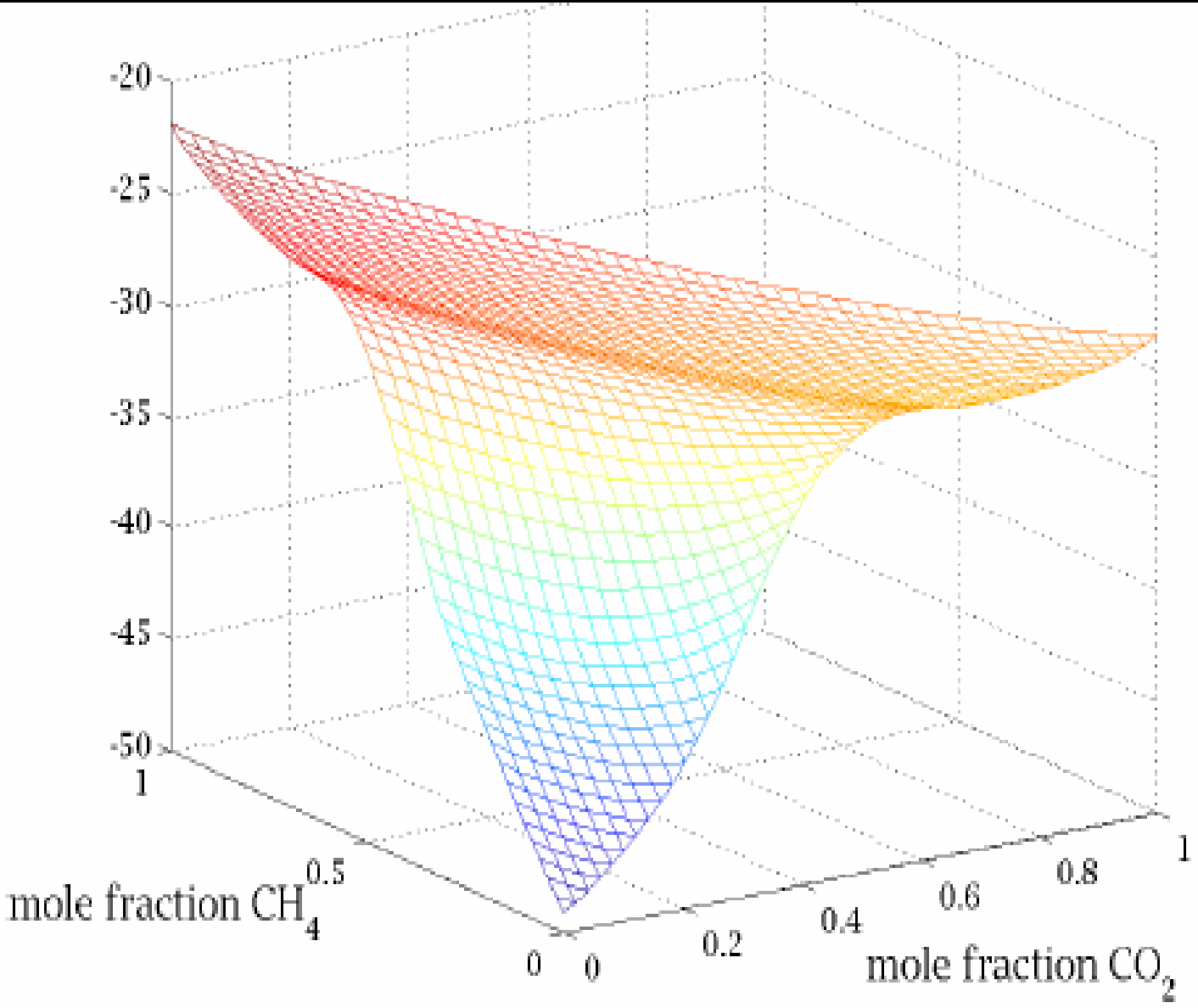

Fig. 2 Free energy density (kJ/mole) as a function of the mole fractions of CH_4 and CO_2 at 1C and 40 bars.

CO2 hydrate equilibrium pressures

Squares :experimental data
Solid line: predicted results

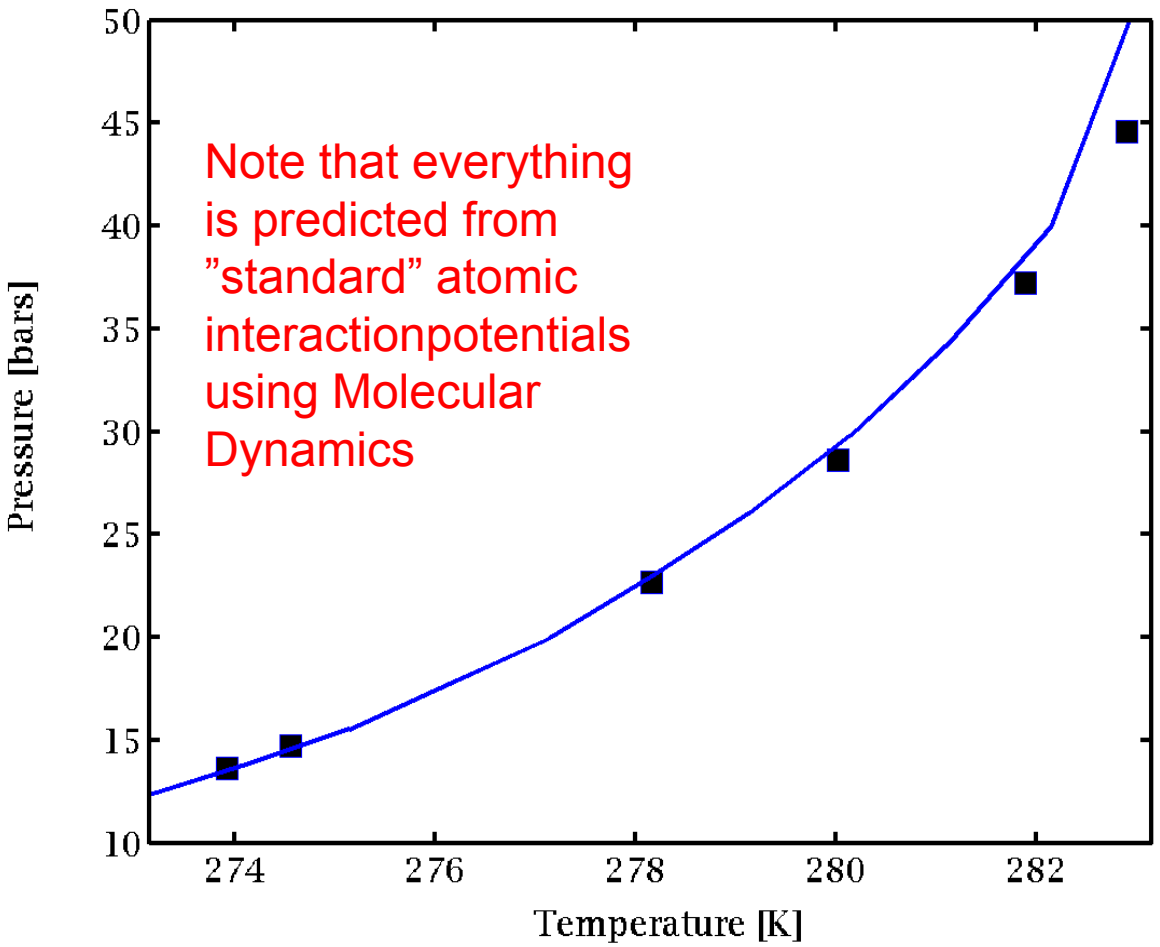

References:

Svandal, A., Kuznetsova, T., Kvamme, B., Physical Chemistry Chemical Physics, 2006, **8**, 1707 - 1713

Svandal, A., Kuznetsova, T., Kvamme, B.,, 2006,Fluid Phase Equilibria, 2006, 246, 177-184

Kvamme, B. & Tanaka, H.,1995, J.Phys.Chem., 99, 7114

Before discussing exploitation schemes we need to look at the most relevant situations

- ***Type 1*** hydrate occurences

  Hydrate on top of liquid water and a gas cap facing the hydrate

- ***Type 2*** hydrate occurences

  Hydrate on top og liquid water with no free gas

- ***Type 3*** hydrate occurences

  Solid hydrate without any contacting fluid

Type 2 and 3 hydrates

- Hydrate is generally not stable toward liquid water undersaturated with hydrate former (realtive to free energy of hydrate!)
- The consequence is that hydrate sections might be interrupted by liquid water sections due to substantial fluid flow (dilution of fluids surrounding hydrate structures) in these regions
- Type 3 hydrates are more common in systems where shale or clay layers separate hydrate blocks

Some very general factors

- Stability of hydrates is very sensitive to temperature – which practically implies that ***efficiency of hydrate exploitation increases with higher in situ temperature.***
- *Production potential increases with intrinsic and relative permeability*

Type 1 hydrates and ***pressure reduction approach***

- Pressure reduction is feasible but slow
- Efficiency can be improved through local fracturing
- Kinetics of hydrate dissociation likely to be dominated by heat transport limitation from surroundings in order to supply the dissociation enthalpy needed

Knowledge gaps and limitations

- *Heat transport dynamics is fairly complex and no satifactory models available*
-
- *Depressurisation reduces temperature and may lead to refereezing and in the worst case also ice formation*

Knowledge gaps and limitations continued

- *It remains unverified how much of the released water that will be transported with the gas*
- *Most efficient exploitation from uncosolidated sediments with significant porosity but this type of sediments are also more sensitive to potential geomechanical implications of the volume reduction (~ 10%) by dissociation of hydrate*
- *Efficiency depends sensitively on types of producuing well(s) (horizontal or vertical)*

Addition of heat?

- Some limited additional heat is necessary anyway to keep producing lines free of possible refrozen hydrate and/or ice.
- Injection of heat through steam or brine is possible but involves heat losses beyond the 5% of reduced hydrocarbon value involved in the dissociation alone.
- System of heat injection wells and possible local fracturing determines efficiency together with heat transport properties of the total system

Injection of inhibitor?

- Injection of inhibitor can also be used as alternative to heat in order to keep production channels open but then again requires corresponding separation facilites of separating inhibitor from produced water.

Summary

- Type I hydrate structures are fairly easy to produce by means of pressure reduction, which will simultaneously produce the free gas below
- And except from strategies for preventing reformation of hydrate and/or ice formation the system does not require any new or special technology
- But geomechanical considerations are needed since primary targets are unconsolidated sand hydrate systems

Type 2 hydrate

- Pressure reduction with/without addition of heat is possible but significant production of water can not be avoided.
- Efficiency still unverified due to limitations in description of hydrate dissociation dynamics.
- Horisontal producing wells will be an efficient completion and no special technology is needed for producing these hydrates

Type 2 hydrate cont.

- Dissociation rates will be low but can be increased by local fracturing as well as chemical injection
- This type of situation is also an ideal target for exploitation though CO2 injection, as will be explained later

Type 3 hydrate

- As discussed earlier there is no unique type 3 hydrate.
- It all depends on the actual permeability due to the state of dynamics (”tight” reservoirs with little fluid flow to dynamic reservoirs with substantial fluid flow)
- Dynamic reservoirs with significant permeability can be produced by pressure reductionwith the aid of some local fracturing to increase exposed hydrate surfaces and increase average permeability

Alternatives?

- Chemical injcetion is possible for type 2 and all ranges of type 3 hydrates but is not likely to be economically feasible
- Injection of carbon dioxide
- Injection of flue gas

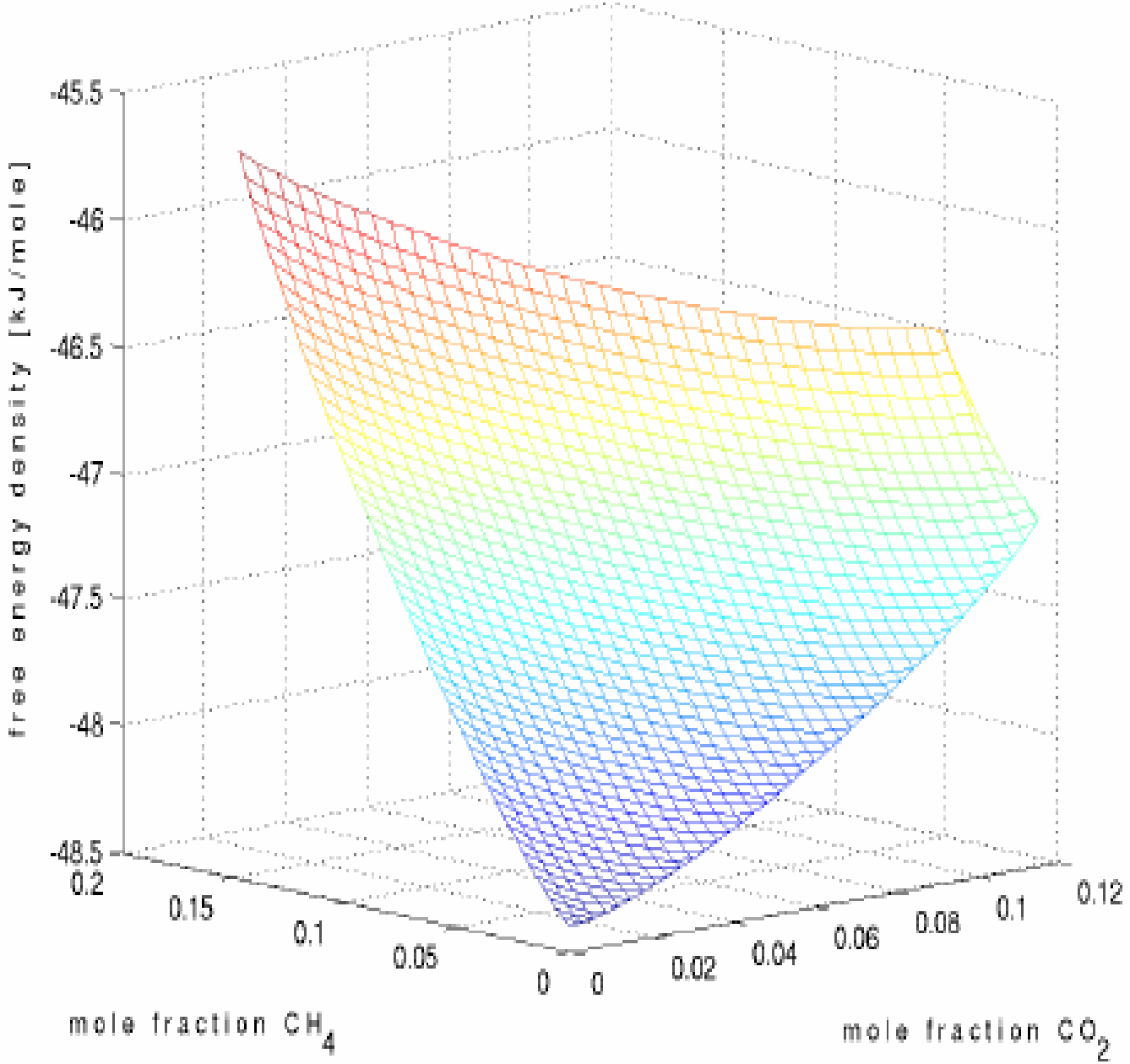

Fig. 1 Free energy density of the hydrate as a function of the mole fractions of CH_4 and CO_2 at 1°C and 40 bars.

Storage of CO2

and

exploitation of hydrate reservoirs?

Can it be experimentally verified that this will practically work in porous medium?

Project Objective

Experimentally Verify:

- Sequestering Greenhouse Gas (CO_2)
  - Determine hydrate formation and distribution
- Gas Production from Hydrates
  - Determine the rate of CO_2-CH_4 exchange

Numerically Predict:

- The hydrate reformation and gas production

Experimental Approach

Use Magnetic Resonance Imaging (MRI) to Image the Formation and Dissociation of Gas Hydrates In Porous Media.

Hydrate Experiments Setup

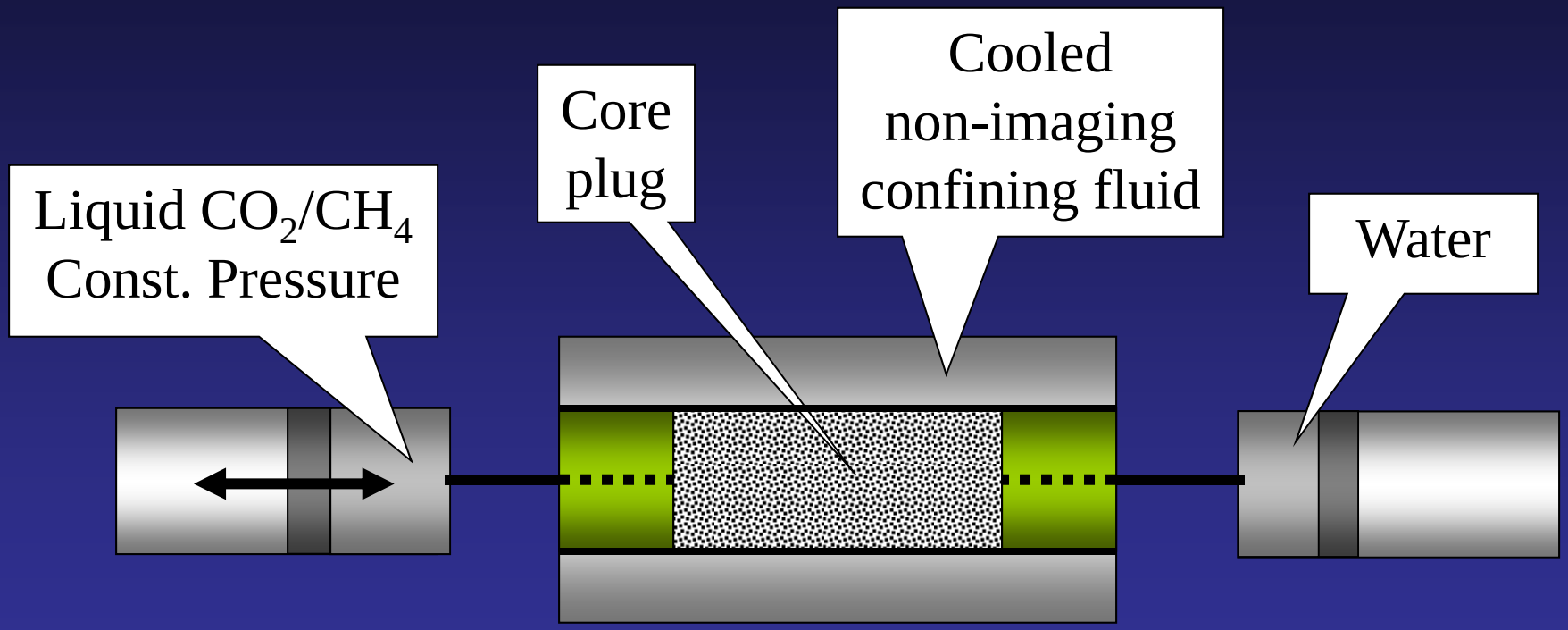

Experimental Setup

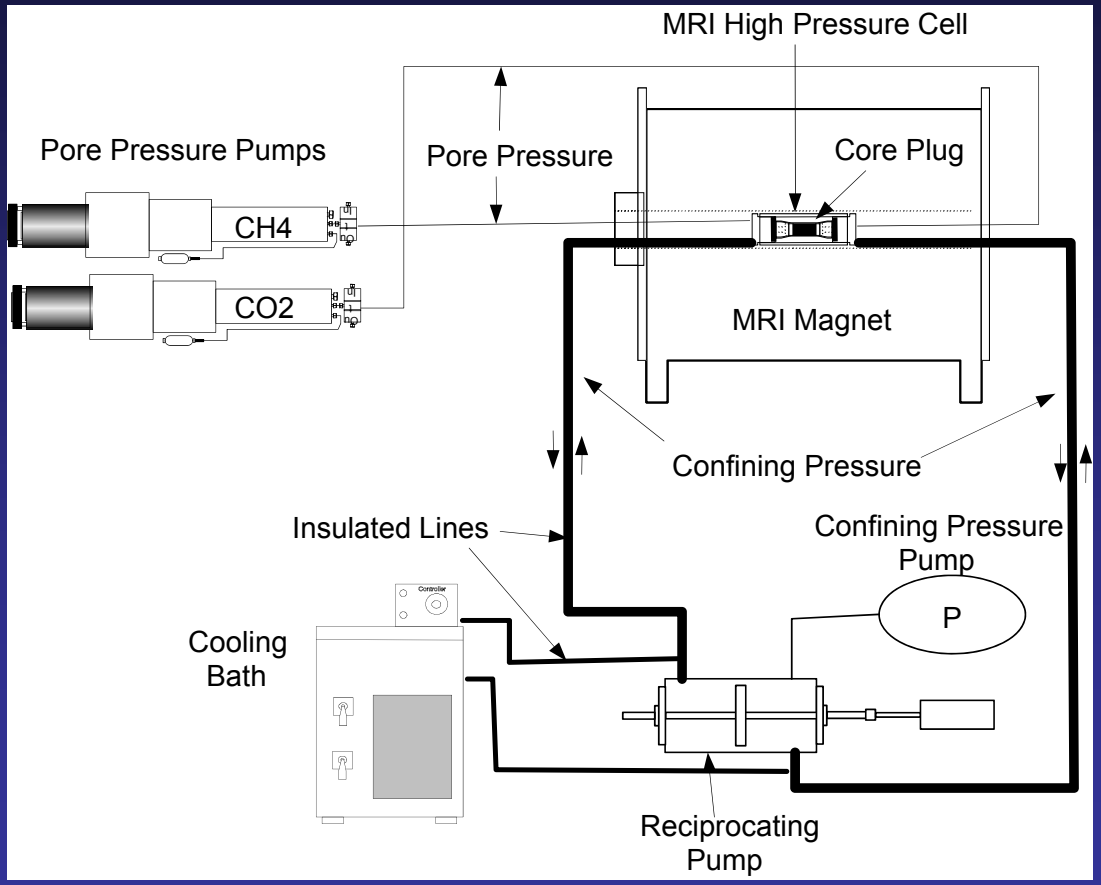

Experimental Setup

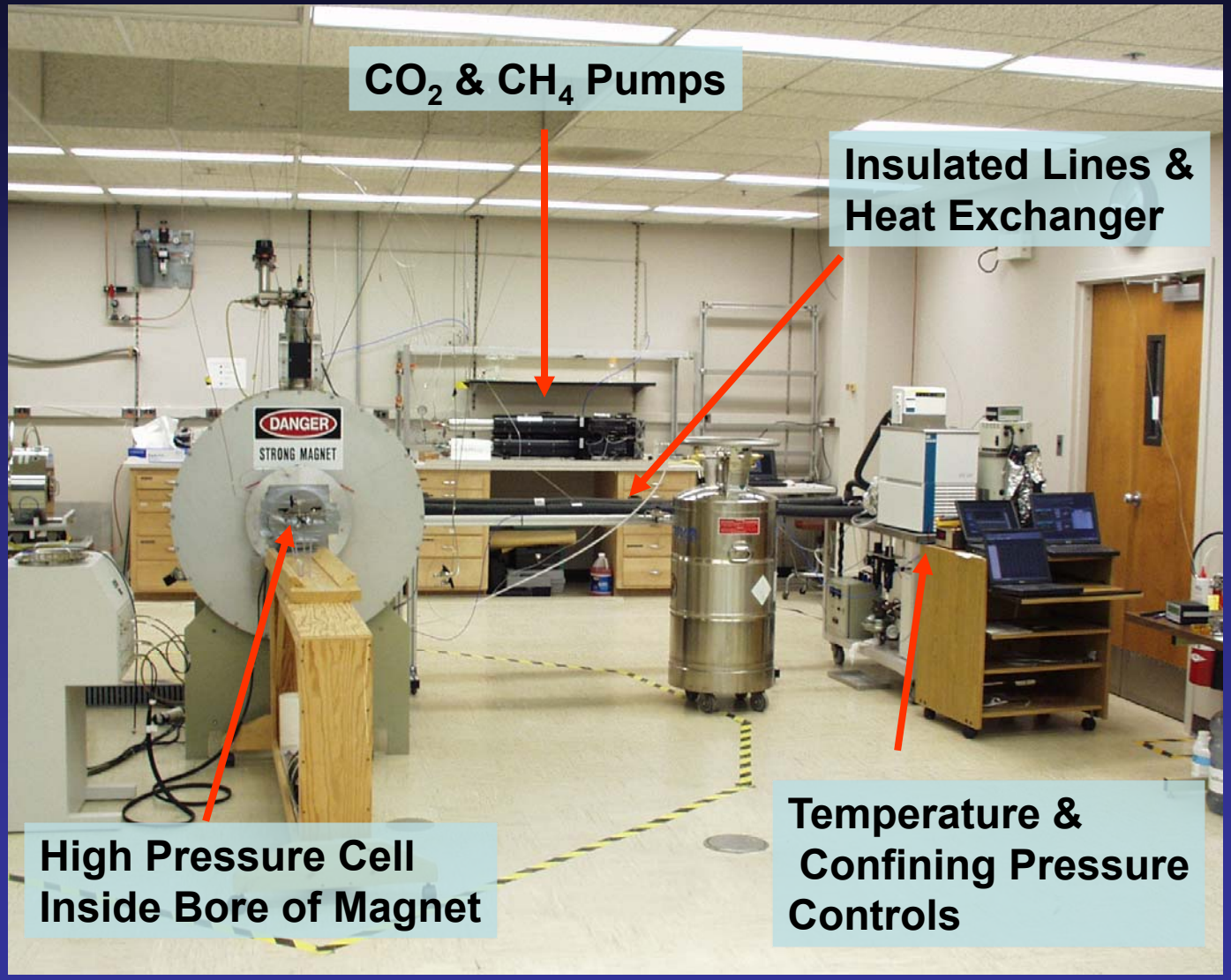

Core Sample Design

- Bentheim Sandstone – Water-Saturated
- Longitudinal Cut – Fitted Spacer Simulates Open Fracture
- Experimental Conditions:

  Flow Loop ~ 4^{o}C – 8.3 MPa *(1200 psi)*.

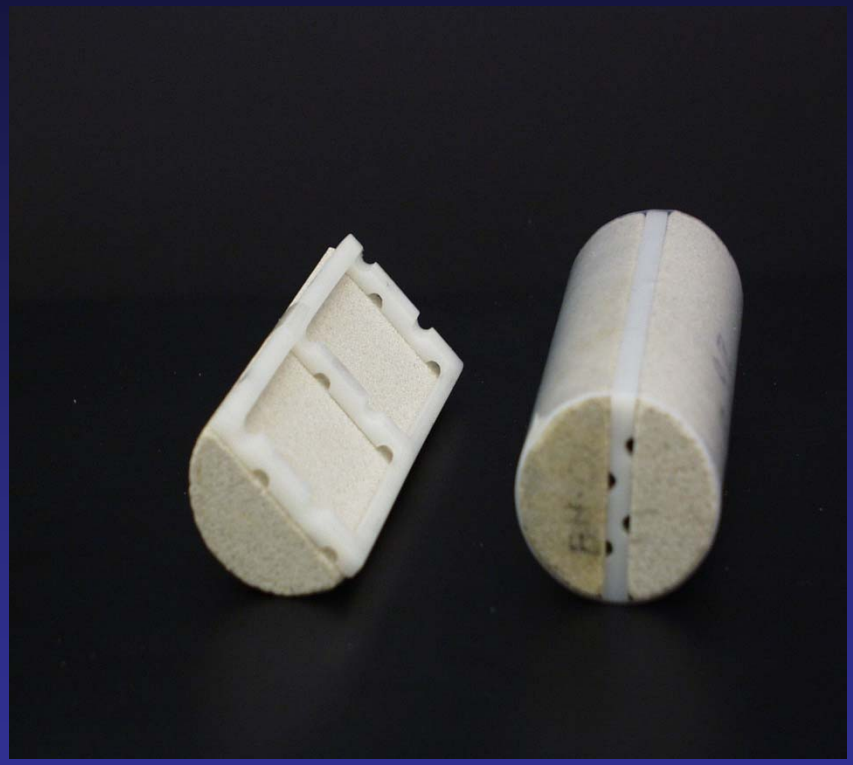

Sample – BH-01

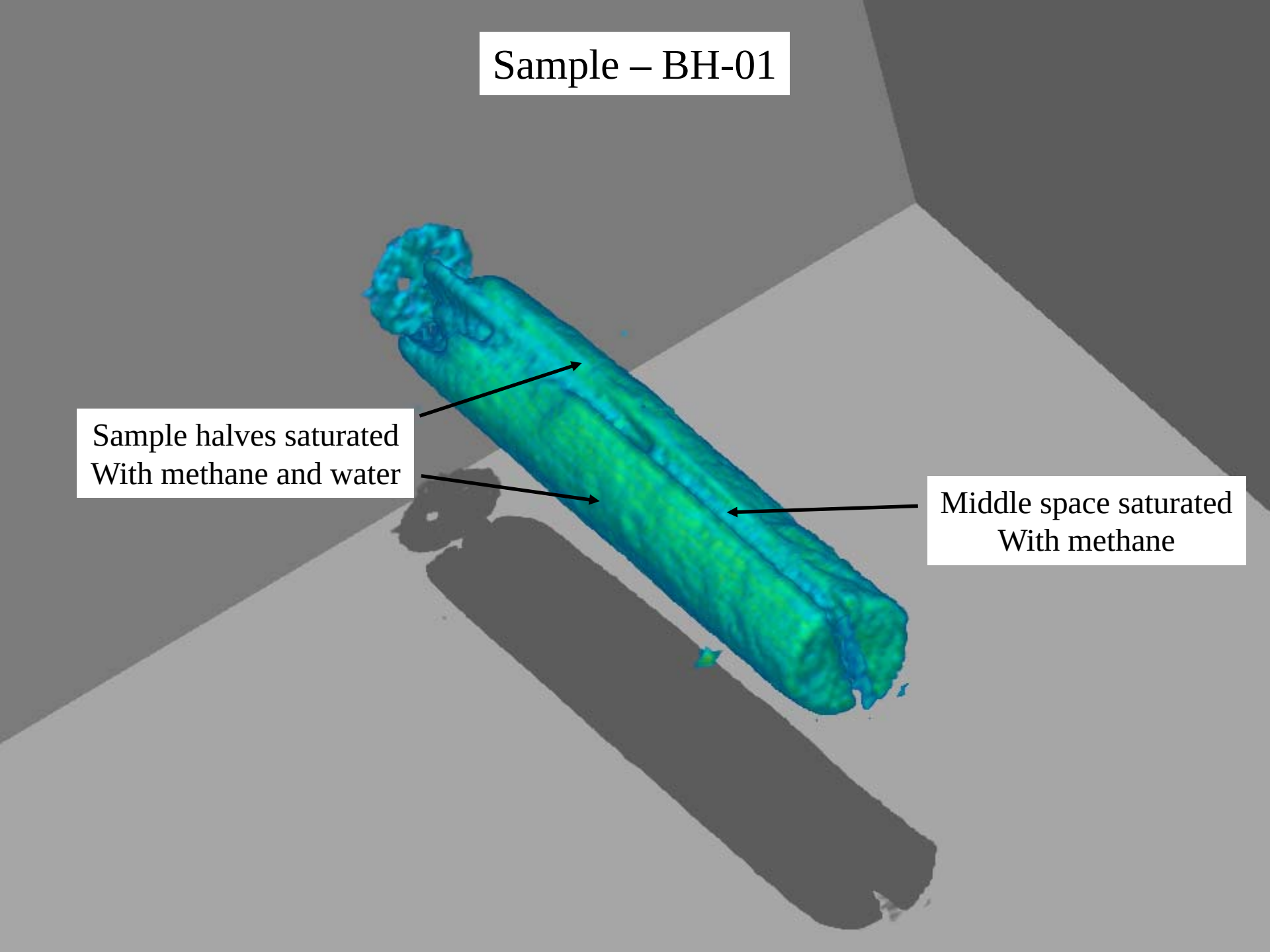
Sample halves saturated
With methane and water
Middle space saturated
With methane

Sample – BH-01

Run – 17-39

Time – 0min

Started cooling sample
To 4^0 C

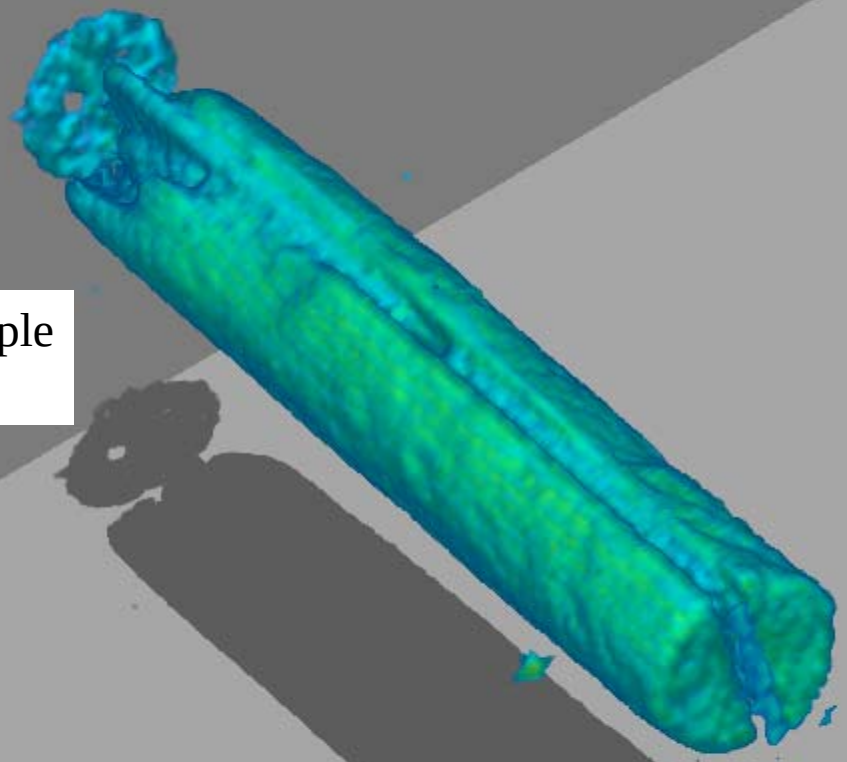

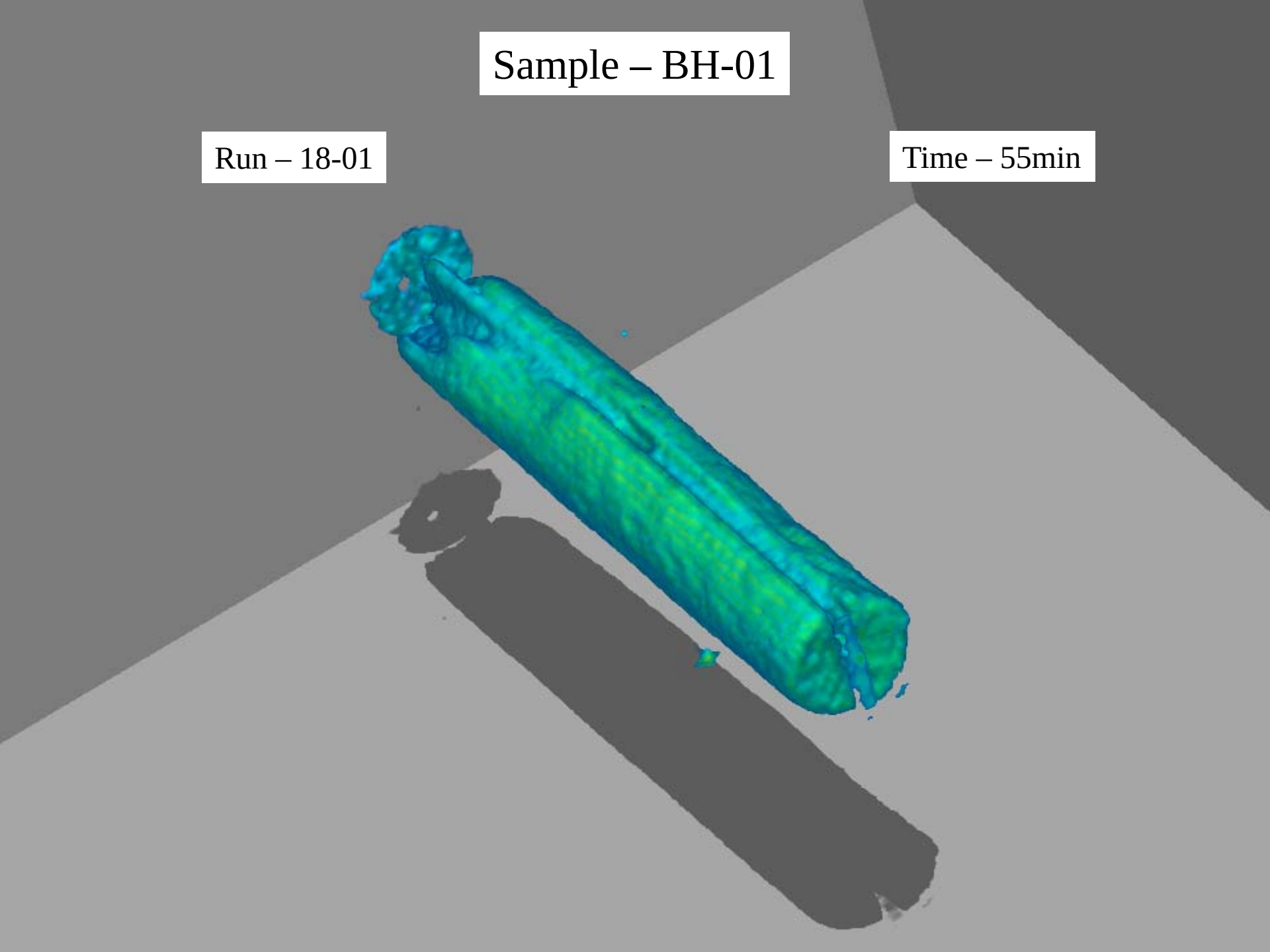
Sample – BH-01
Run – 18-01
Time – 55min

Sample – BH-01

Run – 18-03

Time – 2hr 45min

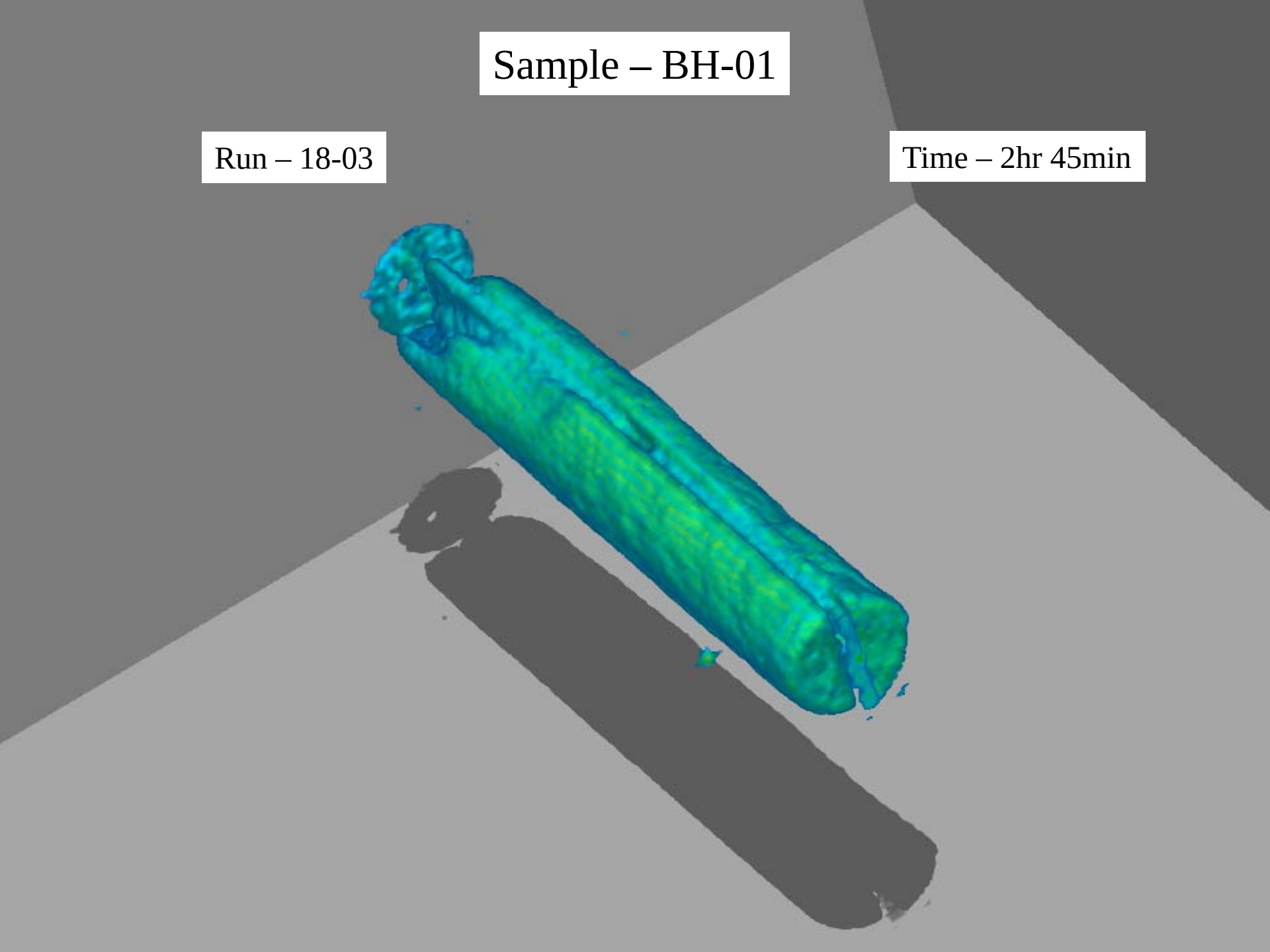

Sample – BH-01

Run – 18-05

Time – 4hr 35min

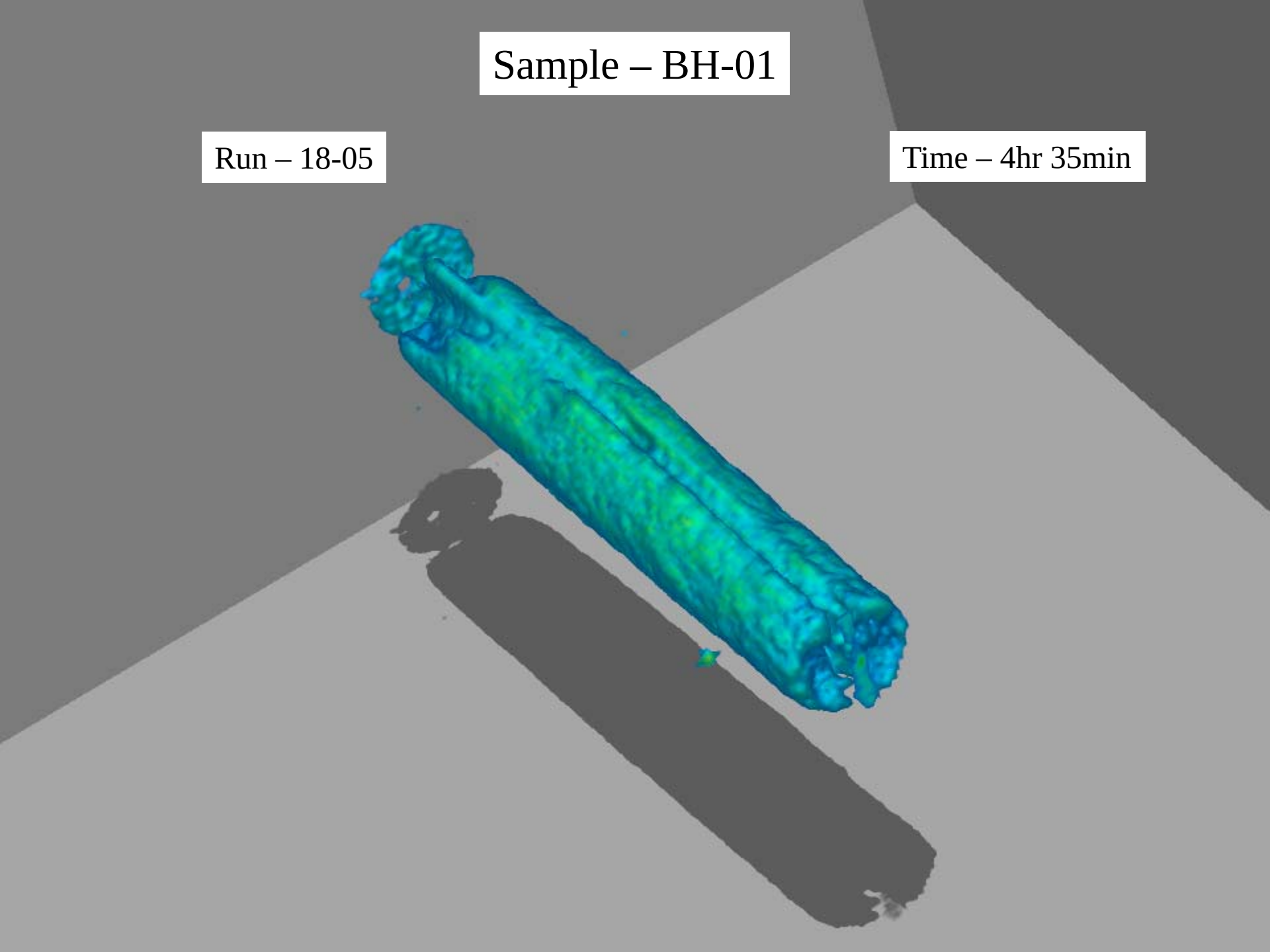

Sample – BH-01

Run – 18-06

Time – 5hr 30min

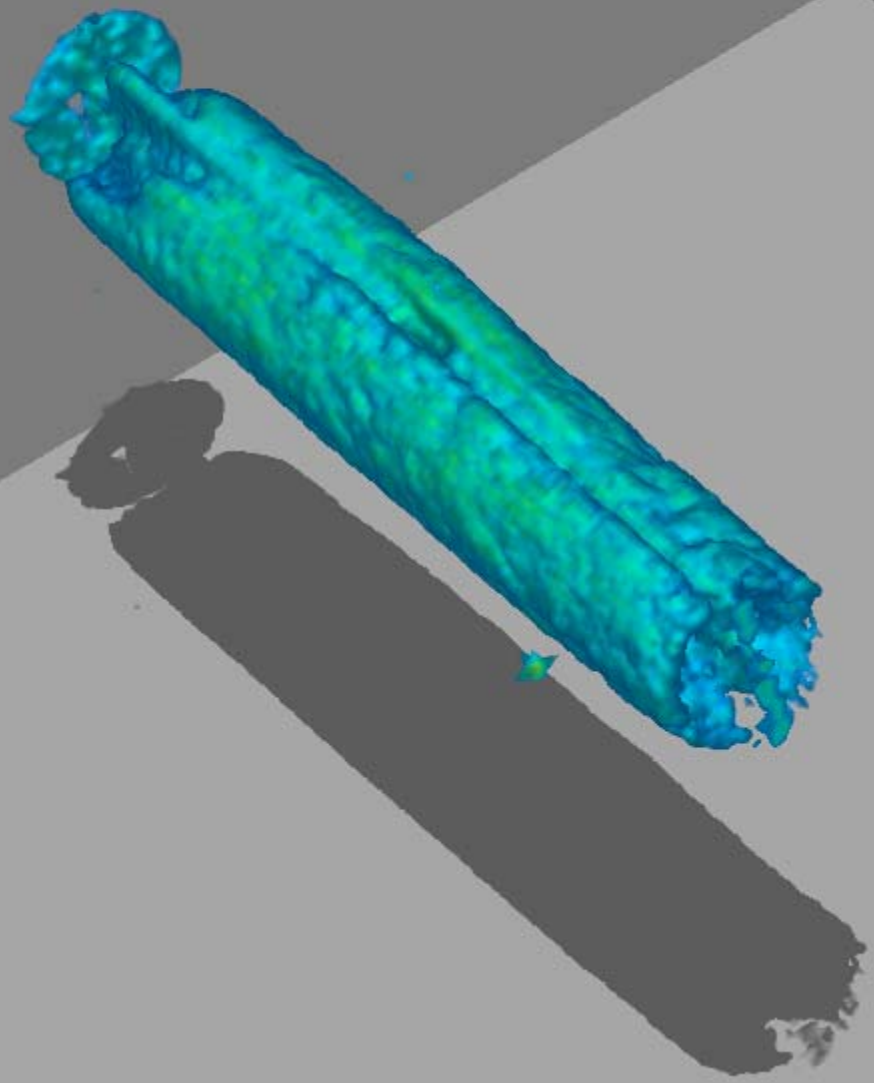

Sample – BH-01

Run – 18-07

Time – 6hr 25min

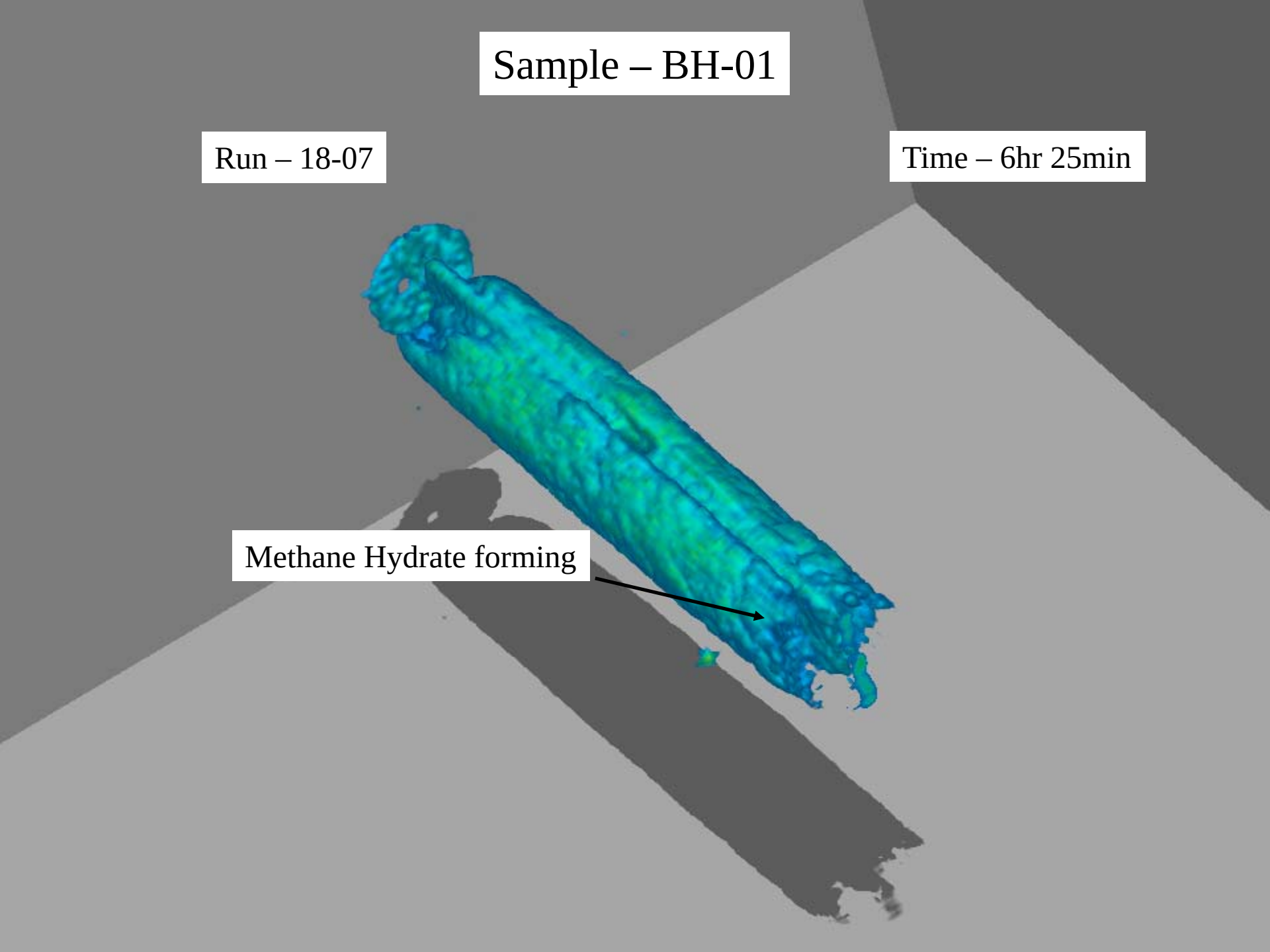

Sample – BH-01

Run – 18-08

Time – 7hr 20min

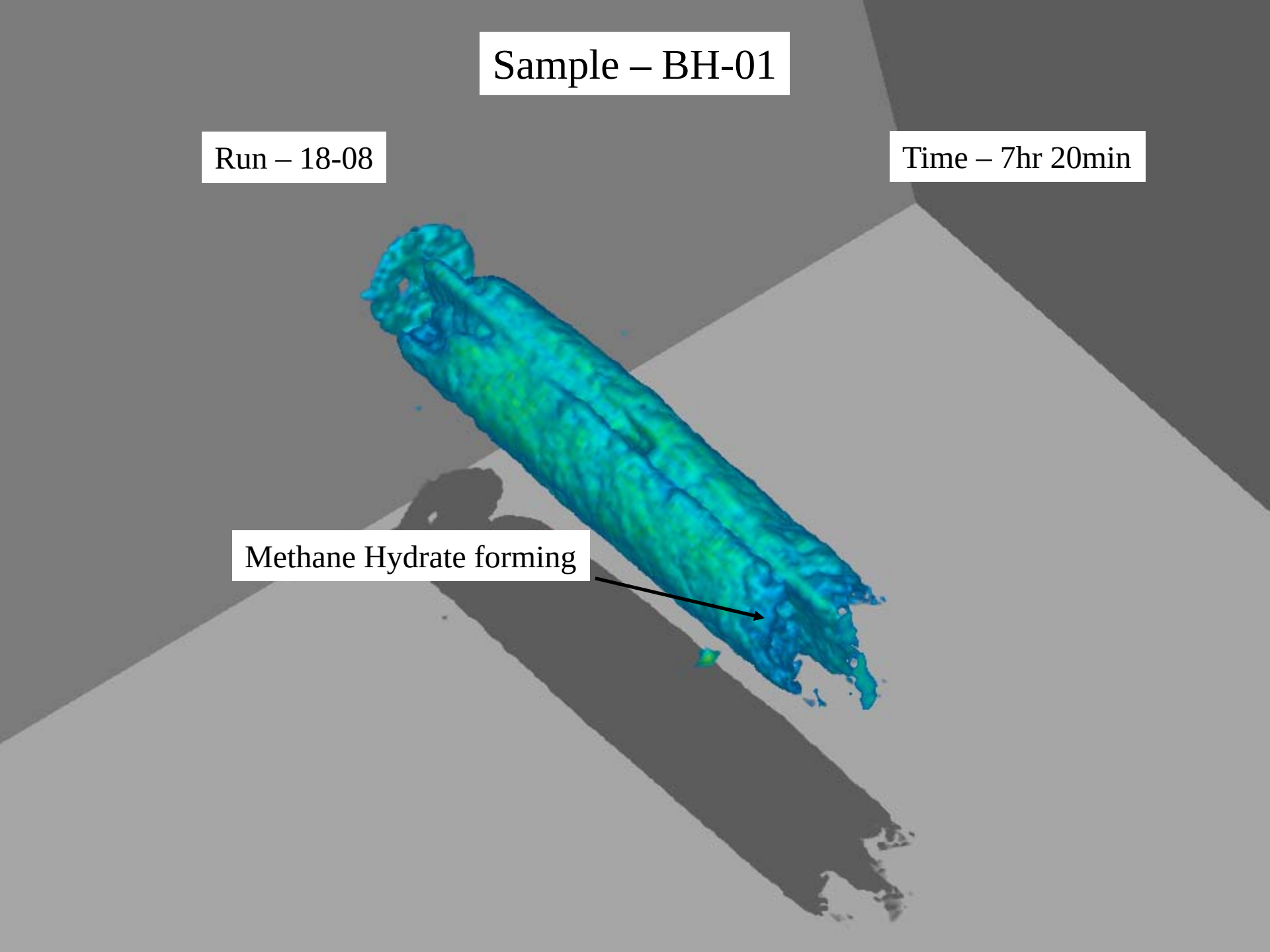

Sample – BH-01

Run – 18-09

Time – 8hr 15min

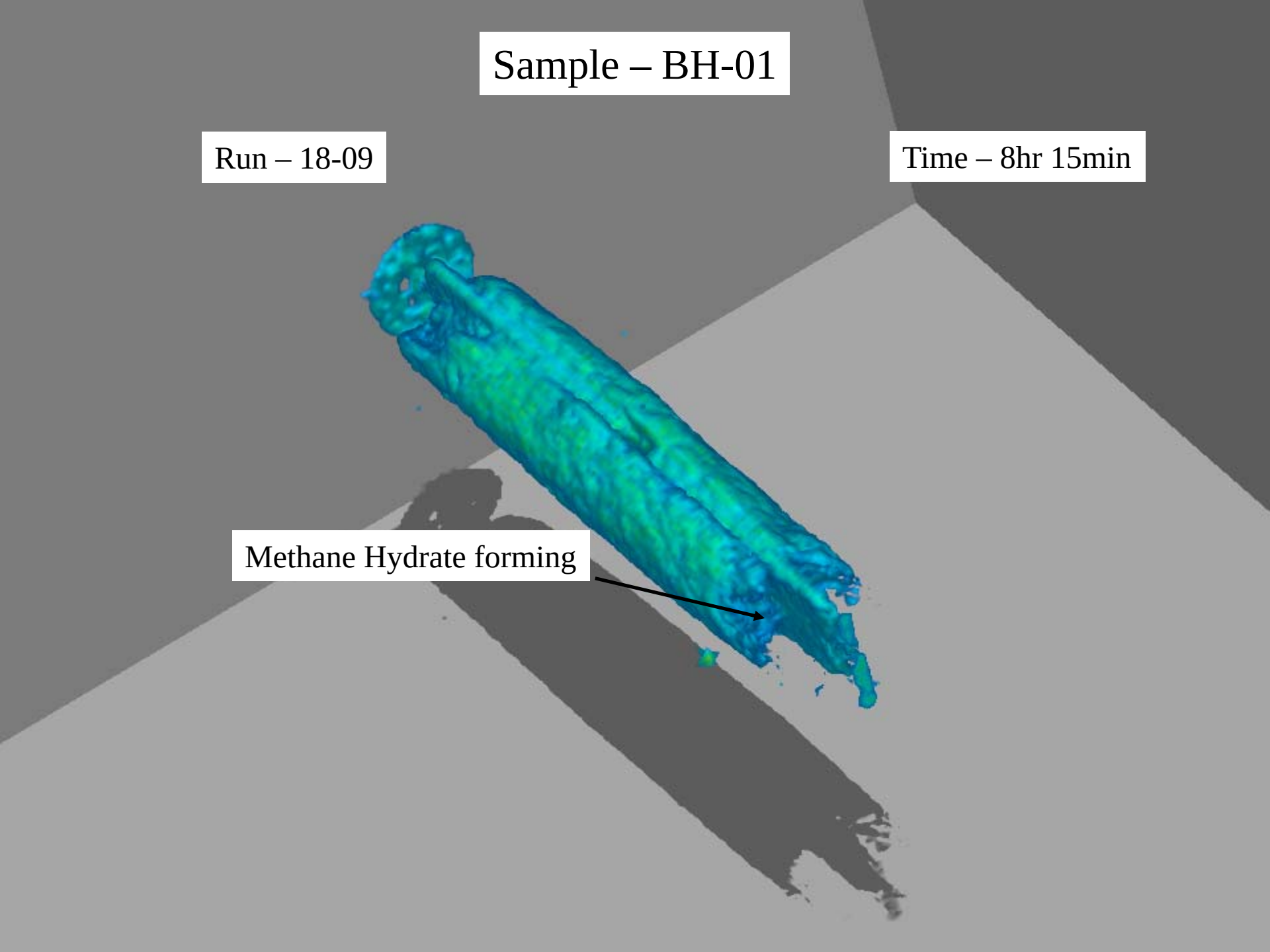

Sample – BH-01

Run – 18-10

Time – 9hr 10min

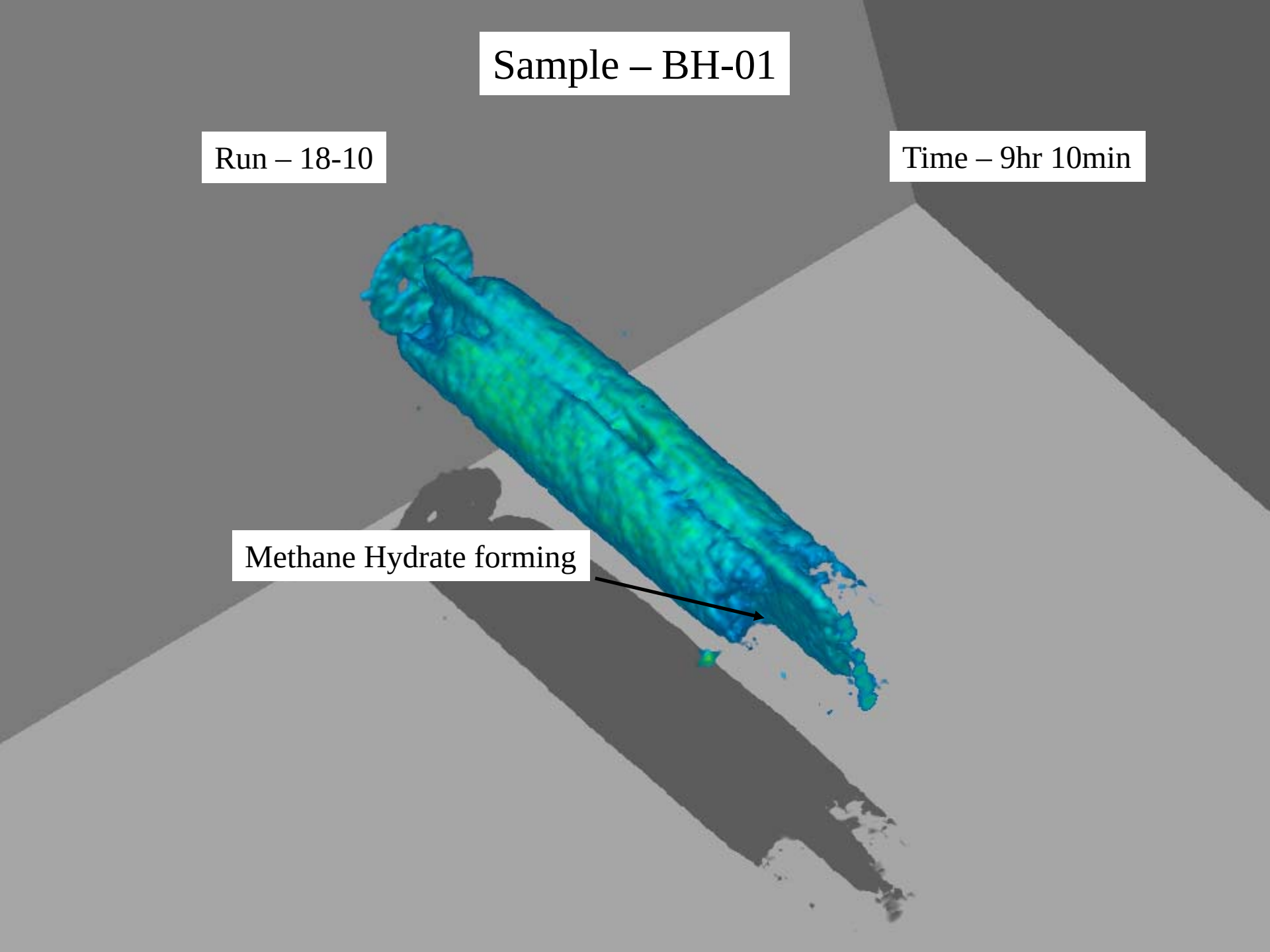

Sample – BH-01

Run – 18-11

Time – 10hr 05min

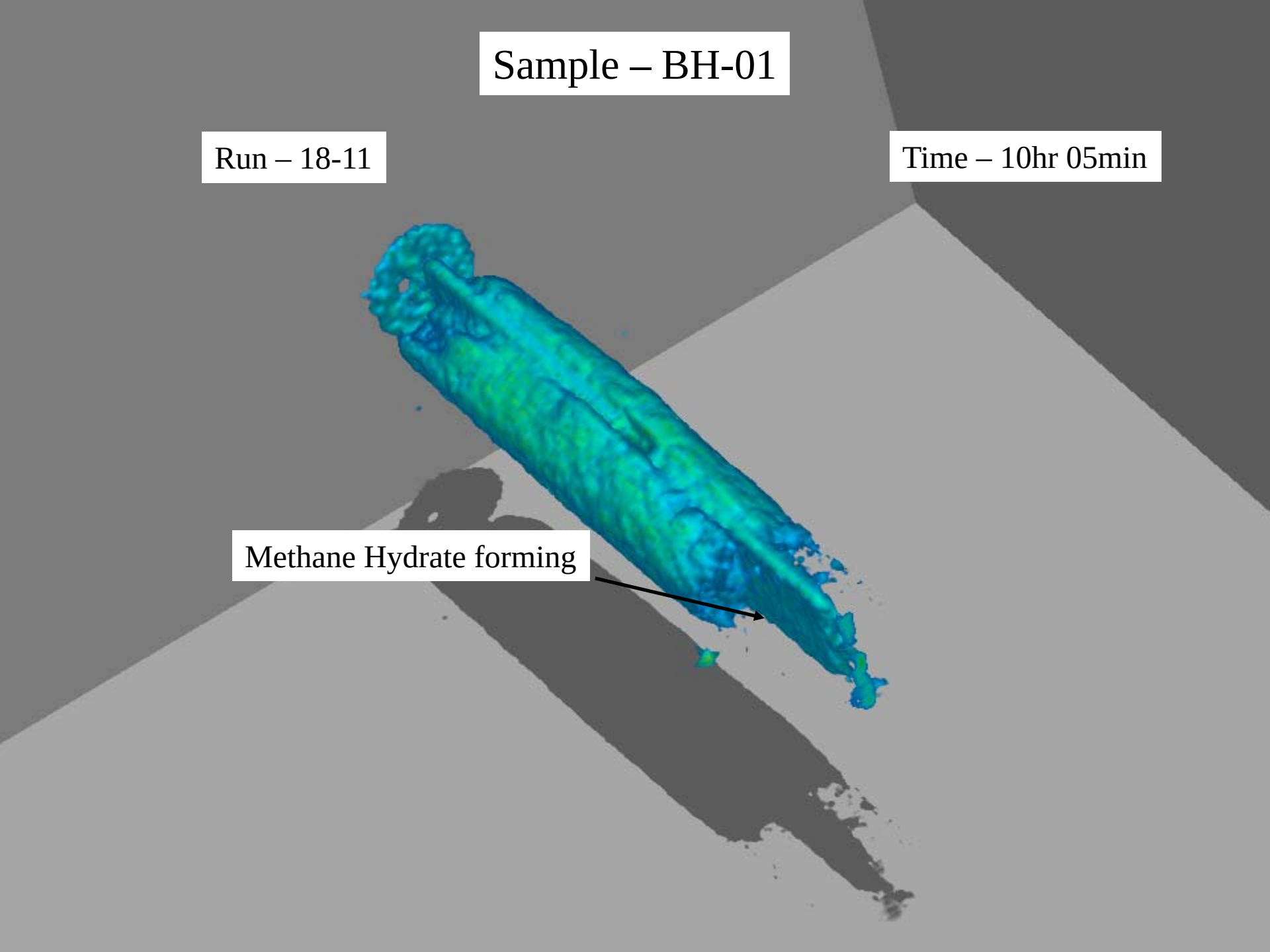

Sample – BH-01

Run – 18-12

Time – 11hr 00min

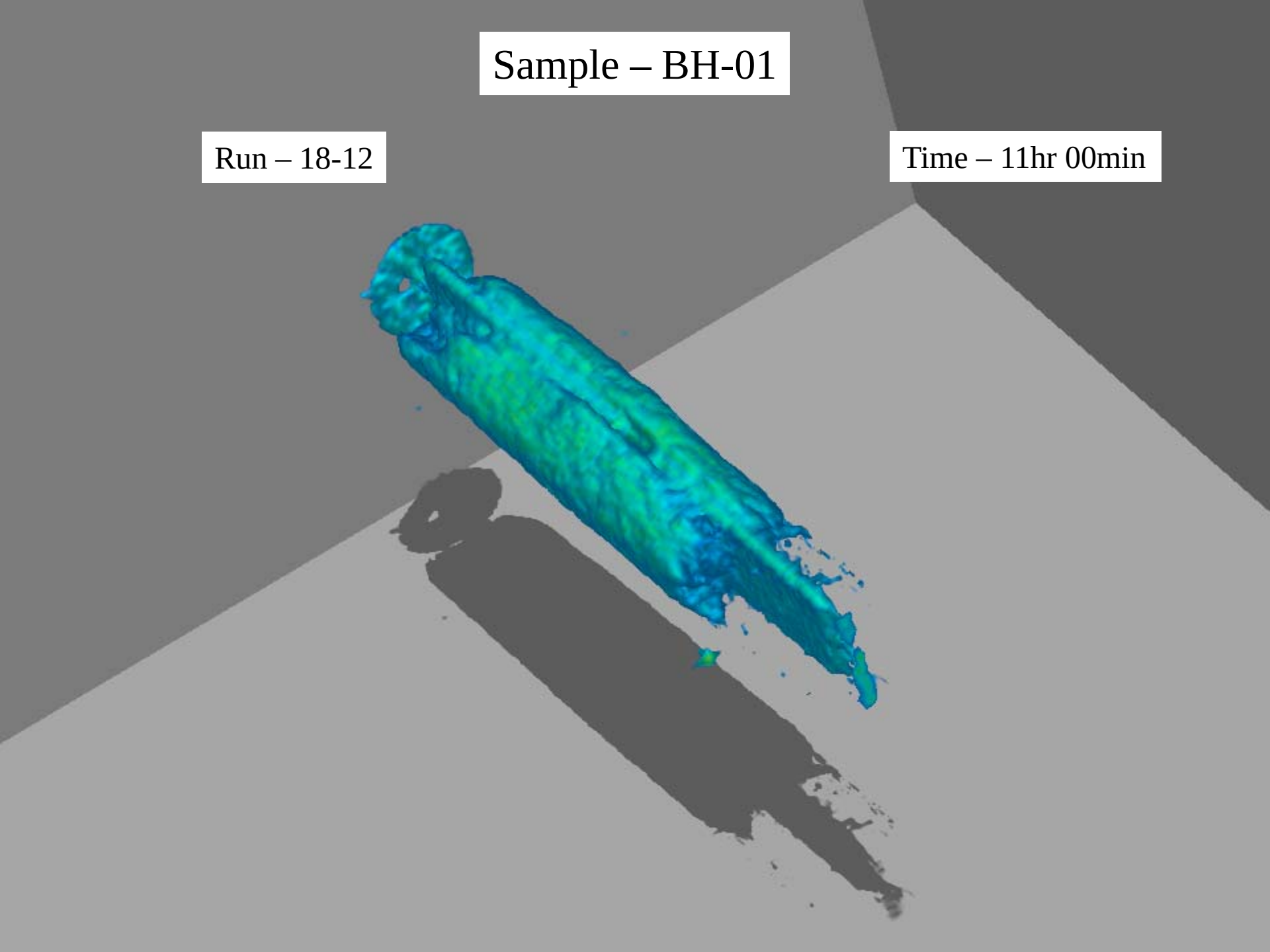

Sample – BH-01

Run – 18-14

Time – 12hr 50min

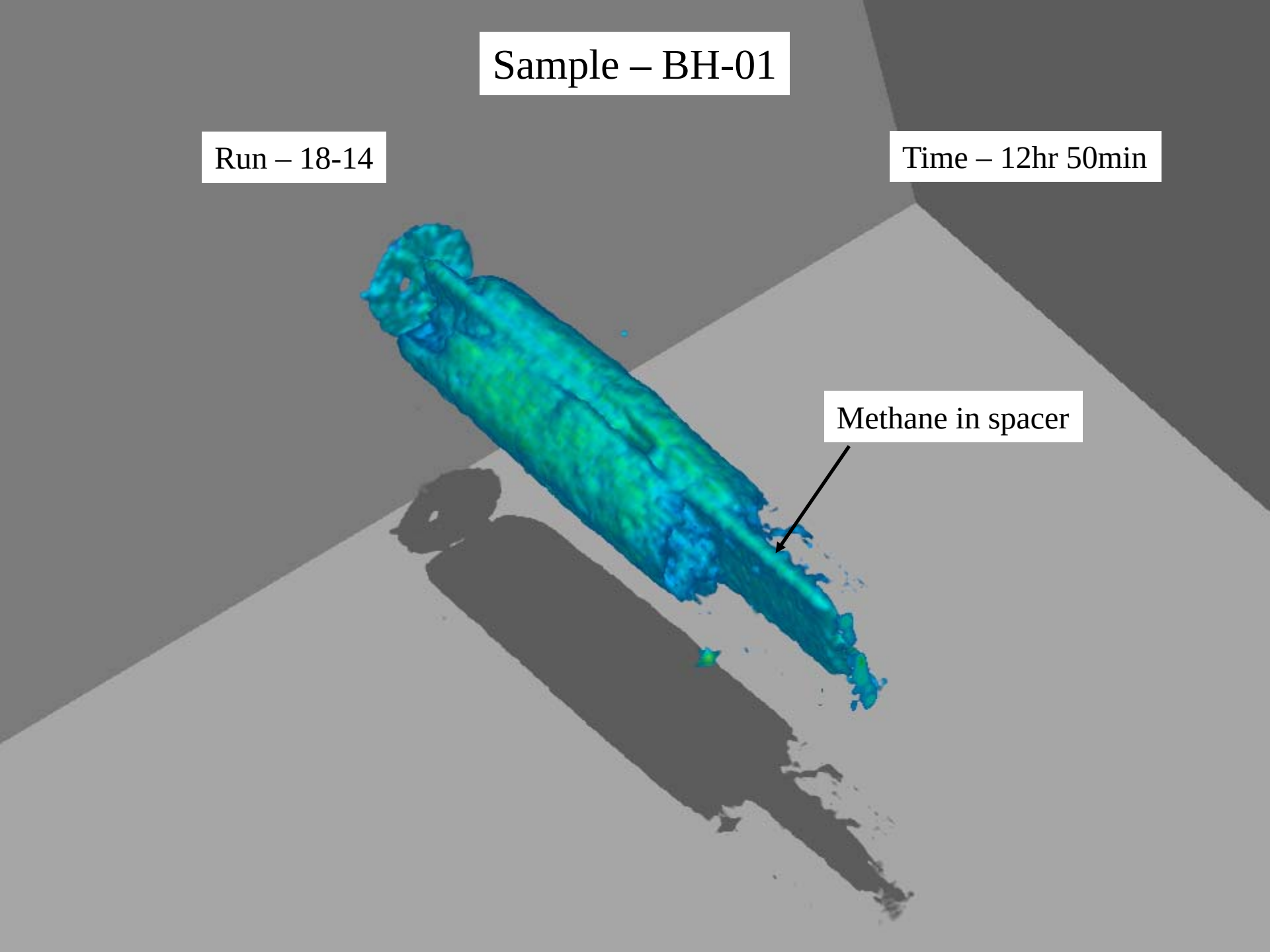

Sample – BH-01

Run – 18-16

Time – 14hr 40min

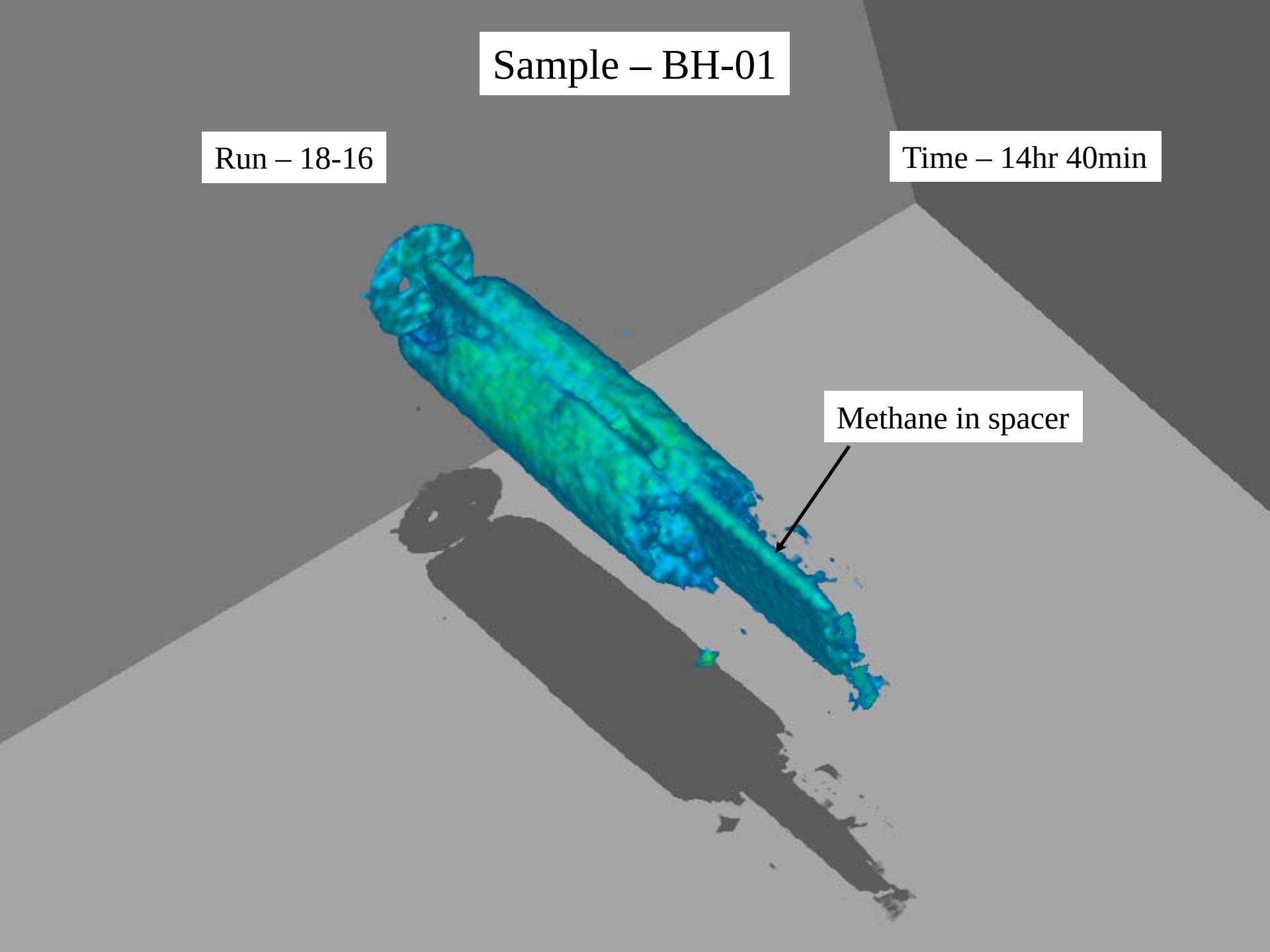

Sample – BH-01

Run – 18-17

Time – 15hr 35min

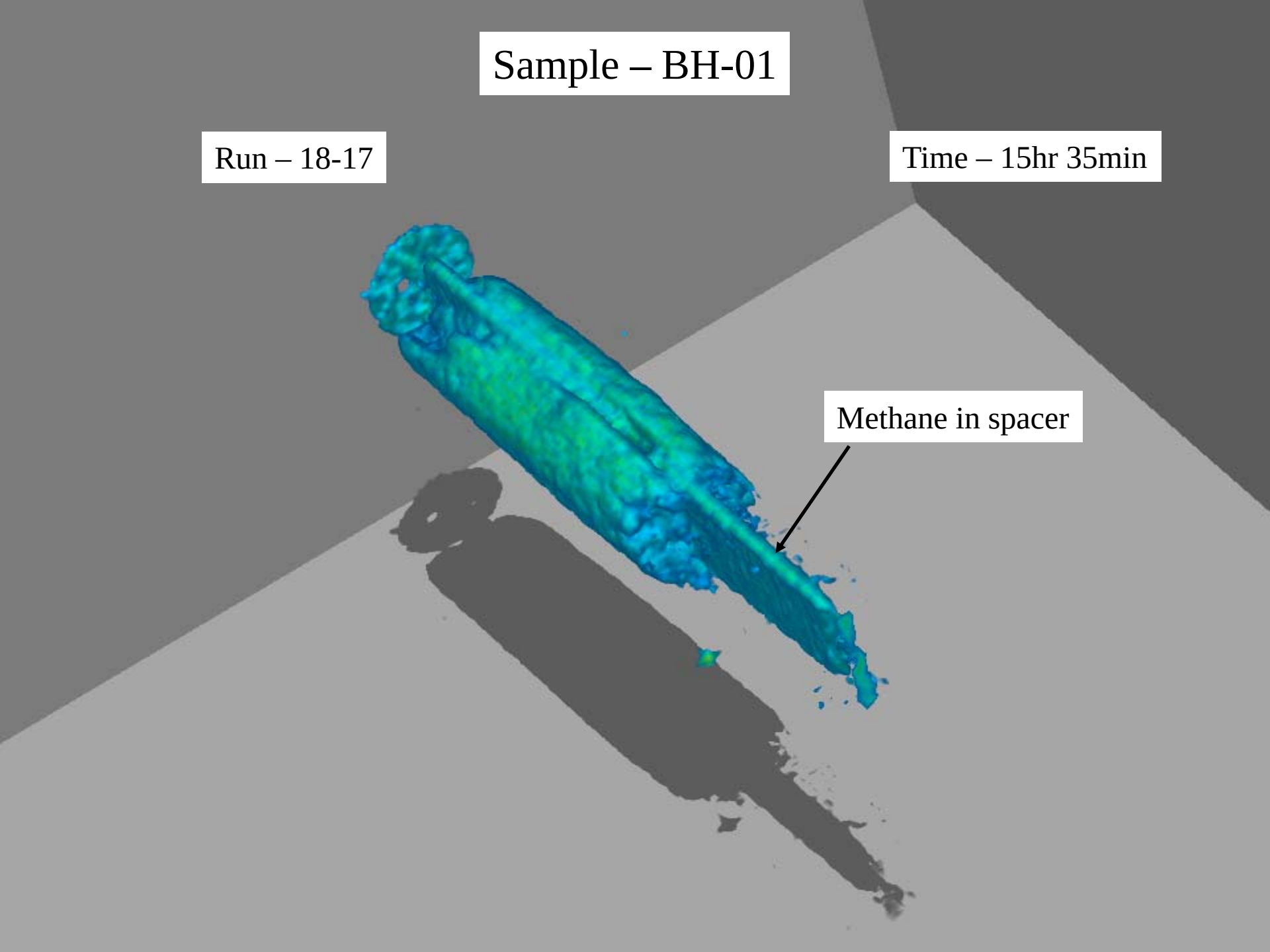

Sample – BH-01

Run – 18-19

Time – 17hr 25min

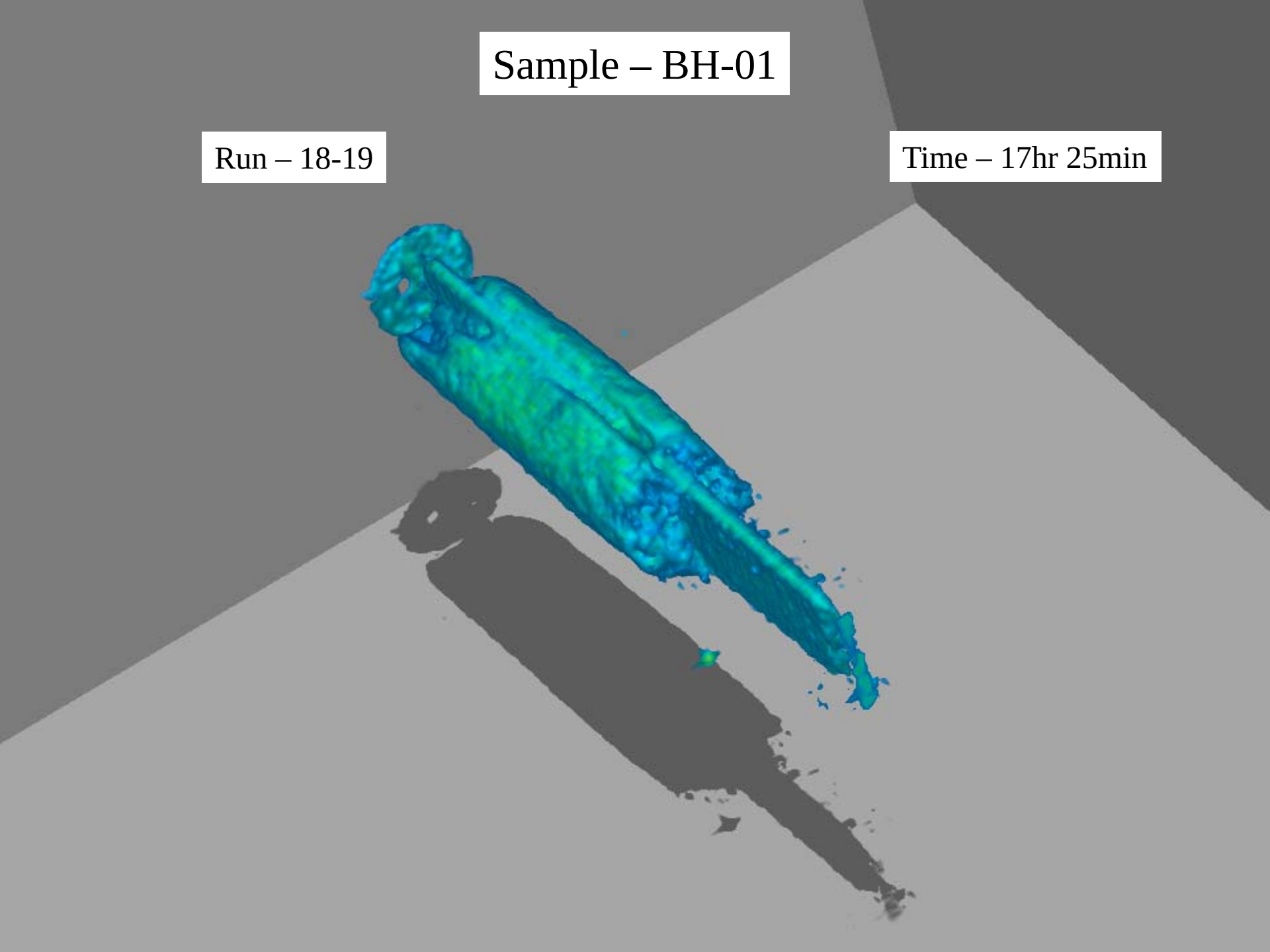

Sample – BH-01

Run – 18-37

Time – 31hr 05min

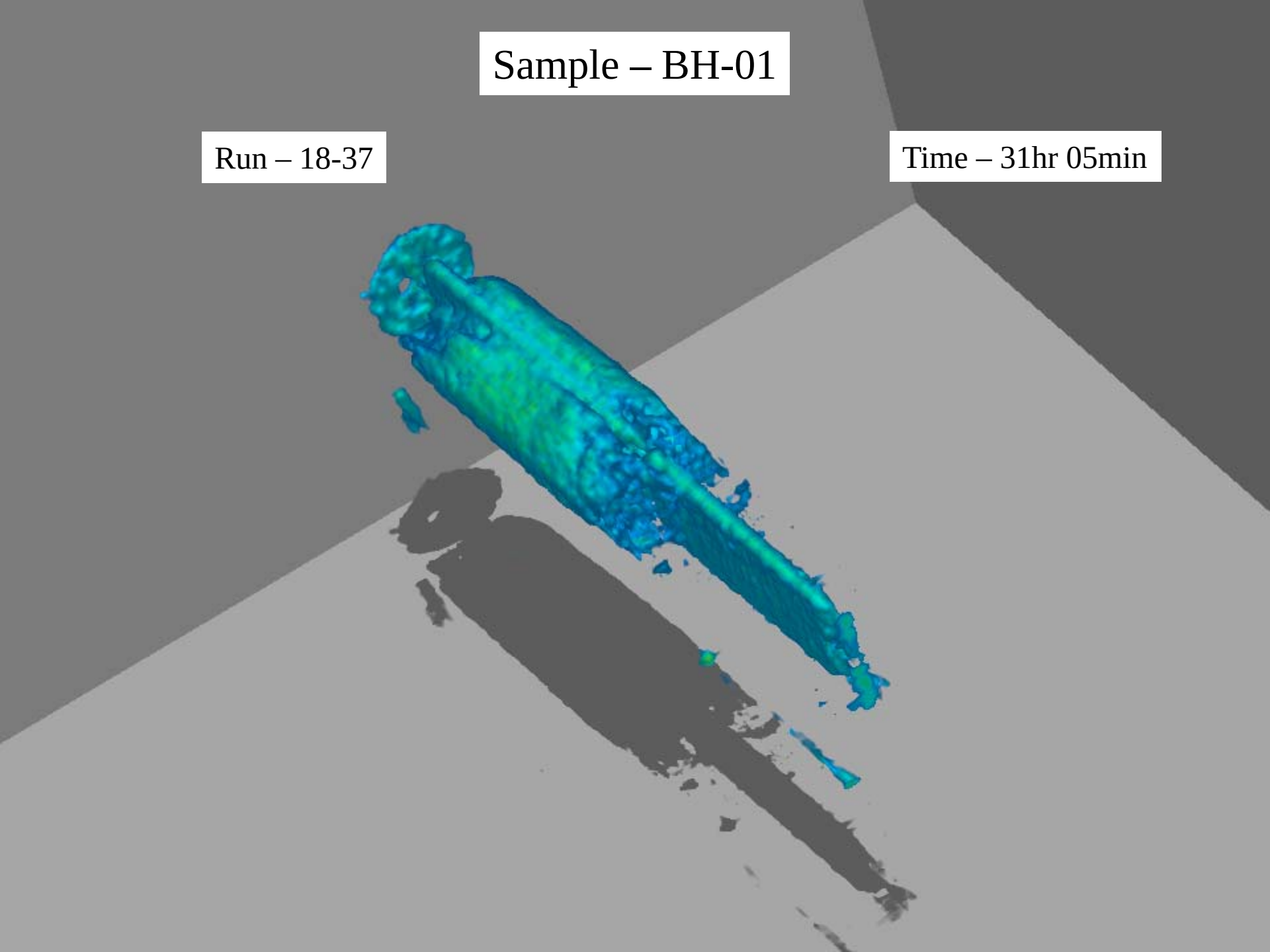

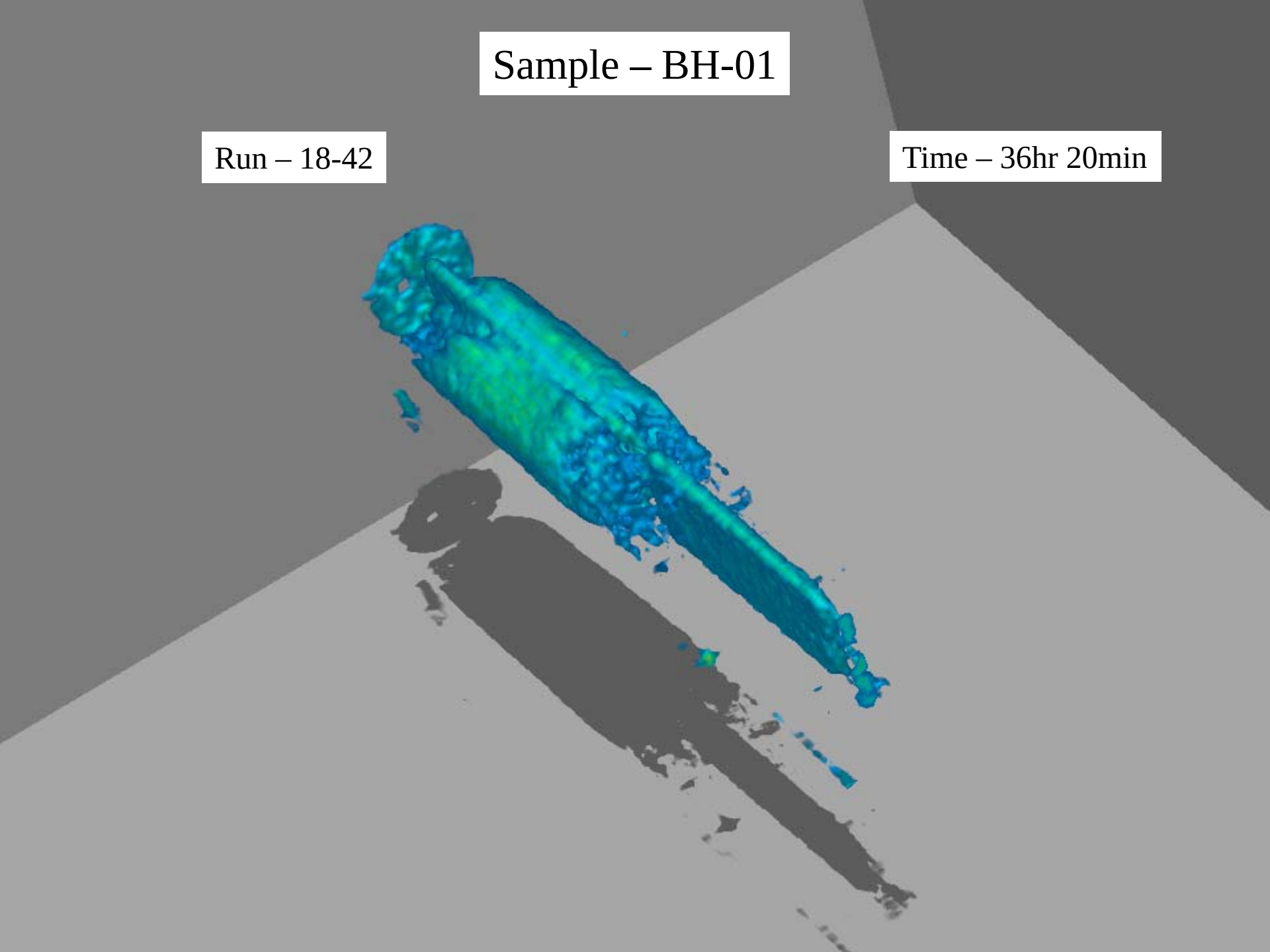
Sample – BH-01
Run – 18-42
Time – 36hr 20min

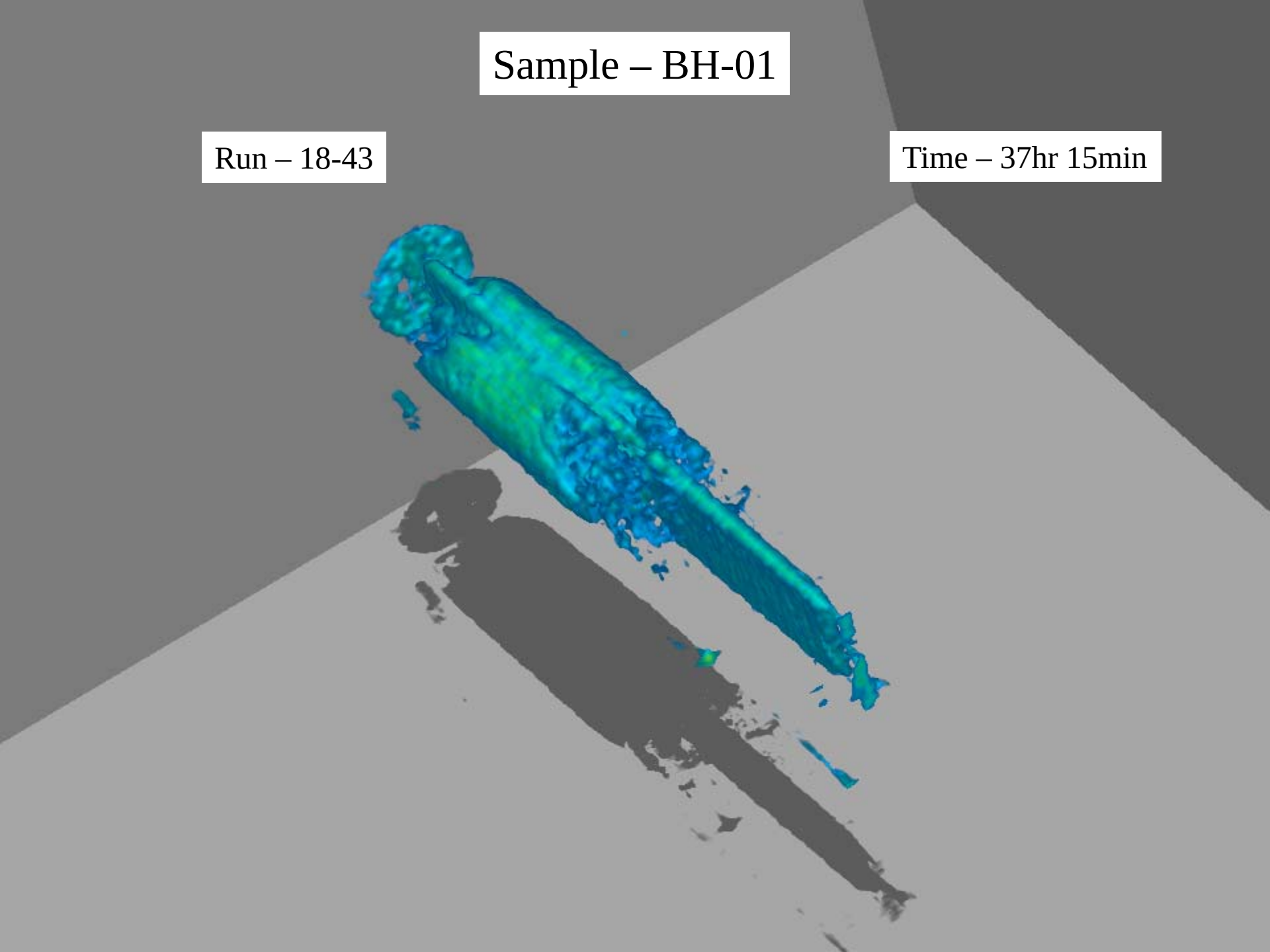
Sample – BH-01
Run – 18-43
Time – 37hr 15min

Sample – BH-01

Run – 18-57

Time – 54hr 10min

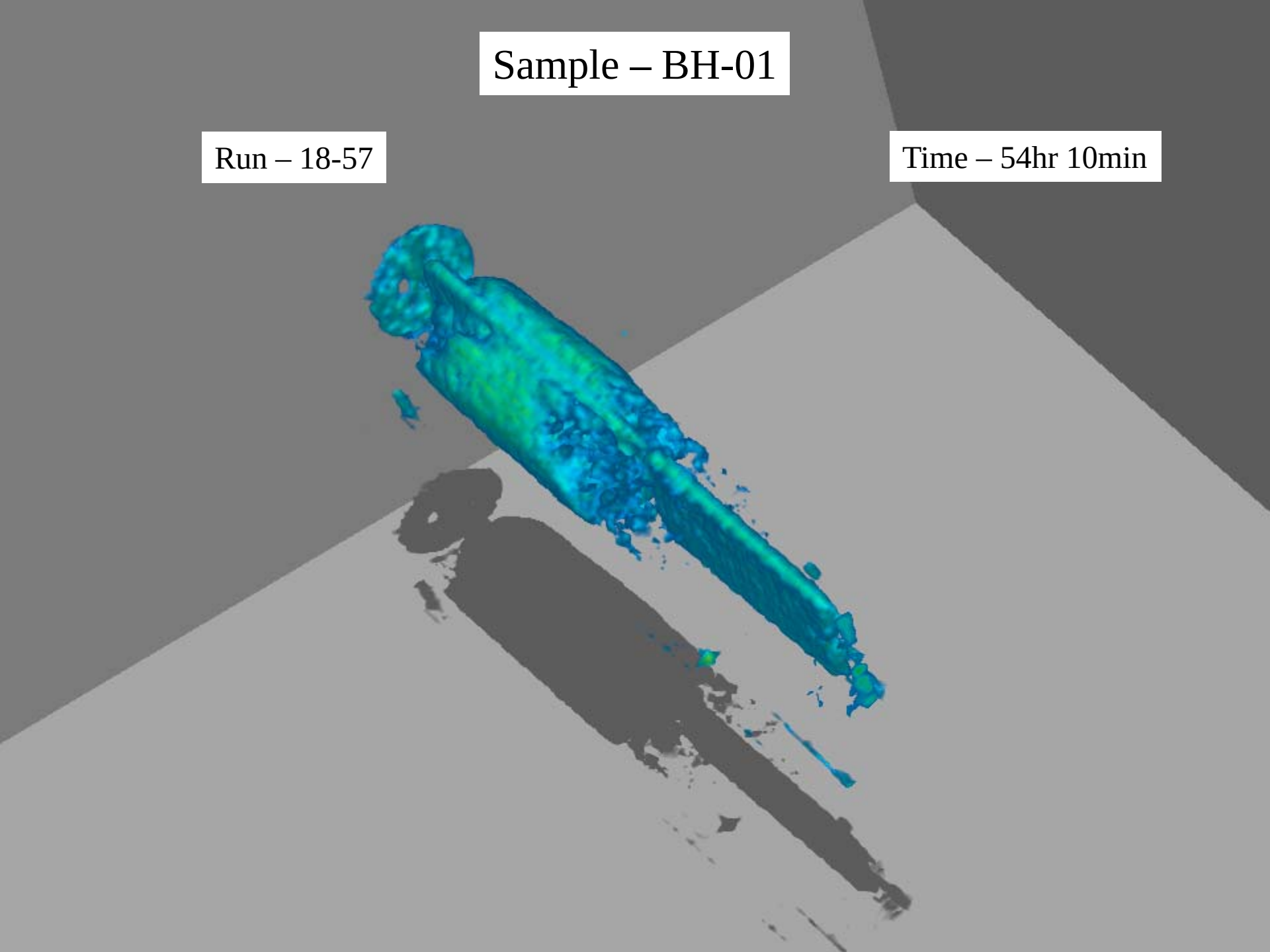

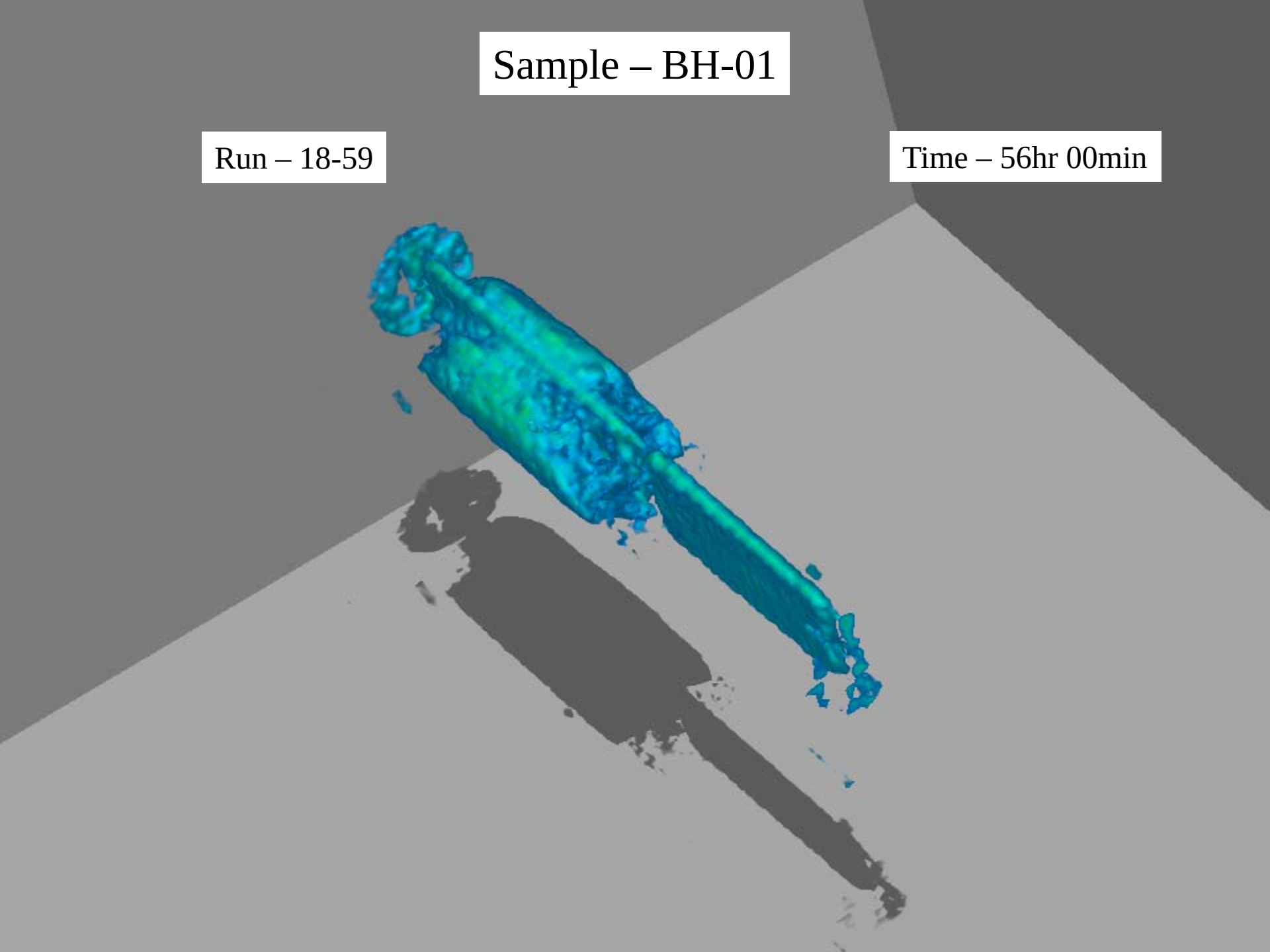
Sample – BH-01
Run – 18-59
Time – 56hr 00min

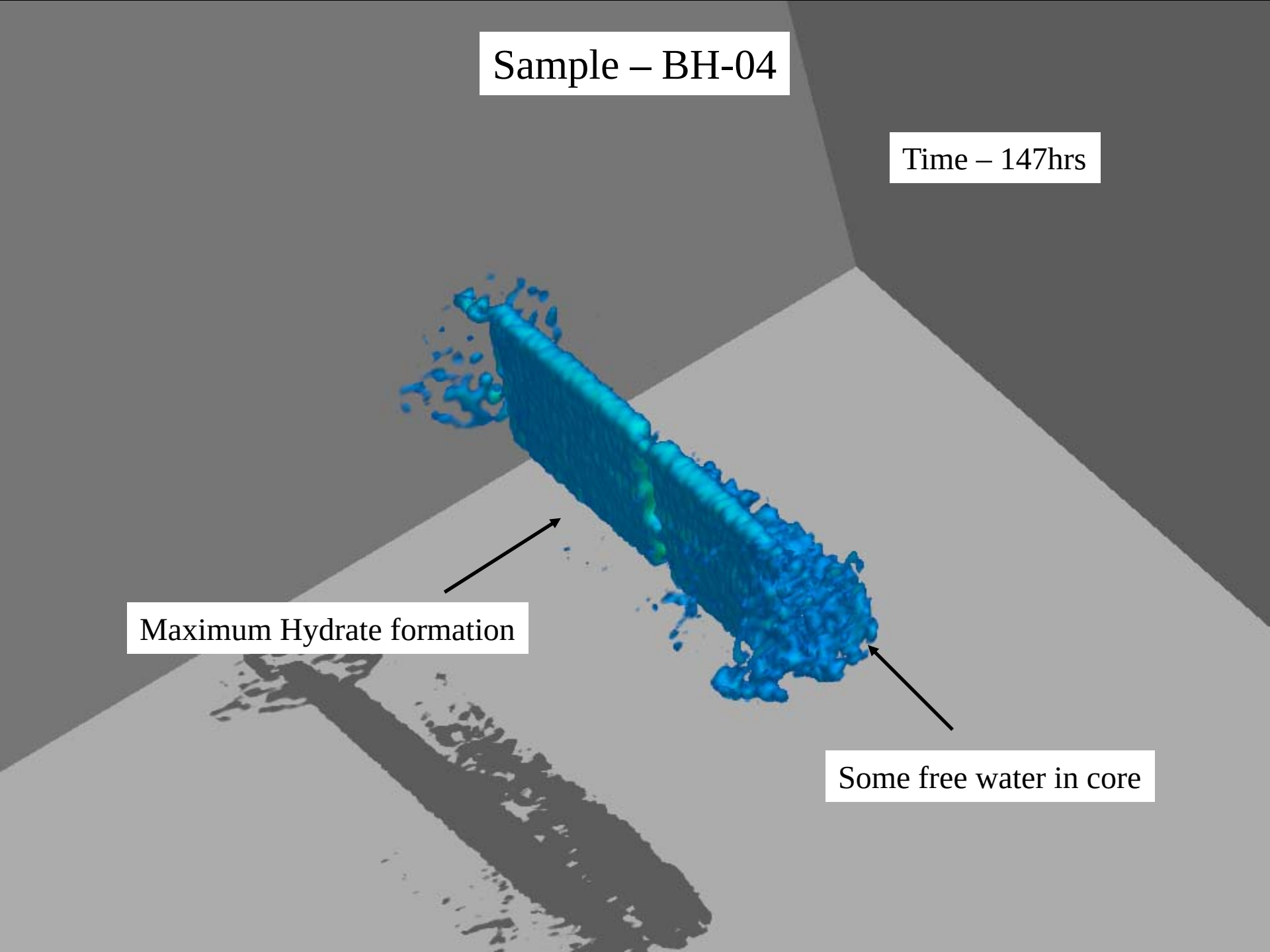
Sample – BH-04
Time – 147hrs
Maximum Hydrate formation
Some free water in core

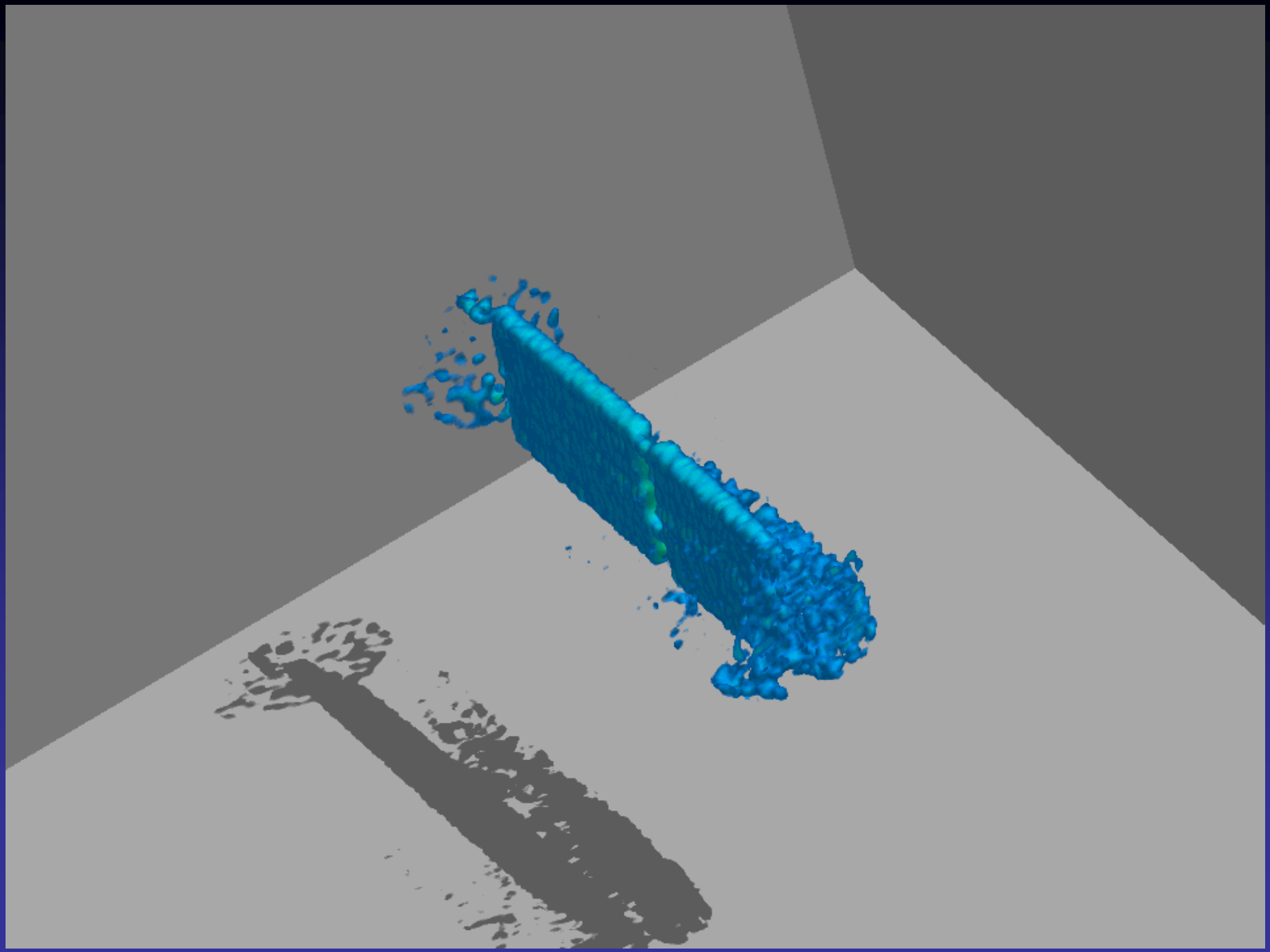

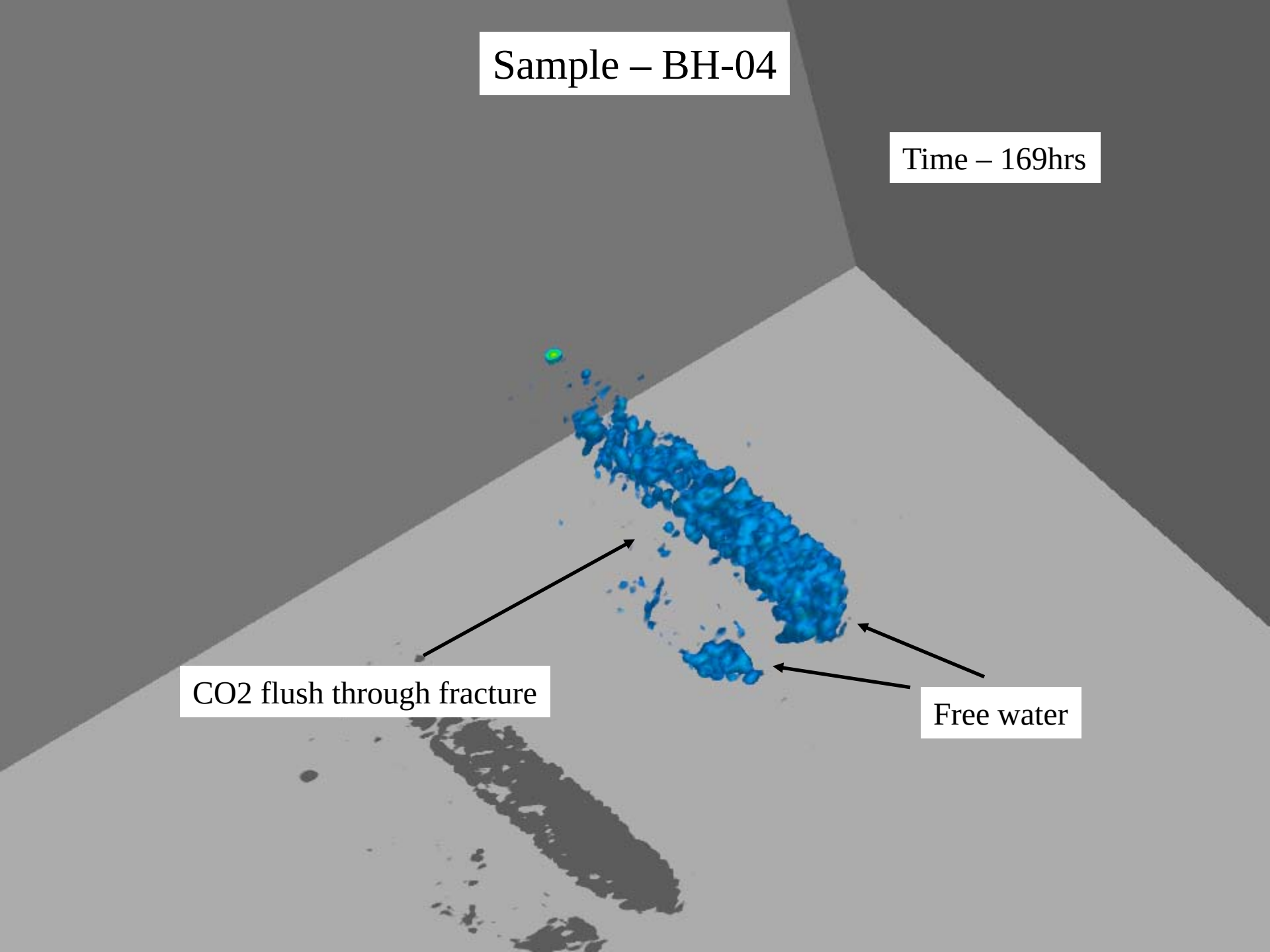
Sample – BH-04
Time – 169hrs
CO2 flush through fracture
Free water

Sample – BH-04

Time – 190hrs

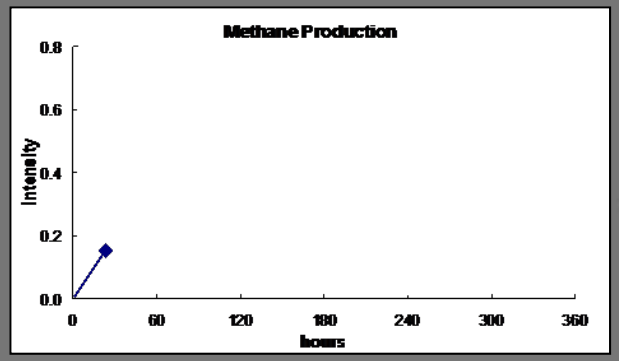

Sample – BH-04

Time – 214hrs

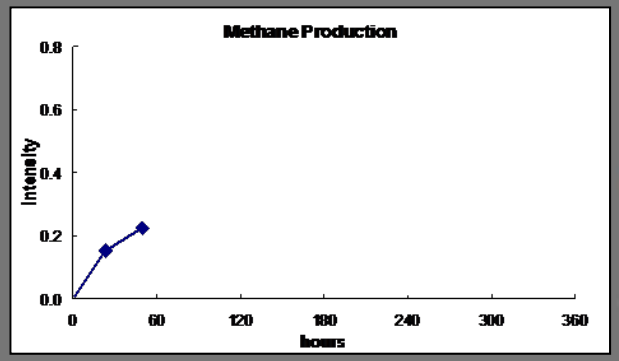

Methane starts to fill fracture

Sample – BH-04

Time – 230hrs

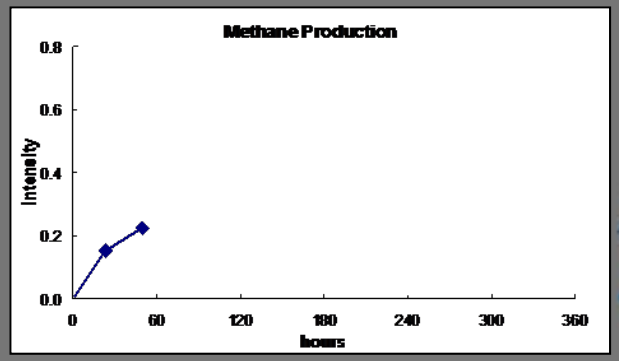

Methane starts to fill fracture

Sample – BH-04

Time – 238hrs

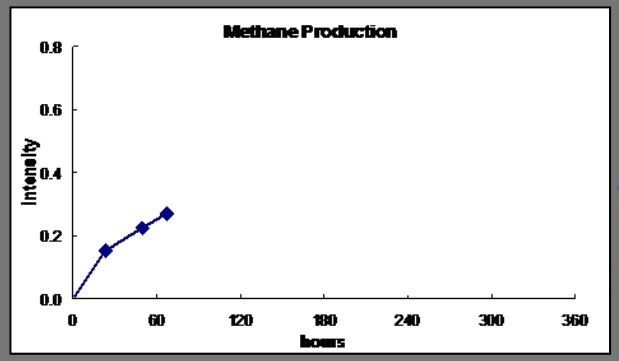

Methane starts to fill fracture

Sample – BH-04

Time – 253hrs

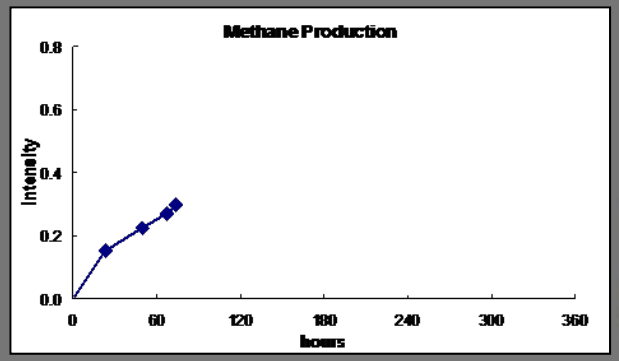

Methane starts to fill fracture

Sample – BH-04

Time – 264hrs

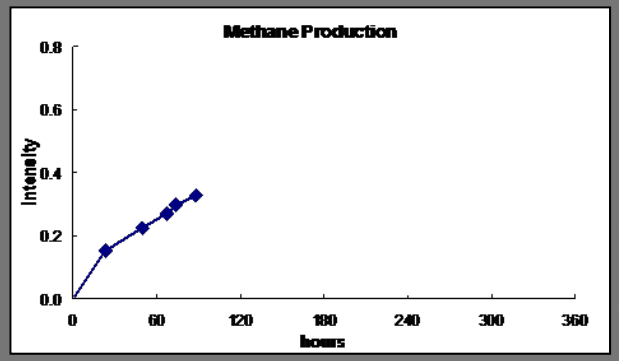

Methane starts to fill fracture

Sample – BH-04

Time – 278hrs

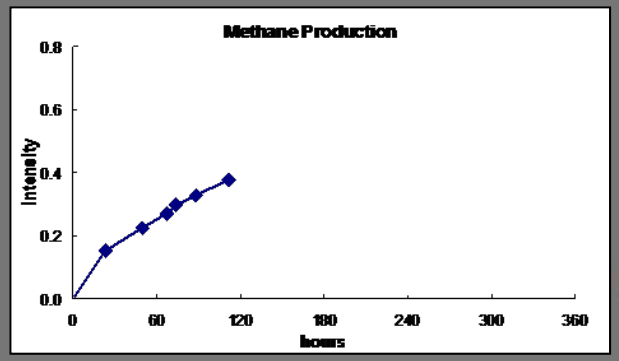

Methane starts to fill fracture

Sample – BH-04

Time – 302hrs

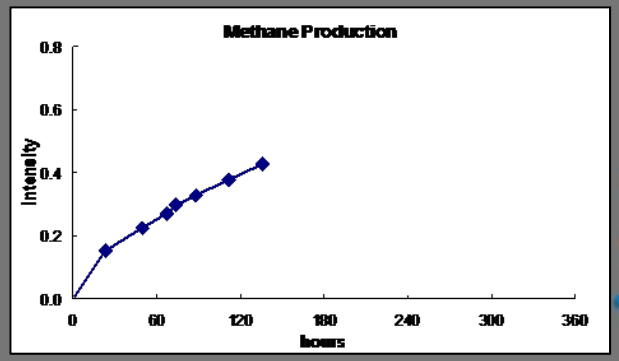

Sample – BH-04

Time – 327hrs

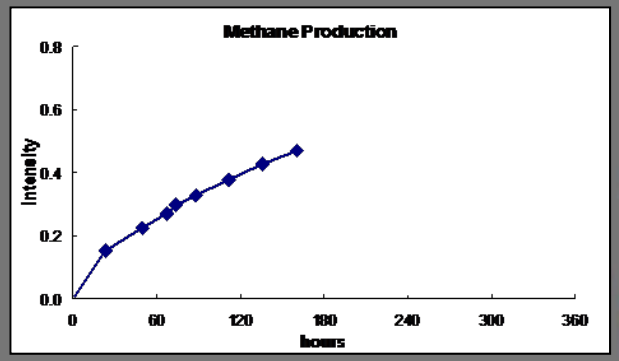

Sample – BH-04

Time – 381hrs

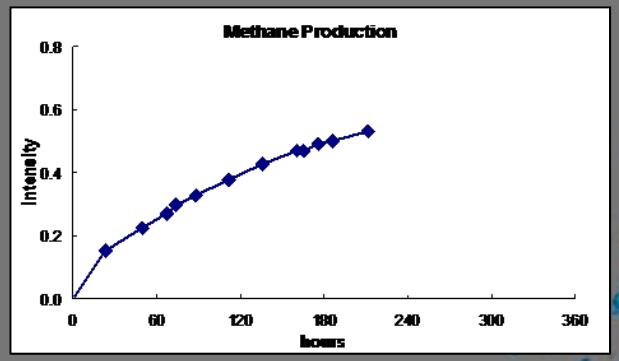

Sample – BH-04

Time – 429hrs

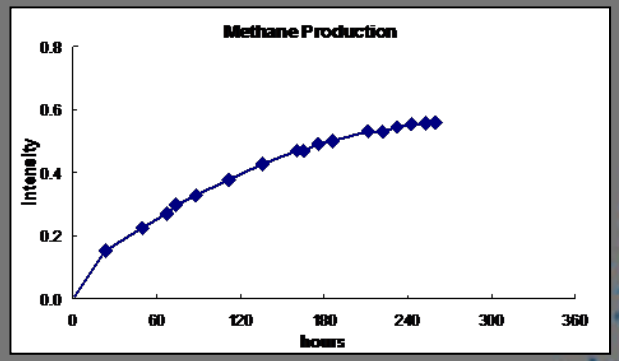

Sample – BH-04

Time – 483hrs

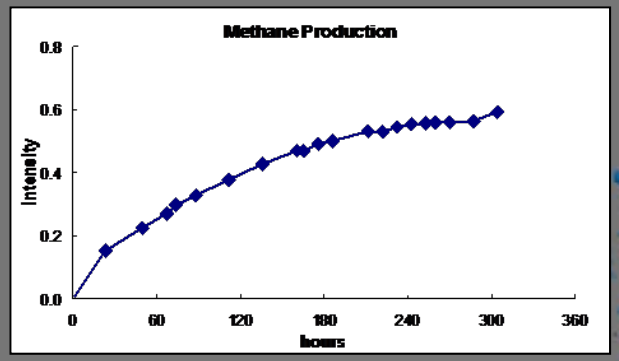

Sample – BH-04

Time – 484hrs

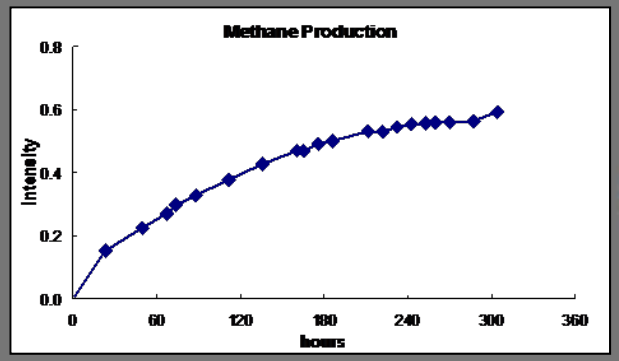

315hrs Methane production

Sample – BH-04

Time – 703hrs

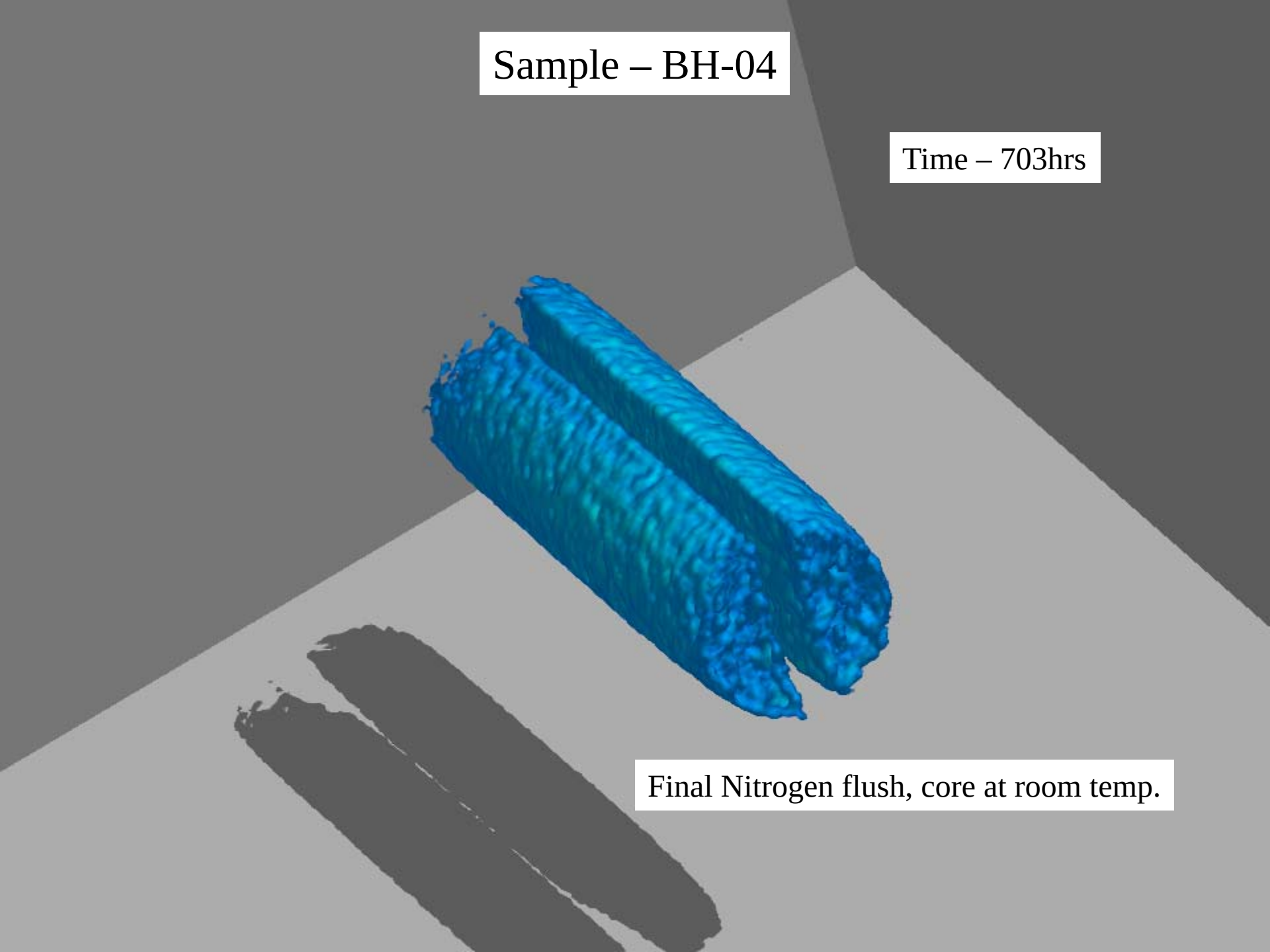

Final Nitrogen flush, core at room temp.

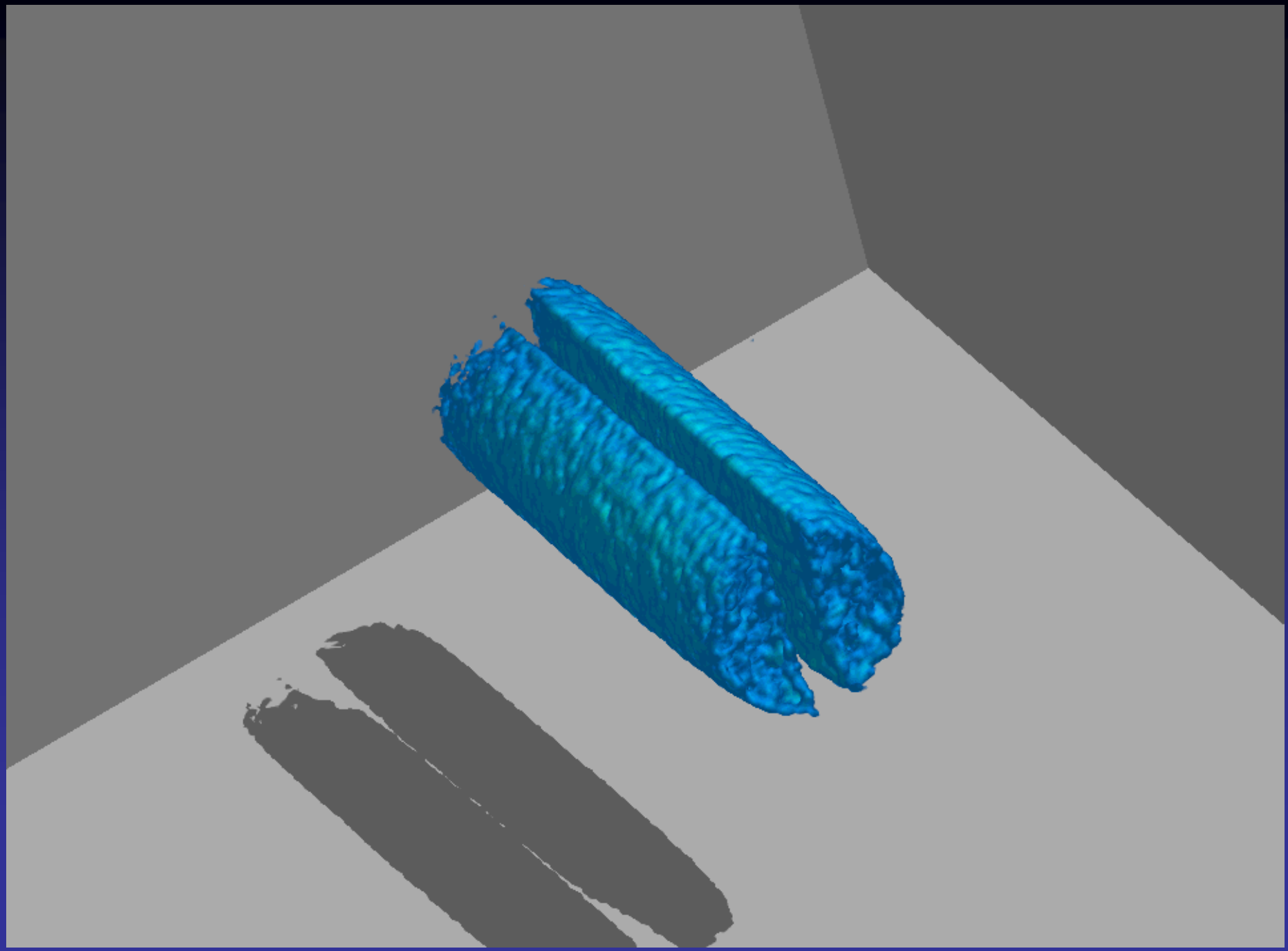

CH_4 Production Rates & Amounts from Hydrate

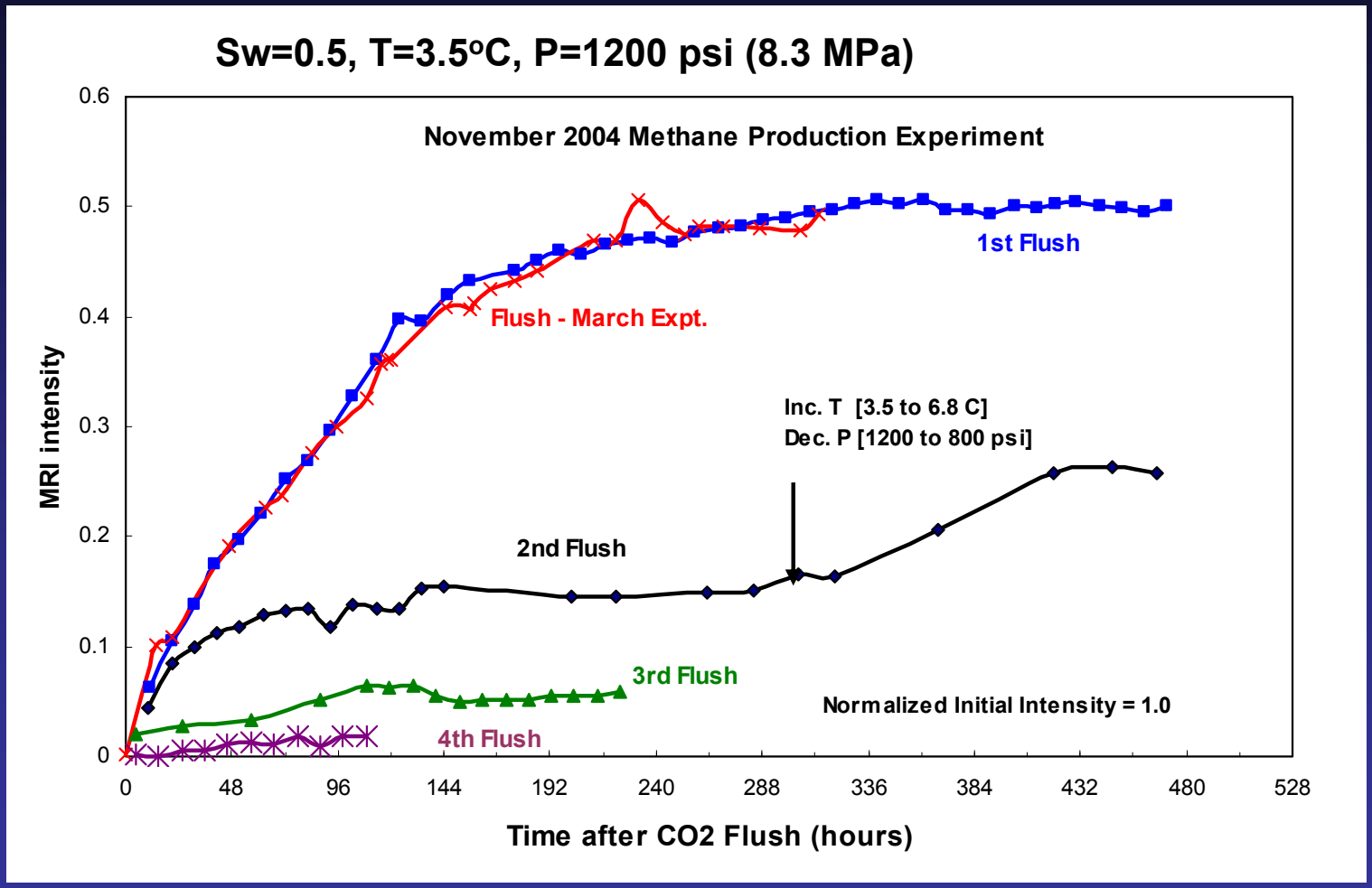

Theoretical modelling

- The conversion of CH4 hydrate over to CO2 hydrate releases limited amounts of energy
- Heat transport is, however, 2 orders of magnitude or more faster than mass transport.
- As a first approximation we may treat this particular exchange as isothermal

Phase Field Theory

- Density Functional Theory links the kinetics of phase transition to the change in molecular structure across the phase boundaries
- Molecular structures is uniquely linked to corresponding free energies via statistical mechanics
- Phase Field Theory uses free energy changes directly as the driving forces for kinetic progress of the phase transition

Three component Phase Field Theory

$$F = \int d\underline{r}\left\{\frac{\varepsilon^2 T}{2}(\nabla\varphi)^2 + \sum_{i,j=1}^{3}\frac{\varepsilon_{i,j}{}^2 T}{4}\left(c_i\nabla c_j - c_j\nabla c_i\right)^2 + f_{bulk}(\varphi, c_1, c_2, c_3, T)\right\}$$

$$f_{bulk} = wTg(\varphi) + [1 - p(\varphi)]f_S(c_1, c_2, c_3, T) + p(\varphi)f_L(c_1, c_2, c_3, T)$$

$$\dot{\varphi} = -M_\varphi \frac{\delta F}{\delta\varphi} + \zeta_\varphi$$

$$\sum_{i=1}^{3} c_i = 1$$

$$\dot{c}_i = \nabla M_{ci}(c_1, c_2, c_3)\nabla\left(\frac{\delta F}{\delta c_i} - \zeta_i\right)$$

Parameters ε and w can be fixed from the interface thickness and interface free energy. ε ij set equal to ε

Interface density profiles for aqueous solution and hydrate

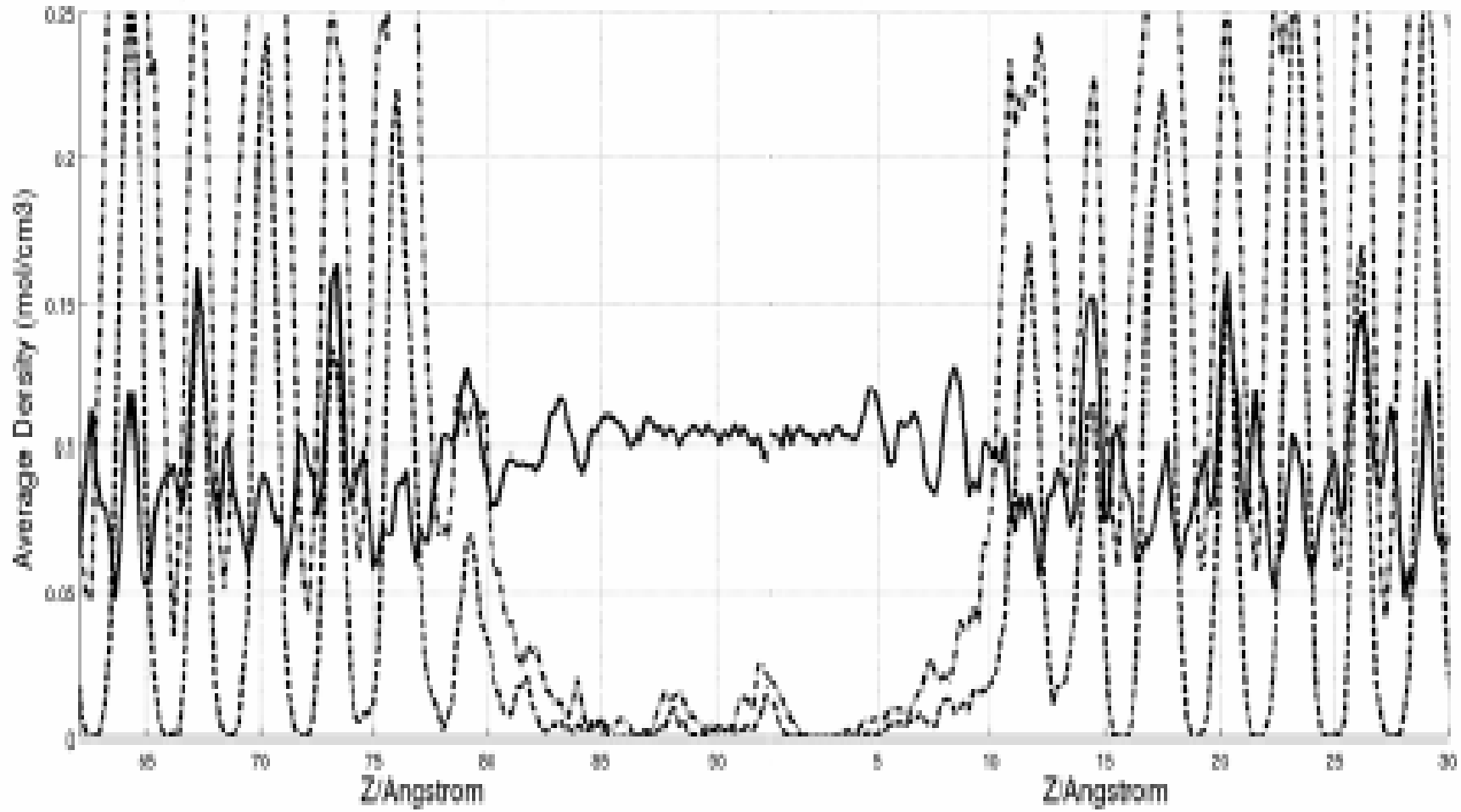

Fig. 6 Full line -- hydrogen density profile; dashed line – oxygen in CO_2 dashed-dotted line – oxygen in water (both hydrate and liquid).

TABLE I. 10%–90% interface widths from MD simulations

	d (nm)
H_2O D↑	0.93
H_2O D↓	0.86
CO_2 D↑	0.79
H_2O CD↑	0.61
H_2O CD↓	0.69
CO_2 CD↑	1.21
CO_2 CD↓	0.88
Average	0.85
H_2O DGF	1.21
CO_2 DGF	1.07

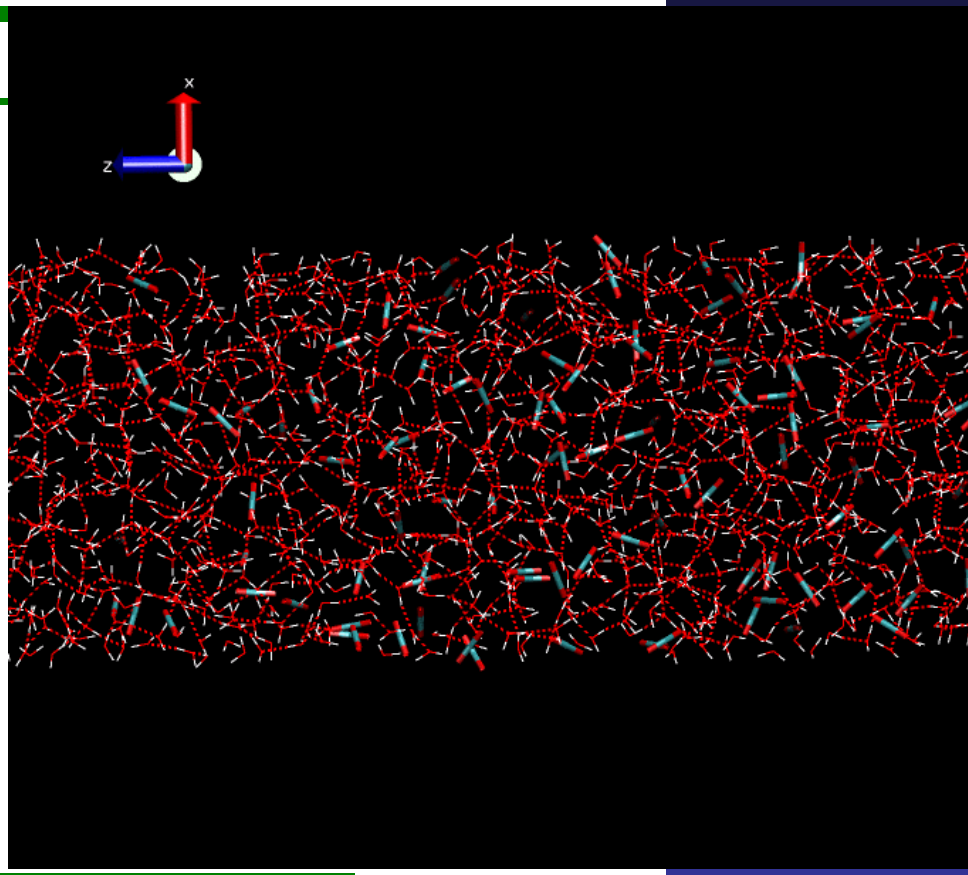

Notation: D – mass density, CD – charge density, ↑ – envelope of peaks, ↓ – envelope of wells, GF – Gaussian filtered.

Cleaving the water -- CO_2 hydrate system by adding repulsive interactions:

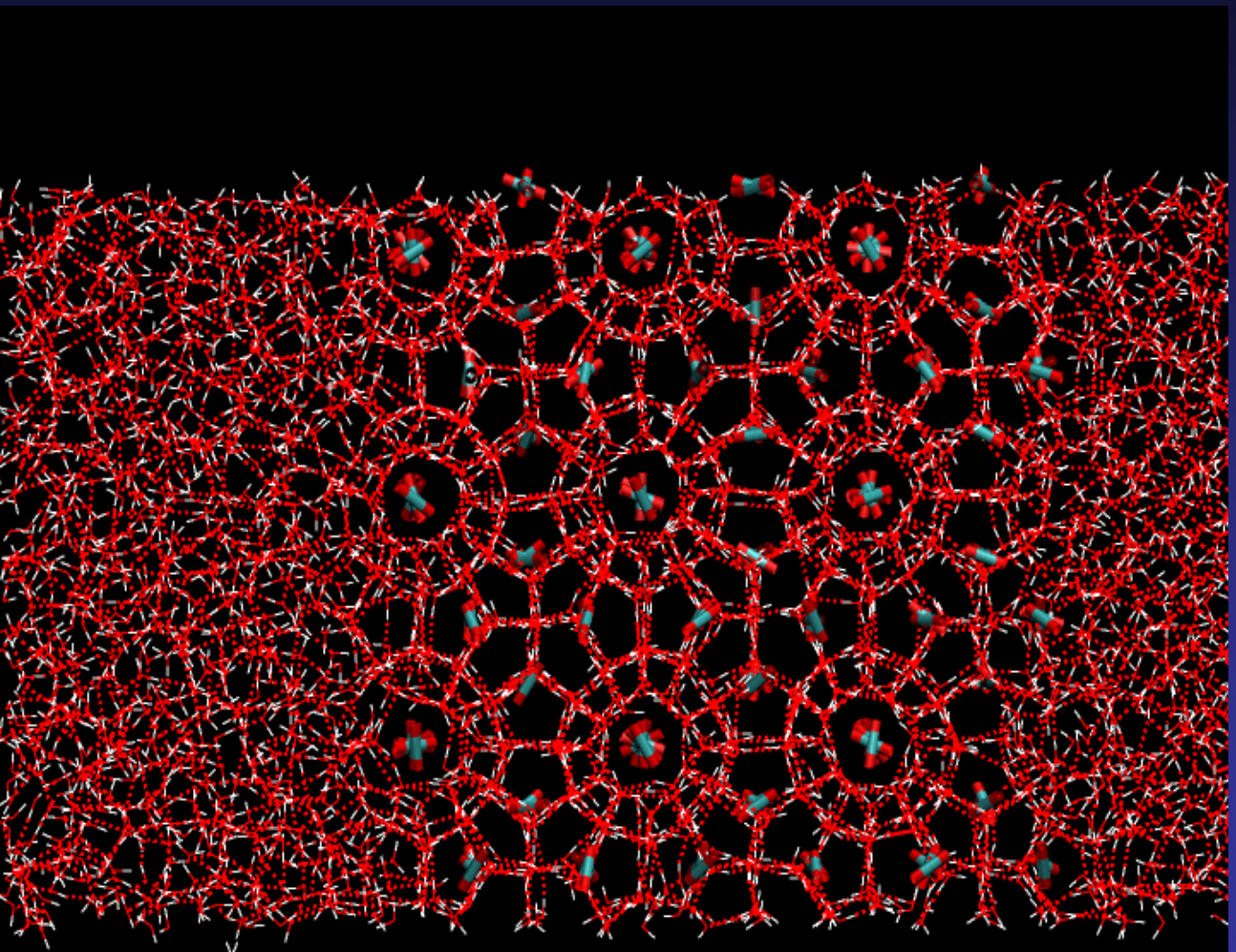

Estimated γ 30 +/- 4 mJ/m^2

Error bars too large
and enhanced by tendencies of hydrate dissociation at the interface.

Work on alternative approach according to cappilary wave theory
is in progress

Interface thickness d and interface free energy fixes the two model parameters *w* and ε in the Phase FieldTheory. Evaluation of these parameters from model systems by Molecular Dynamics simulations of model systems

Estimated to 8.5 Å – see previous overhead

$$d = \left(\frac{\varepsilon^2 T}{2}\right)^{1/2} \int_{0.05}^{0.95} d\xi \left\{\Delta f[\xi, c(\xi)]\right\}^{-1/2}$$

Phase Field Theory parameter w is in the free energy f (see PFT slide)

$$\gamma_\infty = (\varepsilon^2 T)^{1/2} \int_0^1 d\xi \left\{\Delta f[\xi, c(\xi)]\right\}^{1/2}$$

Phase Field Theory parameter ε

where $\Delta f = f - f_0$, and

$$f_0 = f_L(c_L^{eq}) + \left(\frac{\partial f_L}{\partial c}\right)\Big|_{c_L^{eq}} (c - c_L^{eq})$$

$$= f_S(c_S^{eq}) + \left(\frac{\partial f_S}{\partial c}\right)\Big|_{c_S^{eq}} (c - c_S^{eq})$$

Interface free energy ≈ 30 mJ/m^2

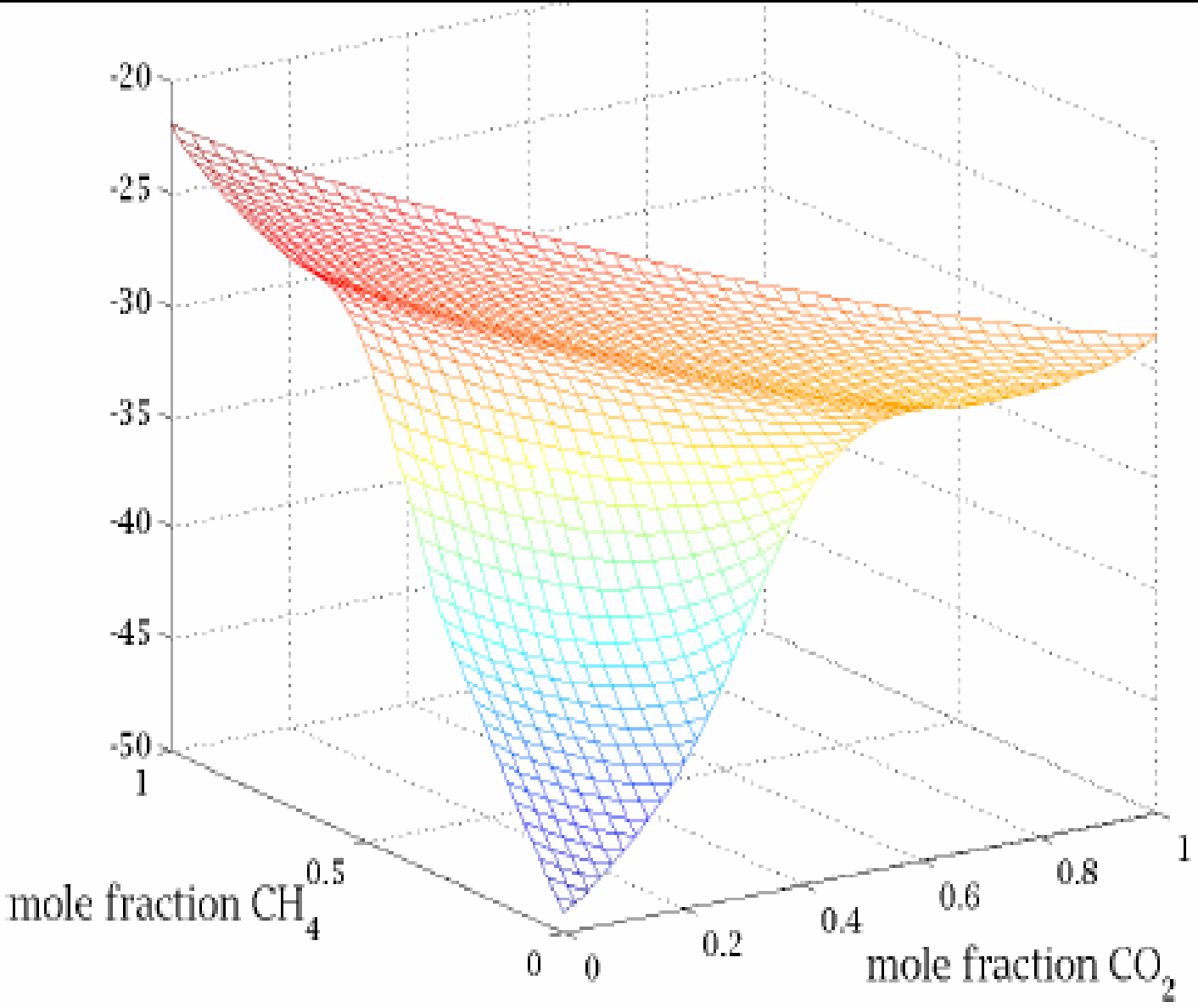

Fig. 2 Free energy density (kJ/mole) as a function of the mole fractions of CH_4 and CO_2 at 1C and 40 bars.

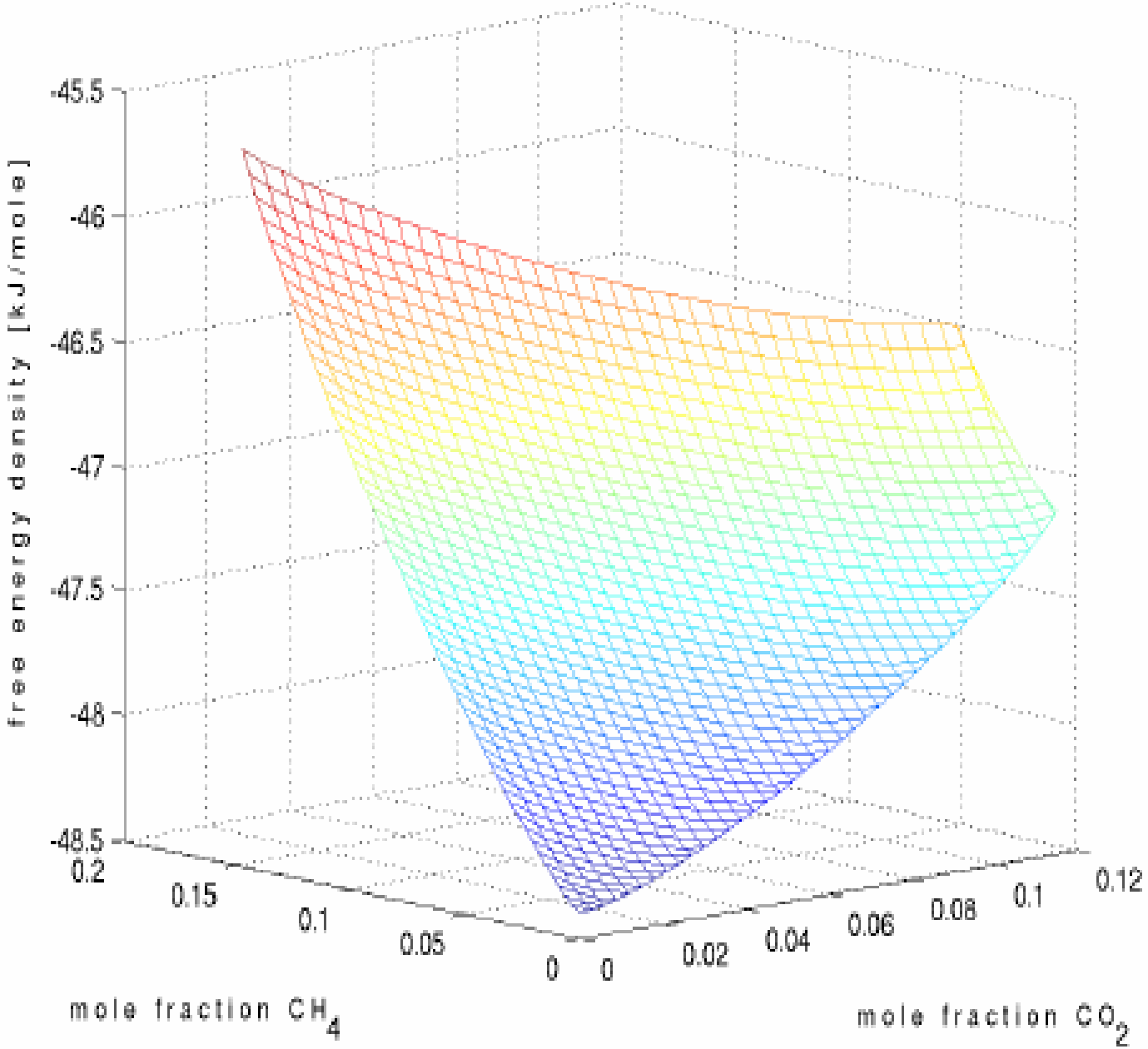

Fig. 1 Free energy density of the hydrate as a function of the mole fractions of CH_4 and CO_2 at 1°C and 40 bars.

Phase field predictions for the conversion of a 10 nm thick methane hydrate layer into mixed CO2 – CH4 hydrate in the presence of liquid CO2 at T = 276.15 K and p = 8.3 MPa. The liquid CO2 phase is on the right. The spatial step size is Δx = 0.05 nm.

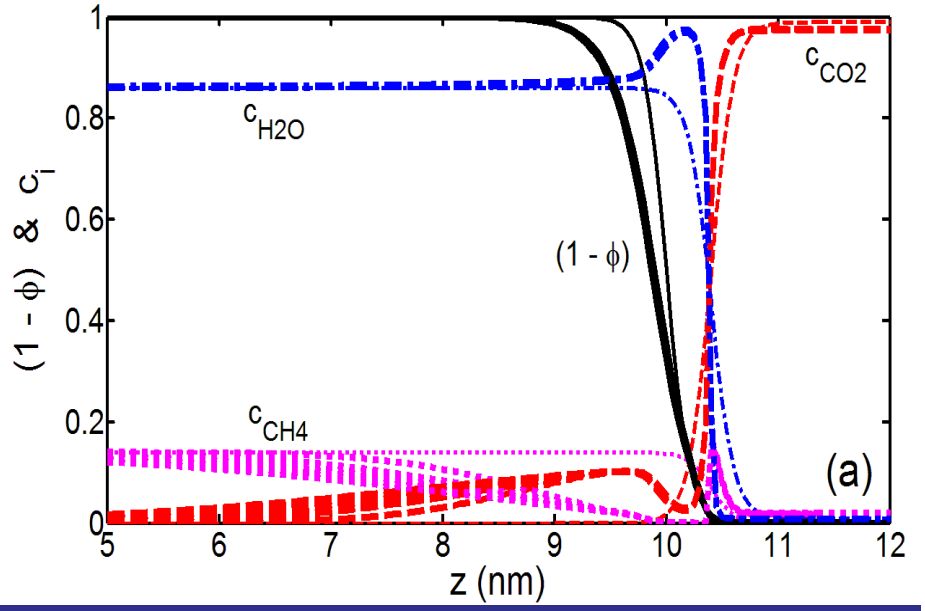

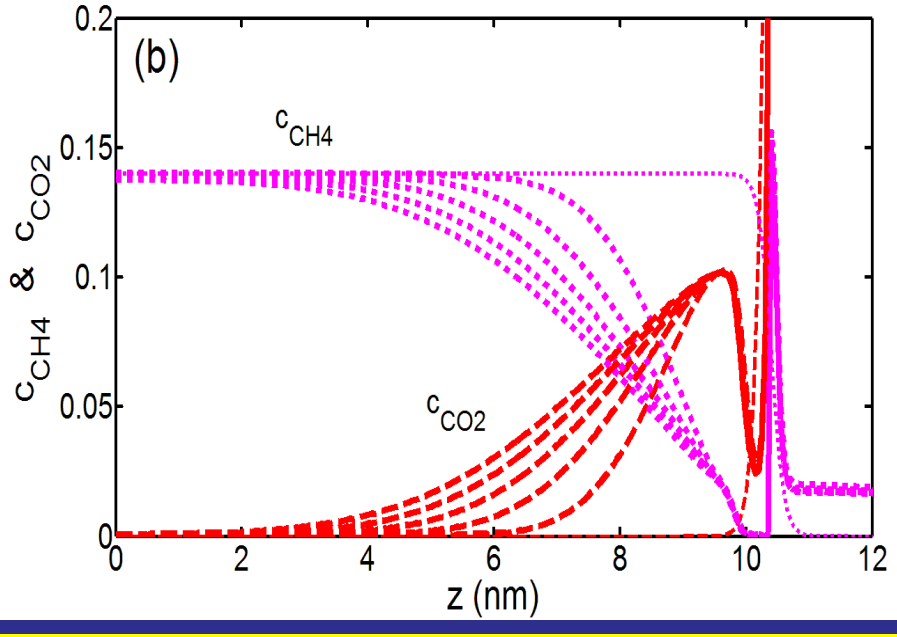

(a) the phase field (solid), CO2 (dashed), CH4 (dotted), and H2O (dash-dot) concentration profiles corresponding to instances t = 0.0, 0.08, 0.16, 0.24, 0.32, and 0.4 μs. The initial profiles are shown by thinner lines. Note the thin water layer slightly right of the z = 10 nm position, and the respective depletion of methane and carbon-dioxide in the same region.

(b) An enlarged view of the methane and carbon-dioxide profiles in the solid hydrate phase is presented in panel (b).

Detailed analysis of the simulated results indicate that the conversion process is essentially dominated by transport limitations. I.e.: we should expect that Fick's law would represent the kinetic progress of conversion to a fair extent

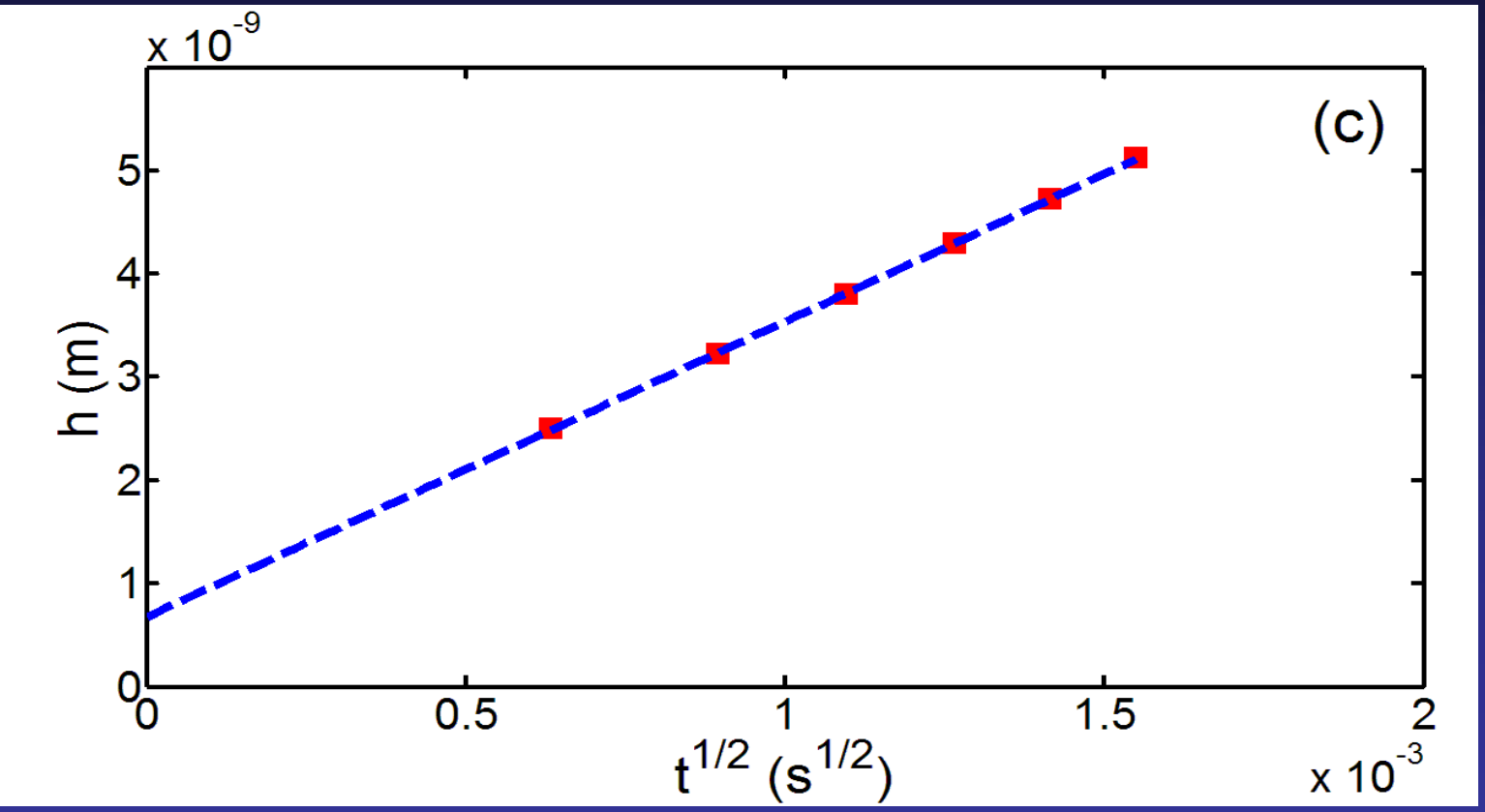

Fitting the phase field simulated progress to Fick's law gives a nice fit. Initial deviations from zero due to initial relaxation of the hydrate interface

Displacement h of the half-height (c_{CO2} = 0.055) position for the CO_2 profile as a function of $t^{1/2}$. $D_s = 5 \times 10^{-12}$ m^2/s is assumed.

So how does this value of diffusivity match experimental results

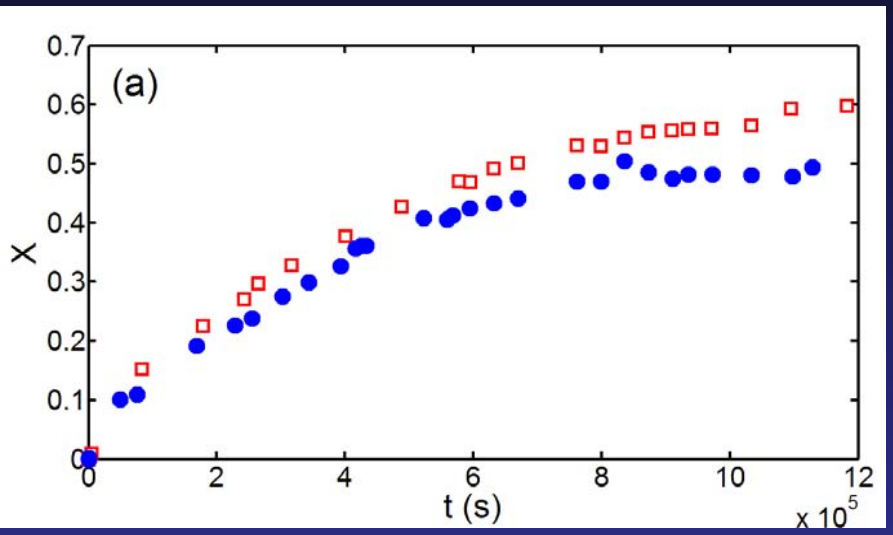

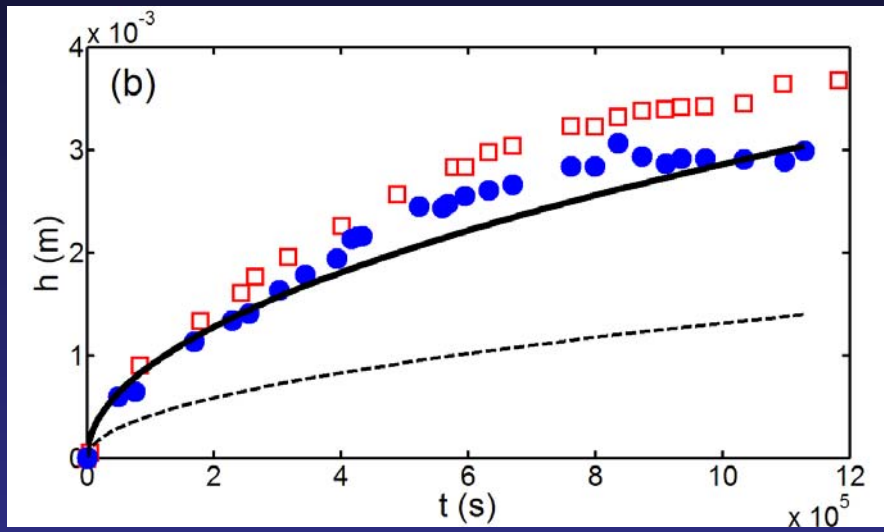

”Bulk” experiment without porous medium indicate D ~ $1.1 \cdot 10^{-11}$

Effects of liquid channels separating the hydrate from the mineral surfaces and the state of non-equilibrium is systems with mineral surfaces (adsorption is an additional phase which reduces the number of degrees of freedom with 1) may account for the difference

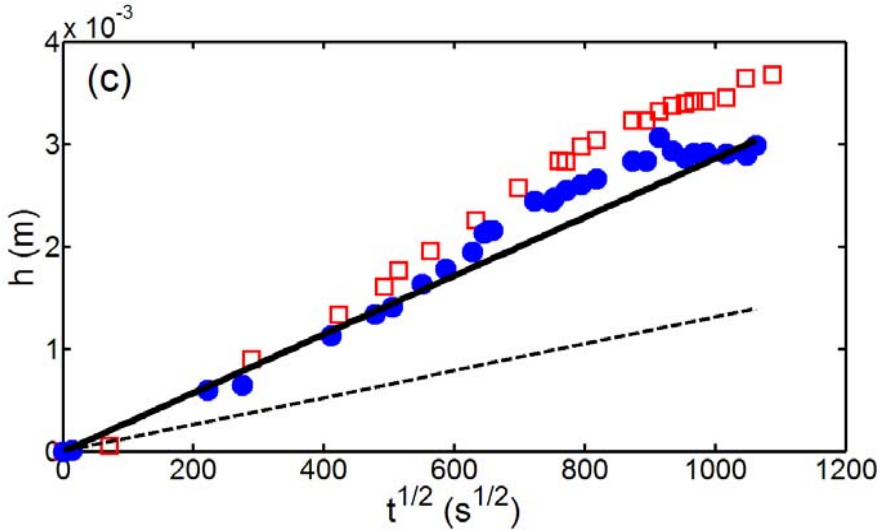

Conclusions

- All hydrate reservoirs do have permeability for the simple reason that water hydrogen bonding in hydrate does not match any favorable interactions with mineral surfaces
- Hydrate phase transition dynamics and corresponding producability depends on type of situation (underlying gas cap, underlaying water or hydrate block alone) depends on the flow dynamics of the actual reservoir in consideration

Conclusions cont.

- Type I reservoirs (undelying gas cap) can be produced initially by pressure reduction but as produced gas is replaced by groundwater it will gradually turn into type II, which is very suitable for production through CO2 injection.
- Local fracturing and horisontal wells for injection of CO2 between water and hydrate will increase injectivity and at the same time create escape pathways for methane

Conclusions cont.

- We have demonstrated experimentally that injection of CO_2 into CH_4 hydrate results in CH_4 release while at the same time providing safe storage option for CO_2
- Unlike other concepts for releasing the hydrocarbons from hydrate there is not net volume change, which can be a geomechanical concern when dissociating hydrate

Conclusions continued

- No extra production of liquid water associated with the gas exchange
- No additional energy supply needed (the conversion is actually exothermic)
- Visualizations Provide Different and Helpful Insights of Hydrate Growth and Stability
- Theoretical predictions based on molecular simulations and Phase Field Theory reproduce the experimental conversion rates

Fiery Ice from the Seas

A series of workshops arranged by

Bjørn Kvamme, UoB, Norway
Stephen Masutani, UoH, USA
Rick Coffin, ONR, USA,
Tsutomu Uchida, Hokkaido Univ., Japan

7th workshop May 10 – 12, 2008
Te Papa, Wellington, New Zealand
http://www.gns.cri.nz/fieryice/
Organized by: Ingo Pecher

Purpose: Contribute to the establishment of large international interdisciplinary research programs on fundamental properties of hydrate reservoirs, hydrate quantification and feasible exlotitation